

POLITECNICO DI TORINO

**Master's degree course
in Aerospace Engineering**

Master's Degree Thesis

**Rendezvous manoeuvres of small satellites equipped with
miniaturized propulsion systems**



Relatore/i

Prof. Sabrina Corpino

Eng. Fabrizio Stesina

Candidato

Alfonso Picerno

Academic Year 2020-2021

*A mio padre,
A mia madre,
per i loro sacrifici grazie ai quali posso
iniziare a trasformare i sogni in futuro*

Summary

- List of figures**..... 6
- List of tables**..... 7
- Abbreviations**..... 8
- Abstract**..... 9
- 1 Introduction** 10
- 2 SROC mission** 12
 - 2.1 Mission Objectives and SROC mission statement** 12
 - 2.1.1 Safety Aspects..... 13
 - 2.2 Proximity operations** 13
 - 2.3 Orbit inspection** 14
 - 2.4 Main phases of a rendezvous mission**..... 15
 - 2.5 Concept(s) of Operations**..... 16
 - 2.6 Nominal Operations** 17
 - 2.7 Retrieval operations** 19
 - 2.8 Off-nominal operations** 19
 - 2.9 Mission architecture**..... 20
 - 2.10 Mission Analysis**..... 22
 - 2.10.1 Assumptions 22
 - 2.10.2 Mission Phases..... 23
 - 2.10.3 Design and definition of trajectories 24
 - 2.11 Baseline design** 26
 - 2.11.1 Trajectory..... 26
 - 2.12 DeltaV budgets** 27
 - 2.13 SROC technology** 29
 - 2.13.1 Propulsion..... 30
- 3 Propulsion system overview** 31
 - 3.1 Interactions between the propulsion system and other SROC’s subsystems**..... 31
 - 3.1.1 Interaction between the propulsion system and ADCNS..... 32
 - 3.1.2 Interaction between the propulsion system and PRNS 33
 - 3.1.3 Interaction between the propulsion system and the payload..... 33

3.1.4	Interactions between the propulsion system and docking subsystem.....	33
3.1.5	Interactions between the propulsion system and CDH	33
3.1.6	Interactions between propulsion system and structure / mechanism.....	33
3.1.7	Interactions between the propulsion system and TCS	33
3.1.8	Interaction between the propulsion system and the EPS.....	34
3.2	Drivers.....	34
3.3	Technologies.....	36
3.3.1	Cold Gas.....	36
3.3.2	Liquid monopropellant propulsion systems	39
3.4	Trade-off analysis	53
4	Engine Model	55
4.1	Cold gas technology.....	55
4.2	SROC propulsion system.....	57
4.3	Thrusters position.....	60
4.4	SROC propulsion system model	61
4.4.1	Thrust and I_{sp} modelling	61
4.4.2	Thrusters Sets	64
4.4.3	Finite manoeuvres and insertion of the new Thruster Sets created within each manoeuvre segment	65
4.5	Characterization of the fuel tank and estimate of the amount of propellant needed for the mission.....	66
4.6	Simulation results	68
4.6.1	ΔV	68
4.6.2	Duration and fuel used	69
4.7	Thrust profile	70
5	Causes of deviation from the planned trajectory.....	73
5.1	Trajectory deviations due to thrust errors	73
5.2	Trajectory deviations due to thruster failures	74
5.3	Orbital disturbances	74
5.3.1	Drag due to residual atmosphere.....	74
5.3.2	Disturbances due to geopotential anomaly.....	75
5.3.3	Disturbances due to solar pressure	75

5.3.4	Dynamic interaction of thruster plumes between chaser and target.....	76
5.3.5	Trajectory deviations generated by the spacecraft system (navigation errors) .	77
5.4	Simulations	77
6	Conclusions	85
7	References	86

List of figures

FIGURE 1: CONCEPTUAL CONFIGURATION OF SROC	11
FIGURE 2: LVLH AND RIC FRAMES COMPARISON	14
FIGURE 3: SROC MISSION- NOMINAL OPERATIVE SCENARIO.....	17
FIGURE 4: SROC OPERATIONS-RETRIEVAL DRM	19
FIGURE 5: SROC MISSION- OFF-NOMINAL SCENARIO AND REDUCED SCENARIO.....	20
FIGURE 6: SPACE RIDER CONSIDERED ORBITS.....	22
FIGURE 7: SPACE RIDER'S REFERENCE ORBITS (SCENARIO 1, 2, 3, 4, 5 RESPECTIVELY).....	25
FIGURE 8: ΔV BUDGET FOR BASELINE SCENARIO.....	28
FIGURE 9: PROPOSED THRUSTER MODULE SPECIFICATIONS	30
FIGURE 10: INTERACTIONS BETWEEN THE PROPULSION SYSTEM AND ALL THE OTHER ON-BOARD SUBSYSTEMS	32
FIGURE 11: COLD GAS STATE OF THE ART	37
FIGURE 12: GREEN PROPULSION SYSTEMS.....	41
FIGURES 13: ADVANTAGES OF GREEN PROPULSION	43
FIGURE 14: MPS-120	44
FIGURE 15: MSP-130	44
FIGURE 16: BGT-X5	45
FIGURE 17: ADN MICRO PROPULSION SYSTEM.....	46
FIGURE 18: ECAPS HPGP THRUSTER.....	47
FIGURE 19: HYDROS-M.....	48
FIGURE 20: HYDROS-C	48
FIGURE 21: GREEN PROPULSION SYSTEM	49
FIGURE 22: PALOMAR MICRO PROPULSION SYSTEM.....	50
FIGURE 23: JPL PROJECT OF A HYBRID PROPULSION SYSTEM	51
FIGURE 24: ARGO MOON PROPULSION SYSTEM.....	52
FIGURE 25: SCHEMATIC OF A COLD GAS PROPULSION SYSTEM	55
FIGURE 26: PERSEUS GENERAL CONFIGURATION FLUIDIC SCHEMATIC.....	57
FIGURE 27: THRUSTER MODULE SPECIFICATIONS	59
FIGURE 28: PERSEUS 6U FULL CONFIGURATION AT PRELIMINARY DESIGN	59
FIGURE 29: THRUSTERS POSITION	60
FIGURE 30: PERSEUS MODEL ON STK.....	63
FIGURE 31: EDIT THRUST COEFFICIENTS	63
FIGURE 32: EDIT I_{sp} COEFFICIENTS.....	64
FIGURE 33: SROC THRUSTER SETS ON STK	65
FIGURE 34: FINITE MANOEUVRES AND INSERTION OF THE NEW THRUSTER SETS CREATED.....	66
FIGURE 35: CHARACTERIZATION OF THE FUEL TANK	67
FIGURE 36: THRUST PROFILE ALONG THE 3 BODY AXES IN THE NOMINAL CASE.....	71
FIGURE 37: DENSITY VS ALTITUDE AT VARIOUS LEVELS OF SOLAR FLUX.....	75
FIGURE 38: SOLAR PRESSURE FORCE ON SURFACE AREA	76
FIGURE 39: THRUSTER PLUME FORCE ON SURFACE AREA.....	77
FIGURE 40: NOMINAL VALUES.....	78
FIGURE 41: ADDED 1 DEGREE OFFSET ON BOTH AZIMUTH AND ELEVATION ANGLE.....	78
FIGURE 42: THRUST PROFILE FOR THE CASE WITH 5 DEGREE / 5 DEGREE OFFSETS	81
FIGURE 43: THRUST PROFILE FOR THE CASE WITH 5 DEGREE / -5 DEGREE OFFSETS	83

List of tables

TABLE 1: SROC PHASES AND SCENARIO 16

TABLE 2: SROC BASELINE MISSION-CONOPS 1-PHASES AND SCENARIO DESCRIPTION (IN-PLANE STRATEGY) 18

TABLE 3: SROC MISSION ARCHITECTURE 21

TABLE 4: DRIVERS WEIGHTS 53

TABLE 5: TRADE-OFF OF THE DIFFERENT TECHNOLOGIES FOR THE SROC PROPULSION SYSTEM..... 54

TABLE 6: COEFFICIENTS FOR THRUST MODELLING 62

TABLE 7: COEFFICIENTS FOR I_{sp} MODELLING..... 62

TABLE 8: THRUSTER SETS 64

TABLE 9: ΔV OF THE SIMULATION WITH PERSEUS MODEL 68

TABLE 10: DURATION OF MANOEUVRES AND FUEL CONSUMED DURING THE MISSION 69

TABLE 11: DURATION AND THRUST VALUES ALONG THE 3 BODY AXES FOR ALL MANOEUVRES 72

TABLE 12: RESULTS OF SIMULATIONS WITH OFFSETS 79

TABLE 13: DURATION AND THRUST VALUES ALONG THE 3 BODY AXES FOR THE CASE WITH 5 DEGREES / 5 DEGREES OFFSETS 81

TABLE 14: DURATION AND THRUST VALUES ALONG THE 3 BODY AXES FOR THE CASE WITH 5 DEGREES / -5 DEGREES OFFSETS 83

Abbreviations

SROC	Space Rider Observer Cube
SR	Space Rider
ConOps	Concept of Operations
HP	Hold Point
FRR	Far Range Rendezvous
CRR	Close Range Rendezvous
WSE	Walking Safety Ellipse
DARM	Deployment and Retrieval Mechanism
TPS	Thermal Protection System
SRP	Solar Radiation Pressure
DEP	Deployment Phase
EOP	Early Operation Phase
TCM	Trajectory Correction Manoeuvres
CAM	Collision Avoidance Manoeuvres
CDH	Command and Data Handling
ADCNS	Attitude Determination and Control and Navigation Subsystem
PROP	Propulsion Subsystem
PRNS	Proximity Relative Navigation Subsystem
EPS	Electrical Power Subsystem
TCS	Thermal Control System
MIB	Minimum Impulse Bit
TRL	Technology Readiness Level
I_{sp}	Specific Impulse
ACS	Attitude Control Subsystem
JPL	Jet Propulsion Laboratory
TVC	Thrust Vector Control
STK	System Tool Kit
DOF	Degree of Freedom
GNC	Guidance Navigation and Control

Abstract

In recent years, public and private actors in the field of the small satellites have been concentrating their energies and resources on the development of a technologies that enable operational capabilities that enlarge the set of missions accomplished by small-sats. One valuable example of new small-sats missions is the inspection and monitoring of larger spacecraft (such as the International Space Station) or debris. This kind of missions requires an improvement of miniaturized technologies such as the cameras for navigations, sensors to measure relative distances, interlink communication, high-accuracy attitude control, and the propulsion system. One of the most relevant planned mission in this framework is the Space Rider Observer Cube (SROC) mission, an innovative small satellite mission performed by a consortium formed by Politecnico di Torino and Tyvak international, that would fly around and in formation with the European Space Agency Space Rider vehicle. Space Rider is an uncrewed space vehicle with the aim to provide Europe with an affordable, independent, reusable end-to-end integrated space transportation system for routine access and return from low earth orbit (LEO). SROC has two key objectives: to fly around the Space Rider vehicle performing observations in visible, near infrared and thermal infrared wavelengths and to validate critical small satellite operations and technologies such as deployment and retrieval capabilities from and to the cargo bay of the Space Rider.

The main objective of the thesis is to perform the mission analysis considering the features of the propulsion system. A model of the propulsion system of the SROC mission has been developed, introducing uncertainties and disturbances and the performance has been verified in System Tool Kit (STK) environment. In the initial stages, an analysis was also made of all the possible choices between the technologies of the SROC propulsion system, choosing the best one through a trade-off between all of them. A series of offsets have also been added to the simulation environment that consider the possible disturbances that the spacecraft may suffer during its operational life in order to compare the results with the nominal case and to evaluate the conditions of the system in the worst cases.

After an in-depth analysis, it was shown that the best technology for the SROC propulsion system is cold gas and once a propulsion model was created that best simulated the real one of SROC, the results of the simulations made in STK environment were very positive, finding a reduction in ΔV equal to 35.6% with relative lowering of the fuel consumed compared to the previous simulations carried out considering a non-customized engine model. The results of the simulations obtained after adding a series of offsets to the simulation environment were equally positive, in fact they did not record significant increases in ΔV and fuel consumed (indeed they remained almost unchanged) but there was a variation in the profiles thrust of the mission while remaining in any case within the range of acceptable values demonstrating the feasibility of the SROC mission with the propulsion system chosen.

1 Introduction

In recent years, the space sector has increasingly attracted the attention of public opinion and above all of important private investors who have decided to invest large capital in this sector. The trend is to carry out missions with small satellites, CubeSat, due to their relatively low cost and complexity which have led them to be the first choice over large monolithic satellites.

A CubeSat is a standard for nanosatellites with the characteristic of being modular, where the base unit, 1U, is a cubic satellite with a 1dm^3 volume and a weight not more than 1.33 Kg, therefore it is possible to have 3U CubeSat with dimensions of 10x10x30 cm or 6U CubeSat 10x20x30cm and so on. CubeSats are projected into a brilliant future, but the technology still needs improvements and the process of manufacturing, assembly, integration and verification shall become more efficient. In this framework, miniaturized propulsion systems deeply increase the range of mission concept achievable with multi-unit CubeSats (6U+) in terms of orbit change and raising, station keeping and orbit maintenance against the disturbances, formation flying, proximity operations and deorbit, but an improvement is required from the technological point of view in order to increase the technology readiness level of some enabling technology for the future missions. These enabling technologies are high data rate communication systems, high accuracy attitude and orbit determination and control devices, thermal control systems. Moreover, new logical and physical architectures, and the capability to re-plan the operations during the mission become fundamental for innovative applications and unprecedented missions where CubeSats are main characters. One of the most promising technologies is the small propulsion system that open new scenarios for the modern CubeSats that would perform controlled orbit (and attitude) manoeuvres^[1].

This thesis is focused on the SROC mission of the European Space Agency (ESA). The SROC mission foresees a CubeSat released by the Spice Rider vehicle and able to perform a set of rendezvous and docking manoeuvres, that allows the CubeSat to re-entry in the cargo bay of Space Rider after long phases of fly-around this vehicle.

This is a very ambitious and innovative mission whose main purpose is to carry out the first rendezvous and docking manoeuvre done with a CubeSat. Being an innovative mission, the design of all the subsystems of SROC is a very delicate point to be achieved especially as regards the propulsion system which is the system that must be able to satisfy the greatest number of requirements. The study presented in this thesis focuses mainly on the propulsion system of the SROC mission starting from the main characteristics of the mission defined in previous studies and going to investigate the current state of the art of propulsion systems for CubeSat both in the European and American market in order to identify the best technology to best achieve the mission. Once the best technology for the propulsion system has been identified, it will be modelled in order to validate it in a simulation environment created through the STK software and analyses will be carried out on ΔV and other characteristics of the mission. In the end, off-nominal situations will also be taken into consideration in order to validate the choice of the propulsion system and the analyses made even in the presence of possible offsets.

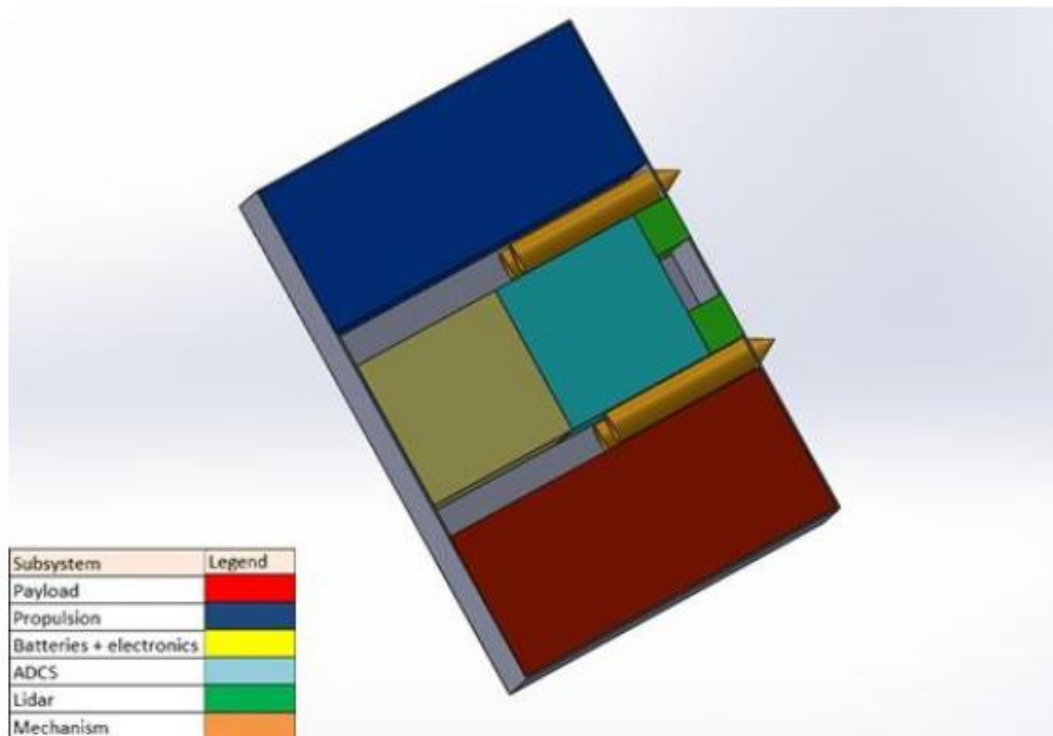


Figure 1: Conceptual configuration of SROC^[2]

The challenge is to develop new miniaturized technologies for CubeSat, which, compared to a large satellite, has the disadvantage of having less volume, mass, and power.

2 SROC mission^{[2][3]}

2.1 Mission Objectives and SROC mission statement

The SROC mission statement is:

SROC mission statement

To deploy a CubeSat in LEO to support operations of Space Rider through multispectral and visual observations taken in proximity of the vehicle during the orbital phase. To enhance CubeSat's capabilities in the proximity operations domain.

Expanding the mission statement and embedding the identified stakeholder needs, the following primary mission objectives are:

- **To observe Space Rider with unprecedented imaging for engineering and outreach purposes**
 - o Imaging capabilities
- **To demonstrate critical technologies and functions related to formation flight missions, in terms of:**
 - o Proximity Navigation
 - o Guidance and Control capabilities
 - o Communication architecture
- **To demonstrate CubeSats in-orbit retrieval and reuse capabilities**
 - o Docking mechanisms

To achieve these objectives, a hyperspectral camera and retrieval mechanism has been chosen as payloads for SROC. For the first one, the imager shall be able to observe SR in thermal infrared, near infrared and visible bandwidths for:

- Identification of the chemical deterioration of Space Rider surfaces;
- Identification of mechanical deterioration of Space Rider surfaces;
- Identification of temperature and temperature distribution on Space Rider;
- Identification of misalignments of components.

2.1.1 Safety Aspects

Safety is a key driver of the SROC mission, and it shall be considered as a critical aspect of the mission to be addressed since the beginning of the concept(s) development. The SROC mission consists of a small spacecraft that is released by and operates in the vicinity of a larger vehicle, and that might be required to re-mate with the mothership and re-enter to Earth. For the moment, no explicit safety requirements are stated for this kind of mission in the framework of the Space Rider project. However, it is expected that safety requirements will affect the mission and system design significantly. The only examples of similar missions available to date are related to CubeSats deployed from the International Space Station (ISS) and from visiting vehicles at the ISS. For the development of the first iteration of the SROC mission design, the safety strategy aims at avoiding any collision with the Rider (meaning that: the SROC demonstrator mission shall not compromise the SR vehicle and its mission) and it is based on the following concept (**minimum risk philosophy**):

- Several “volumes”, in the form of **ellipsoids**, are built around Space Rider. These ellipsoids delimit different zones in which the SROC CubeSat shall be operated in different modes, and in which certain capabilities are required. **Decision points** shall be defined for passing from one zone to the adjacent.
- Exploit the **safe free drift trajectory** approach, i.e. trajectories of SROC shall be passive safe, whenever possible.
- A **collision avoidance system** shall be integrated in the CubeSat design, which shall tolerate at least **one failure**, and be fully **autonomous** (i.e. independent from ground operations) or **semi-autonomous**.

2.2 Proximity operations

Spacecraft proximity operations is the tracking or maintenance of a desired relative separation, orientation or position between or among spacecraft. In this situation, there is not just one orbit (or location on the orbit) to be controlled, but there are many, and the typical approach consists in controlling the orbit of one of the spacecraft (the leader) and regulating the others (the followers) relatively to it. The leader is also called target or chief while the followers are also called chasers or deputies, depending usually on the application. While the leader’s orbit is handled with an absolute reference frame, for the followers a relative frame is considered: this is a local orbital reference frame in which the motion is described relatively to a particular point in orbit or to another spacecraft; in this way the local orbital frame for both the leader and the follower can be defined, but the trajectories of the chaser are defined relatively to the target. For our application, two different frames are proposed: 1) the local-vertical/local-horizontal (LVLH) frame; 2) the Hill’s frame . The LVLH frame has its origin in the centre of mass of the leader spacecraft, the first axis is in the direction of the orbital velocity vector (V), the second axis is in the opposite direction of the angular momentum vector (H) of the orbit and the third one completes the triad. In rendezvous literature, these coordinates are also called V_{bar} , H_{bar} and R_{bar} respectively (the last one refers to the radial direction in case of a circular orbit). The Hill’s frame also has its origin in the centre of the spacecraft mass, the first axis is the radial outwards direction (Radial), the second axis is the direction of the orbital velocity vector (InTrack) and the third one completing the triad is the orbital angular momentum direction (CrossTrack). It is preferable to operate the second reference frame proposed, also called RIC frame (Radial-InTrack- CrossTrack), as it is the one used in the relative equations of motion, described below, and the most widely used in

relative proximity operations literature. Both the frames are compared and shown in Figure 1, together with the absolute position, velocity and angular momentum vectors (\vec{r} , \vec{v} and $\vec{h} = \vec{r} \times \vec{v}$ respectively), assuming a circular orbit for the leader spacecraft.

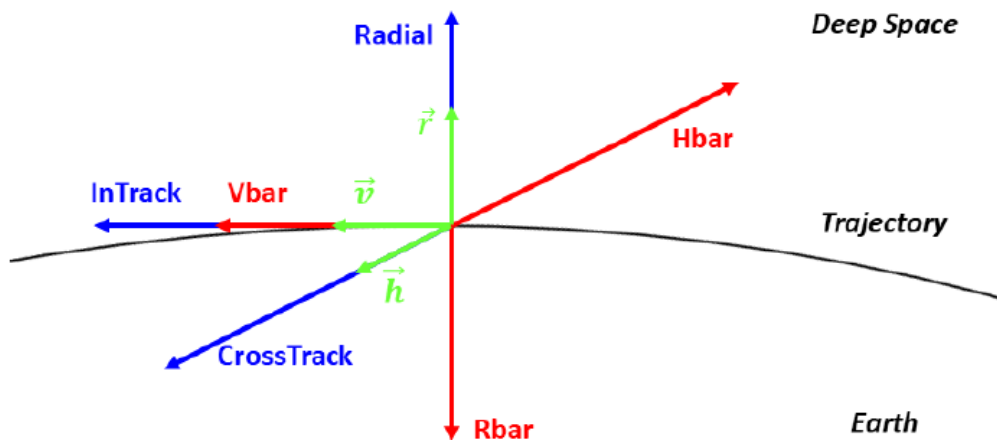


Figure 2: LVLH and RIC frames comparison

2.3 Orbit inspection

There are several strategies to realize inspection of objects in space using a satellite, and they can be broadly divided into three main groups:

- **Close-range observation:** the inspector satellite intercepts and rendezvous with the space object to be observed and continues station-keeping about the space object while collecting sensor data. After data collection is complete, the inspector satellite moves off.
- **Far-range observation:** the inspector satellite is placed in a fixed orbit from which it can observe the target space object. The inspector employs long-range sensors to collect data. No attempt is made to manoeuvre closer to the space object.
- **Fly-by:** the inspector satellite is manoeuvred to an intercept orbit that brings it close to the space object; during the close approach, the inspector satellite collects sensor data then continues along its own trajectory.

In the first two strategies, the inspector satellite keeps its position relative to the target (closer or farther respectively) for a longer time than in the third case, in which the distance from the target is variable as the inspector travels along its orbit.

For the SROC mission, the first option has been chosen because: 1) compared to the long-range strategy, it gives the opportunity to stay closer to the target, while 2) compared to the fly-by solution, it allows a longer inspection time. The benefit of the first option is related to the quality and quantity of mission data that can be collected through a (relatively) simple/small payload (if compared to the payload needed for collecting the same data at a longer distance and/or in a shorter period of time). On the other hand, staying closer to the target for a long period of time in a controlled formation implies several technical challenges that will be addressed in detail in this study. In other words, the close-range observation maximises the scientific return of the mission and challenges the capabilities of the inspector thus maximising also the technological return of the mission. The cost of implementing the close-range strategy is the complexity of the chaser

(which is however linked to the primary objective of the mission, i.e. demonstration of critical technology for proximity operations), and the safety of the mission, which will be driven by the Space Rider mission requirements. When the inspector is in proximity of its target, different strategies for the geometry of the proximity operations have been considered for the SROC mission:

- **InTrack holding at TBD distance from SR:** the inspector satellite is in the same orbit of the target with a small phase angle in true anomaly. The chaser stays stationary near the target, observing always the same portion of the target.
- **Out of plane motion at TBD distance from SR with radial components:** the orbit of the inspector satellite has a different inclination with respect to the orbit of the target. The chaser swings around the leader's orbital plane, increasing the observable area of the target.
- **Safety ellipse with in and out of plane fly around components:** the inspector satellite stays in an orbit with the same period of the target but with different eccentricity and inclination, in order to make the inspector to follow an elliptic trajectory around the target; varying the inclination of the orbit of the inspector, the inclination of the ellipses also changes, and this allows the chaser to access every point of the target.

For the SROC mission, the last strategy has been selected and implemented as it maximises the portion of the target area observed by the inspector, and it gives full control about the area(s) to be observed.

2.4 Main phases of a rendezvous mission

In general, a Rendezvous and Docking mission can be divided into the following phases:

- Phasing
- Far-range rendezvous
- Close-range rendezvous
- Mating

The phasing is the reduction of the orbital phase angle between the chaser and target and it ends with the acquisition of the 'entry gate' (or 'trajectory gate') which shall satisfy a set of margins for position and velocity values at a certain range. The 'gate' (or 'aim point') will be on the target orbit, or very close to it, and represents the beginning of the far-range relative rendezvous operations.

The major objective of the far-range rendezvous phase is the reduction of trajectory dispersions; therefore, its major tasks are the acquisition of the target orbit, the reduction of approach velocity and the synchronisation of the mission timeline. At the end of this phase, the chaser reaches a point near the target in which it can stay indefinitely at zero ΔV cost, and this point can be a V_{bar} holding point, or a forward and backward drifts below or above the target orbit, or an elliptical motion with the mean orbital height equal to the target orbit.

The close-range rendezvous phase includes the closing, which is the reduction of the relative distance, and the final approach, which consists on the achievement of the mating conditions. This phase is safety critical and, because of the resulting relative trajectory, pure tangential thrust manoeuvres are rarely used while radial approaches are preferred. Radial approach starts from a V_{bar} hold point and

precedes flying around the target. The final approach depends on the docking system and shall fulfil the requirements of attitude and relative position and velocity.

The mating includes capture, which is the prevention of escape of capture interfaces and the attenuation of shock and residual motion, and the achievement of rigid structural connection. For the SROC mission, in which the CubeSat will be deployed by the target vehicle itself, the phasing phase does not exist. All other phases shall be considered, with the peculiarities given by the mission concept considered. However, it shall be highlighted that the most critical part of the SROC mission is related to the last phase of the rendezvous, i.e. the final approach, and the mating. These two phases require capabilities and technologies which have never been demonstrated in orbit between nano/micro satellites nor between nano/micro satellites and bigger spacecraft.

2.5 Concept(s) of Operations

In the present study, the SROC baseline mission implies a single deployment and retrieval, with no reuse of the CubeSat during the same mission (CubeSat is retrieved and stowed/secured in the SR cargo bay until the vehicle returns to Earth). The simpler Observe mission concept is considered in this study as the option for handling contingency cases, i.e. it is the basis for the definition of off-nominal scenarios.

In order to isolate the novel and critical operations within the SROC ConOps, the operational scenario is split in four main parts: high-level mission phases, nominal operations, retrieval operations, and off-nominal routines. This will assist operators during the development of flight procedures to deeply analyse mission critical and off-nominal phases.

High-level mission phases define all the activities related to Integration and Launch, Transfer, Main Operations and decommissioning. Pre-launch activities are considered in this study due to their relevance to integration of the systems within Space Rider and the subsequent integration in Vega C.

The high-level mission phases are given in the follow Table. The high-level ConOps starts with the pre-launch phase 6 months before the launch.

Mission Phase	Mission Scenario
Logistic	SROC integration in Space Rider
Launcher integration	Space Rider integration in Vega-C launcher
Launch	Space Rider injection into LEO
System preparation	SROC deployment from Space Rider and free drift
Rendezvous	Rendezvous and approach to enter formation flight with Space Rider
Observation	SROC points its cameras on Space Rider and executes a series of orbits to observe Space Rider exterior in different wavelengths
Docking and Retrieval	SROC returns into Space Rider cargo bay
End of mission	SROC stowed into Space Rider and return to Earth

Table 1: SROC phases and scenario

2.6 Nominal Operations

The SROC baseline mission implies a single deployment and retrieval, with no reuse of the CubeSat during the same mission (CubeSat is retrieved and stowed/secured in the SR cargo bay until the vehicle returns to Earth). The simpler Observe mission concept is considered in this study as the option for handling contingency cases, i.e. it is the basis for the definition of off-nominal scenarios.

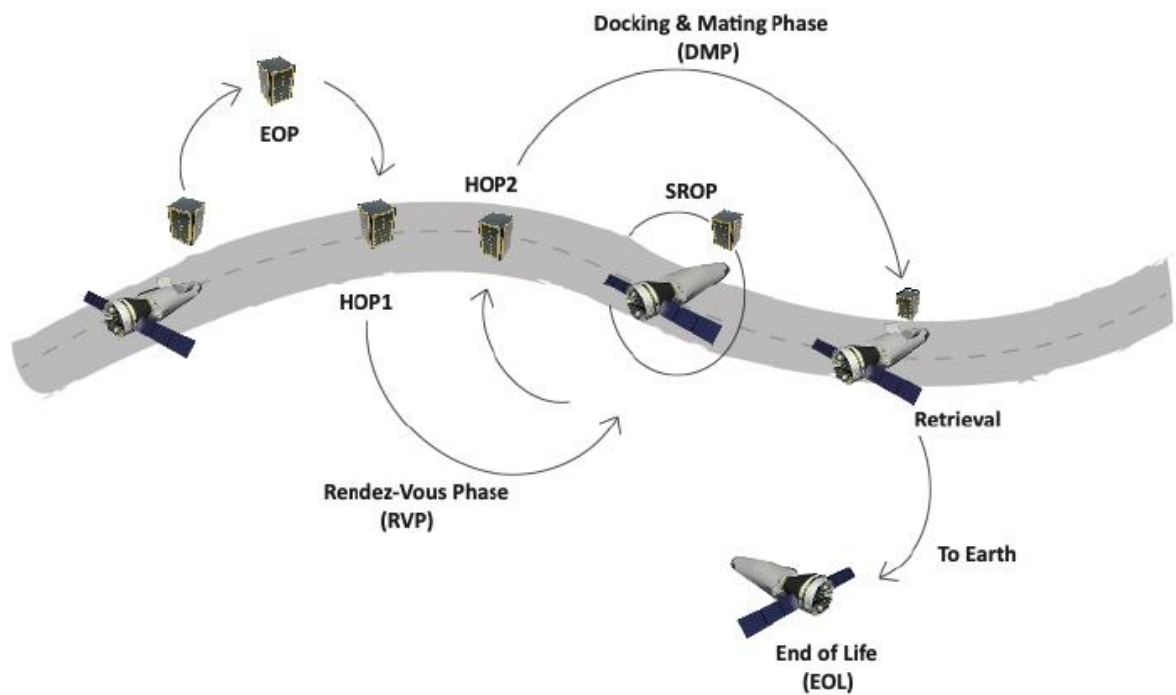


Figure 3: SROC mission- Nominal Operative Scenario

The HP#1 can be also used as virtual point in case rehearsal manoeuvres need to be accomplished. This option would be an action towards risk mitigation of the close proximity operations and docking phase. SROC could carry out the critical manoeuvres around a virtual point (HP#1) before accomplishing them in the vicinity of the rider later in the mission.

Mission Phase	Duration	Mission Scenario
Deployment Phase (DEP)	TBD hours	<i>SROC system preparation SROC spacecraft separation</i>
Early Operations Phase (EOP)	5 days	<i>Link acquisition Detumbling Attitude acquisition Appendices deployment Checkout post deployment Calibration of thrusters Calibration of cameras Test of critical equipment</i>
Holding Phase 1 (HOP1)	4.5 hours	<i>SROC is in hold point 1 (HP#1)</i>
Rendezvous Phase (RVP)	4.5 hours	<i>SROC performs a series of manoeuvres to follow a safe path from HP#1 towards Space Rider to get in the operative orbit. The rendezvous trajectory is split in two segment: Far Range Rendezvous (FRR)→ In-Plane trajectory from HP#1 to InTrack Target Close-Range rendezvous (CRR)→ Out-of-plane trajectory from InTrack Target</i>
Space Rider Observation Phase (SROP)	8 days	<i>Insertion into the Walking Safety Ellipse (WSE) Observation in the Walking Safety Ellipse (WSE) Free Flight Approach to Space Rider (except for the last Inspection cycle)</i>
Holding Phase 2 (HOP2)	4.5 hours	<i>SROC is in hold point 2 (HP#2)</i>
Docking & Mating Phase (DMP)	10-15 hours	<i>Fly-around trajectory from to HP#2 to Rbar Close approach Mating</i>
Retrieval Phase (REP)	5 hours	<i>Capture Post docking check out SROC Retrieval</i>
End of Life (EOL)	TBD	<i>SROC is stored in the Space Rider cargo bay and re-enter with Space Rider</i>

Table 2: SROC Baseline Mission-ConOps 1-Phases and Scenario description (In-Plane strategy)

2.7 Retrieval operations

The operations related to the retrieval routine is represented in Figure 4.

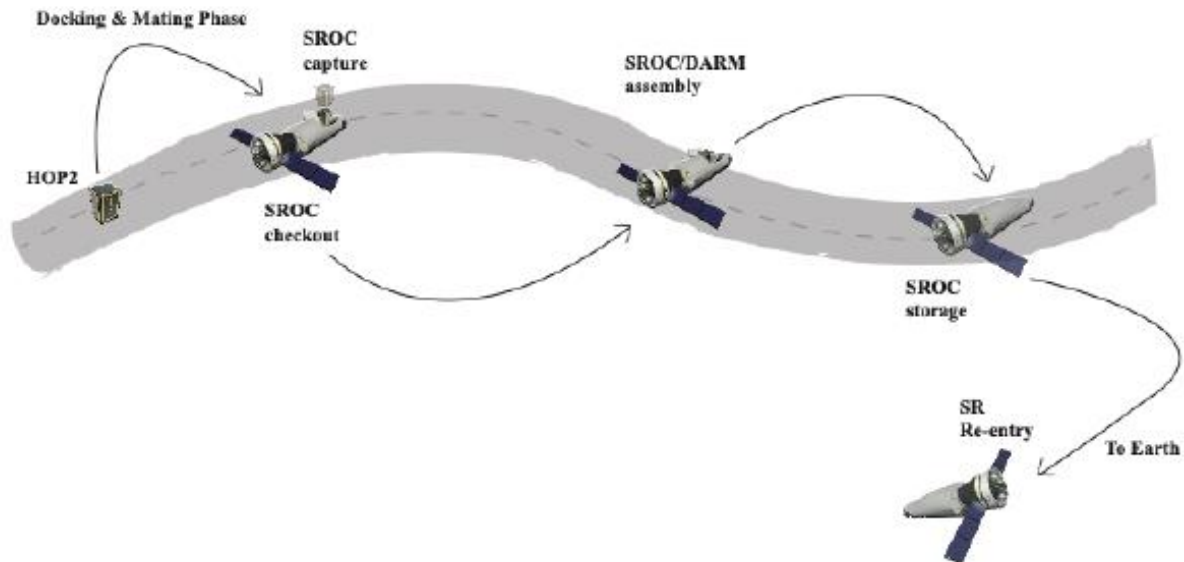


Figure 4: SROC operations-Retrieval DRM

2.8 Off-nominal operations

Off-nominal scenarios refer to all the events that lead to the impossibility of proceeding with the nominal operations. It is necessary to underline that are here considered off-nominal events that might be triggered by either SROC or SR.

From Figure 5 it is possible to observe more details about the off-nominal routine. The routine is based on the Fault Detection Isolation and Recovery (FDIR) approach. The allocation of the functions needed to accomplish each phase depends on the desired autonomy of the system. However, human operator control is always possible to guarantee the success of each phase even in unpredicted situations. Collision Avoidance Manoeuvres (CAM) are foreseen in case of SROC anomalies. Depending on the availability of the main engine, two different CAMs have been taken into account:

- 1) Go away to safe hold point
- 2) Maintain passive safe trajectory

The second option is also the less complex since it keeps the SROC in the operative orbit letting the system naturally drift away from the SR. Final selection of CAM strategy will be also function of SR safety requirements.

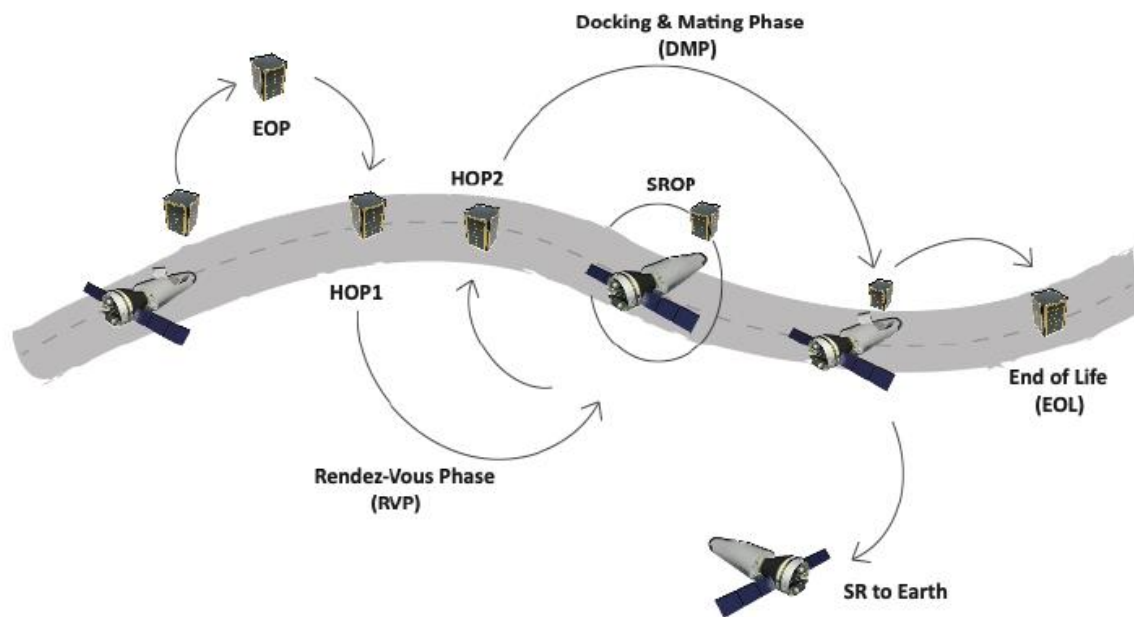


Figure 5: SROC mission- Off-nominal scenario and Reduced scenario

2.9 Mission architecture

The Phase 0/A study led to the conclusion that a 12U CubeSat in formation flying with the Space Rider would best achieve the mission objectives while reducing the encumbrance on the Rider. Therefore, the space segment architecture is composed by one CubeSat with multispectral imager (MSI) as payload, plus a retrieval mechanism. The imager shall be able to observe SR in thermal infrared, near infrared and visible bandwidths in order to meet the identified science goals. In addition, SR could be observed in the ultraviolet bandwidth and stereo imaging technique could be considered, but this is not a priority goal. The choice of the bandwidths shall be done in order to reduce the complexity of the system limiting the need for redesign of the selected instrument. In order to accomplish the mission objectives regarding the retrieval capability. For most options, a dispenser with an active scissor mechanism integrated in SR is considered for complete retrieval of the CubeSat. A Store & Forward architecture and three options for the communication architecture could be tradable: 1) interlink with SR; 2) direct link; 3) both of them. The CubeSat could communicate via direct link with ground station with autonomy level.

Mission element	Description	Trade-offs/Comments
Subject	Space Rider observations; CubeSat Retrieval capabilities	Multi-spectral Observation of Space Rider Single deployment and retrieval of SROC
Space Segment	1 CubeSat 1 Retrieval Mechanism	12U form factor baseline Deployment and Retrieval Mechanism (DARM)
Payload Optics	Multispectral imager	3 bandwidths: Visual, Near InfraRed and Thermal InfraRed
Payload Retrieval	Magnetic mechanism	Ad-hoc customization of AAreST docking mechanism
Orbit & Constellation	Formation flying with respect to Space Rider	SSO midday-midnight assumed as baseline Rendezvous trajectory: in-plane + out-of-plane segments Walking Safety Ellipse with relative inclination change for observation
Communication Architecture	Store & Forward architecture	Direct link to Earth (Interlink is an option to be further assessed in the next iterations)
Ground Segment	Ground station network MCC	Network of 6+ UHF ground stations, 1 S-band main ground station (+ 1 S-band ground station back-up) MCC in Torino
Mission control centres and operations	Professional Operators	CubeSat control centre
Launch Segment	Vega C	Launch assumed June 2023

Table 3: SROC mission architecture

The functional analysis has been carried out for identifying the critical functions that must be enabled by the different elements of the proposed mission architecture. In particular:

- To integrate SROC into the Space Rider cargo bay [Allocation to deployment mechanism]
- To deploy SROC without risk for the Space Rider [Allocation to deployment mechanism]
- To maintain formation with the Space Rider [Allocation to GNC subsystem]
- To mate with the Space Rider [Allocation to retrieval mechanism and GNC subsystem]
- To demonstrate CubeSat reuse capabilities [Whole space segment is interested]
- To take multispectral observations [Allocation to observation payload]

During the second design iteration, it became clear that a 12U form factor would best meet the mission objectives, taking into account the challenges of the SROC mission in terms of proximity operations capabilities and safety constraints.

The critical areas of the mission have been also identified as follows:

- Imaging capabilities
- Guidance and Control capabilities
- Proximity Navigation
- Docking
- Communication architecture

2.10 Mission Analysis

In this section the analysis of orbit geometry and trajectories for the SROC mission is described. Assumptions about Space Rider orbits and system configuration have been made in order to develop formation and rendezvous strategies.

2.10.1 Assumptions

Different Space Rider operational orbits have been considered, adopting as the initial date of the SROC mission 23st June 2023 11:00:00.000 UTG.

Sun Synchronous - midday/midnight		Intermediate Orbit – dawn/dusk	
Apoapsis Altitude	400 Km	Apoapsis Altitude	400 Km
Eccentricity	0.0	Eccentricity	0.0
Inclination	97.03 deg	Inclination	37 deg
RAAN	339.23 deg	RAAN	249.23 deg
AOP	0 deg	AOP	0 deg
True Anomaly	0 deg	True Anomaly	0 deg
Intermediate Orbit – midday/midnight		Quasi Equatorial	
Apoapsis Altitude	400 Km	Apoapsis Altitude	400 Km
Eccentricity	0.0	Eccentricity	0.0
Inclination	37 deg	Inclination	5 deg
RAAN	339.23 deg	RAAN	0 deg
AOP	0 deg	AOP	0 deg
True Anomaly	0 deg	True Anomaly	0 deg

Figure 6: Space Rider considered orbits

Other assumptions are listed below:

- SR Dry Mass: 4165 Kg
- SR attitude is fixed with TPS towards nadir direction, except for the SROC deployment
- SR motion is controlled (i.e. not perturbed except for gravitational J2 effects)
- SROC parameters:
 - Dry Mass: 24 kg

- Drag Coefficient: 2,2
- Drag Area: 0,006 m²
- SRP Coefficient: 1,3
- SRP Area: 0,06 m²
- Deployment conditions has been assumed after a deployment analysis with a standard ΔV of 1 m/s, based on existing technology, and a deployment angle of 5 deg with respect to Rbar direction (anticlockwise wrt nadir vector).
- Holding points are considered for go/no go commands and for possible rehearsal operations in order to increase mission safety
- SROC orbit propagators and environmental models:
 - Integrator: RungeKutta89
 - Gravitational perturbation: JGM-2 at order J4
 - Solar radiation pressure: spherical model
 - Third bodies: Sun and Moon
 - Atmospheric model: MSISE90

Two different synchronised propagators have been used for the follower and the leader: while the first one uses perturbations, the second does not, assuming that SR, being the leader, is always in the correct orbit. The SRP and the third body perturbations influence the trajectories of SROC varying its orbital parameters, but they are much less effective than the atmospheric drag, which slow down the CubeSat. This effect is significant in hold points because varying the semimajor axis, the proximity operations condition is not satisfied.

2.10.2 Mission Phases

Space Rider shall operate in circular orbits at 400 km of altitude with different inclination. For all this possible Space rider scenarios, different strategies and SROC mission phases duration can be adopted.

The SROC mission phases are reported hereafter:

- Deployment Phase (DEP): SROC is deployed from the DARM system inside the SR cargo bay
- Early Operations Phase (EOP): the duration may vary, between the best case of 5 days and the worst of 10 days
- Hold Point Phase 1 (HOP#1): the first hold point is needed to stop the drift away motion after EOP
- Rendezvous Phase (RVP): the goal is to reduce the distance between SROC and SR, after the free drift during the EOP phase, and to achieve the relative position to start the observation phase. Two different strategies are developed to accomplish this task.
- SR Observation phase (SROP): this phase is divided into different scenarios that are repeated several times, according to the number of desired observations. This phase is composed by:
 - WSE insertion: SROC performs a manoeuvre to enter the WSE which, thanks to the contribution of the atmospheric drag, will advance along the positive InTrack direction allowing the observation of SR in total passive safety
 - SR observation: SROC passively maintains its motion in the WSE to observe SR, guaranteeing the payload operating range
 - Free Flight: after the observation period, SROC continues its motion without manoeuvring to allow the downlink with ground stations

- Approach: SROC manoeuvres to approach again SR and to start another observation cycle. This scenario is not performed for the last observation cycle, where instead a Hold Point trajectory is executed.
- Hold Point Phase 2 (HOP#2): the second hold point is needed to stop the drift away motion after the last free flight segment and prepare for docking
- Docking & Mating Phase (DMP): the last phase is composed by three different segments to perform the mating with Space Rider:
 - Fly Around: SROC exits the Hold Point trajectory to approach SR along the radial direction
 - Close Approach: SROC stops its relative motion wrt SR and reduces the distance between the two spacecraft
 - Mating: SROC manoeuvres to mate with Space Rider

2.10.3 Design and definition of trajectories

Space Rider shall operate in circular orbits at 400km of altitude with an inclination that can vary from quasi-equatorial to Sun-Synchronous orbits; therefore, the following different scenarios have been simulated: the chosen starting time for each scenario is the UTC Gregorian time 23st of June 2023 11:00:00:

- Scenario 1: sun synchronous midday/midnight orbit with inclination of 97.03 deg and RAAN of 94.79 deg
- Scenario 2: sun synchronous down/dusk orbit with inclination of 97.03 deg and RAAN of 4.79 deg
- Scenario 3: intermediate orbit with inclination of 37.00 deg and RAAN of 4.79 deg
- Scenario 4: intermediate orbit with inclination of 37.00 deg and RAAN of 94.79 deg
- Scenario 5: quasi-equatorial orbit with inclination of 5.00 deg and RAAN of 0 deg

The five mission scenarios are depicted in Figure 7.

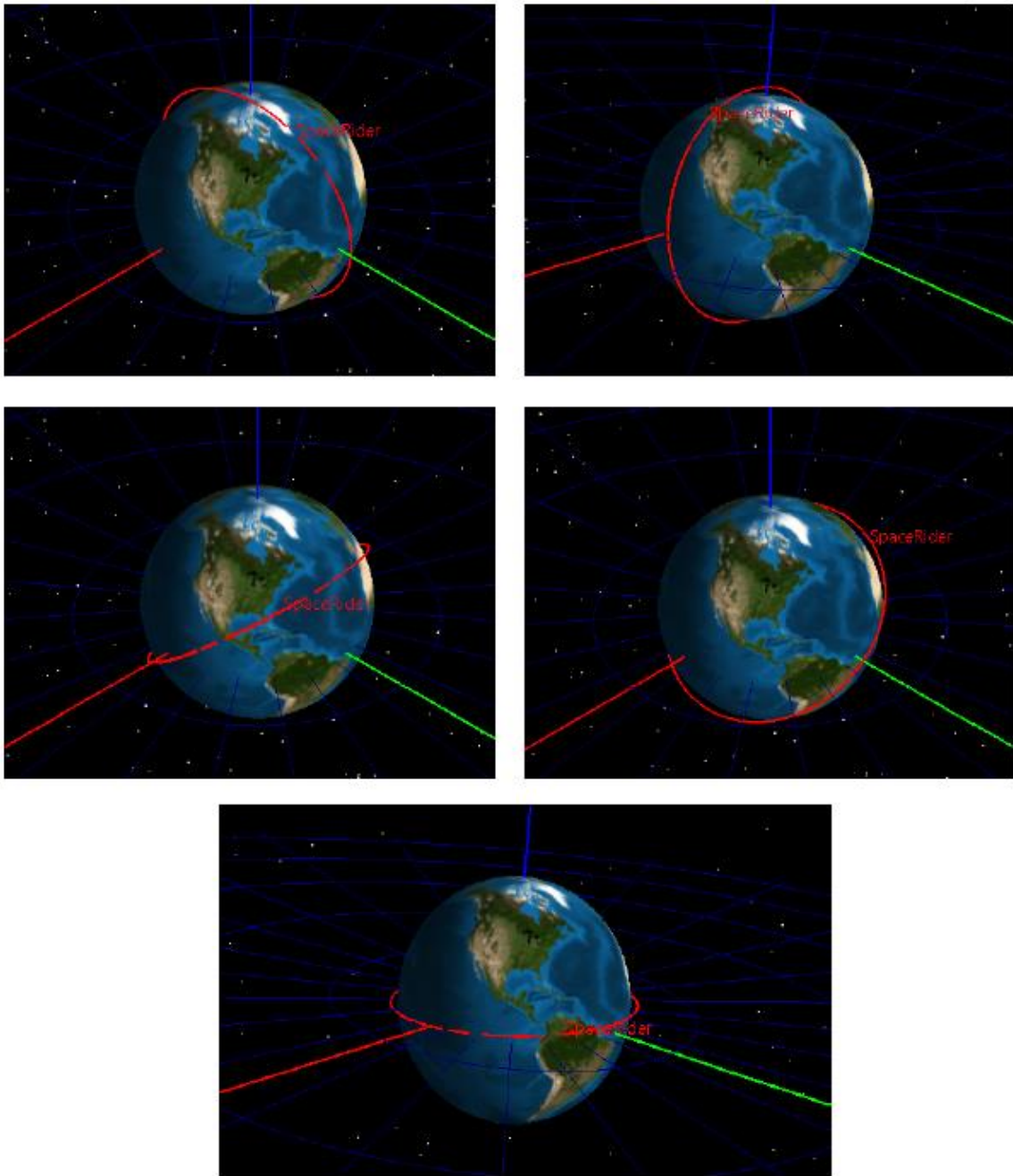


Figure 7: Space Rider's reference orbits (scenario 1, 2, 3, 4, 5 respectively)

At the beginning, an ideal case has been studied, with just gravitational perturbation JGM-2 at order J4, then other perturbations have been considered. For the propagation, the RungeKutta89 integrator has been adopted and manoeuvres have been considered impulsive. Every scenario starts with SR true anomaly set at 0 deg and, to define the starting position of SROC and to handle the output data, a reference LVLH frame centred on SR has been created. To represent SROC inside SR cargo bay, null starting relative position and velocity have been set. The deployment is executed after 2000s from the beginning of the scenario and it has been first modelled with an impulsive manoeuvre of 1 m/s.

2.11 Baseline design

2.11.1 Trajectory

According to the nominal concept of operations for the baseline mission (Observe & Retrieve), the trajectory of SROC can be divided into the following segments:

- 1) Deployment;
- 2) Drift Away;
- 3) Hold Point 1 (HP#1);
- 4) Rendezvous;
- 5) Walking Safety Ellipses + Free Flights + Approaches (repeated observation cycle);
- 6) Hold Point 2 (HP#2);
- 7) Approach and Docking.

The **deployment** has been chosen to be coplanar, with negative components of R_{bar} and V_{bar} ; the ΔV applied is 1 m/s. Once deployed, the scenarios have been propagated for 5 days (worst and conservative scenario) in order to simulate the required time for the operations of detumbling, check and calibration of SROC (EOP).

Both **hold points** have been chosen to be in positive InTrack direction because the natural effects of the perturbations make SROC to drift away from SR. Following the trade-off study for the selection of the strategy for the operative phase, the safety ellipse trajectory has been chosen. For **the approach and docking** after HP#2 the correct strategy depends on the attitude of the target and the docking mechanism, which are unknown at this point of the project. For this reason, for the simulations a classic R_{bar} approach has been used. The soft-docking condition is achieved at a velocity of 0.15 m/s, but further analysis will be carried out for the final phase of docking.

For the baseline design, the **Sun-Synchronous orbit noon/midnight** has been assumed for Space Rider. The SSO noon-midnight was assumed as baseline orbit for several reasons:

- it is the best for illumination conditions at docking. For example, SSO dawn-dusk is not suitable because of poor illumination during docking from R_{bar} . For the other two suitable options (intermediate orbit and quasi-equatorial), beta angle is variable from -20 to 60 deg. For cases from -20 to 20 deg: the same "good" illumination during docking is guaranteed for most part of the orbit. For cases from 20 to 60 deg, suitable illumination during docking is guaranteed only orbital noon
- it is a popular orbit for CubeSats, and it is well covered by an appropriate network of Ground Stations and suitable for mission operations from the CubeSat Control Centre. The intermediate orbits are also suitable from the ground coverage perspective, while the quasi-equatorial orbit would require additional stations to be considered for an appropriate coverage of the mission.

ConOps (in-plane + out-of-plane rendezvous) with 5 days EOP duration is proposed as baseline, with SROC in formation according to the Walking Safety Ellipse with in and out of plane fly around components strategy for the observation. ConOps, and in particular the strategy adopted for the rendezvous, provides more decision points along the trajectory leaving room for corrections if needed without affecting the strategy itself. Moreover, in case a manoeuvre should be missed, SROC never goes behind SR (negative InTrack), thus excluding the collision with SR in the nominal case. Using an

in-plane segment reduces the duration and the cost (in terms of ΔV) of the rendezvous in most scenarios. The duration of the EOP for the baseline mission is set to 5 days to leave margin to the mission design should any changes occur in later development stages, and for accounting uncertainties related to the system design and operations (e.g. time needed for calibration of instruments, need for rehearsal operations).

2.12 DeltaV budgets

All the considerations reported in this section refer to impulsive manoeuvres without considering in the simulations the model of the engine that will be used for the SROC mission. In the next chapters of this thesis all these considerations will be integrated in order to obtain a ΔV budget more and more conforming to reality.

The ΔV budget for the baseline scenario is reported in Figure 8. A 5% margin has been adopted for ΔV calculation where performed by analytical means. Regarding non nominal manoeuvres, such as TCMs (Trajectory Correction Manoeuvres) and CAMs (Collision Avoidance Manoeuvres): the former are already considered in the budget since they have been simulated (although not optimised), while for the latter 2.5 m/s ΔV is considered (plus 100% margin). Instead of a ΔV allocated to reaction wheels desaturation (which would be accomplished by the magnetorquers), an extra system margin is added to represent losses due to thruster inefficiency in 3-DOF manoeuvring. Since 8 canted thrusters are employed to achieve 6-DOF manoeuvring, most impulses can only be achieved by firing combination of nozzles which have a net effect along one direction but also zero-sum thrust in other directions; this parasitic thrust component gets cancelled out among the active nozzles, but nonetheless consumes propellant. A margin of 16% has been assumed, as if on average active nozzles pointed 30 deg away from the actual net thrust direction.

The final value of ΔV for sizing the system is **20 m/s**. A small fuel reserve is taken in case rehearsal manoeuvres are carried out in HP#1. This value of ΔV is conservative even in the worst-case scenario, represented by the Quasi-Equatorial Orbit of SR.

Sun Synchronous Orbit
ConOps #1
5 days of EOP

Manoeuvre	Total [m/s]	Margin	Total with Margin [m/s]
Hold Point 1	0.40	5%	0.42
FRR In-Plane	0.36	5%	0.38
CRR 1	0.33	5%	0.35
WSE Insertion 1	0.44	5%	0.47
CRR 2	0.12	5%	0.13
WSE Insertion 2	0.38	5%	0.40
CRR 3	0.16	5%	0.17
WSE Insertion 3	0.27	5%	0.28
CRR 4	0.12	5%	0.13
WSE Insertion 4	0.39	5%	0.40
CRR 5	0.16	5%	0.16
WSE Insertion 5	0.26	5%	0.28
CRR 6	0.12	5%	0.12
WSE Insertion 6	0.39	5%	0.41
Hold Point 2	0.08	5%	0.08
Fly Around	0.38	5%	0.40
Close Approach	0.24	5%	0.25
Mating	0.06	5%	0.06
Burn inefficiency (16%)	0.74	100%	1.49
CAM	2.50	100%	5.00
DeltaV TOT [m/s]	7.89	DeltaV TOT with Margin [m/s]	11.36

Figure 8: ΔV budget for baseline scenario

2.13 SROC technology^[4]

The implementation of the SROC mission includes the following items:

1. Spacecraft Platform

- 1.1. Command and Data Handling subsystem (CDH)
- 1.2. Attitude Determination & Control, and Navigation Subsystem (ADCNS)
- 1.3. Propulsion subsystem (PROP)
- 1.4. Proximity Relative Navigation Subsystem (PRNS)
- 1.5. Space-to-Ground communication subsystem
- 1.6. Space-to-Space communication subsystem (if applicable)
- 1.7. Docking subsystem (if applicable)
- 1.8. Electrical Power Subsystem (EPS)
- 1.9. Thermal Control Subsystem (TCS)
- 1.10. Mechanical/Structure

2. Spacecraft Payload

- 2.1. Primary Hyperspectral payload
- 2.2. Secondary payload(s), if applicable

3. Deployment & Retrieval Mechanism (DARM) onboard Space Rider

- 3.1. Deployer main structure
- 3.2. Electrical and Mechanical interfaces with Space Rider
- 3.3. Deployment/Docking/Retrieval mechanisms (if applicable)
- 3.4. CDH (Command and Data Handling) subsystem (if applicable)
- 3.5. Space-to-Ground communication subsystem (if applicable)
- 3.6. Space-to-Space communication subsystem (if applicable)

2.13.1 Propulsion

In this thesis we will mainly deal with the propulsion system, so in this section we report only a figure with the requirements that the propulsion system must comply with and we do not deal in detail with the other SROC systems.

	Tyvak proposed Prox-Ops Cold Gas 12U config	Tyvak proposed Prox-Ops Cold Gas 6U config
Safety	2+ Fault Tolerance Cold Gas (R134a) No hot exhaust No plasma	2+ Fault Tolerance Cold Gas (R134a) No hot exhaust No plasma
Max Thrust	35 mN	35 mN
Minimum Impulse Bit	< 5 mNs	< 5 mNs
Total Impulse	960 Ns	480 Ns
Delta-V	40 m/s	40 m/s
Thrust Vectoring / Degrees of Freedom	6 DOF (3+3) Full 3-axis thrust vectoring Full 3-axis attitude control	6 DOF (3+3) Full 3-axis thrust vectoring Full 3-axis attitude control
Envelope	< 210 x 200 x 150 (6.0 U)	< 210 x 95 x 150 (3.0 U)
Performance Density	160 Ns/U	160 Ns/U
Mass	< 8 kg wet	< 4 kg wet
Power	< 2 W keep-alive 15 W peak power	< 2 W keep-alive 15 W peak power

Figure 9: Proposed thruster module specifications

3 Propulsion system overview

In this chapter we will deal with identifying drivers on the basis of which to evaluate the best technology for the propulsion system of the SROC mission and in the end make a trade-off between all the technologies considered.

3.1 Interactions between the propulsion system and other SROC's subsystems

Before starting the analysis on the best propulsion technology for the mission in question, we carried out an analysis of all the interactions between the propulsion system and all the other subsystems of the SROC spacecraft. This analysis was fundamental to identify all the drivers on the basis of which to evaluate the best propulsion system for our mission.

The implementation of the SROC mission includes the following subsystems:

- Command and Data Handling subsystem (CDH)
- Attitude Determination & Control, and Navigation Subsystem (ADCNS)
- Propulsion subsystem (PROP)
- Proximity Relative Navigation Subsystem (PRNS)
- Space-to-Ground communication subsystem
- Space-to-Space communication subsystem
- Docking subsystem
- Electrical Power Subsystem (EPS)
- Thermal Control Subsystem (TCS)
- Mechanical/Structure
- Spacecraft Payload

The propulsion system interacts with all except the Space-to-Ground communication subsystem and the Space-to-Space communication subsystem.

The figure shows a diagram that summarizes all the interactions between the propulsion system and other subsystems which we will discuss in detail later.

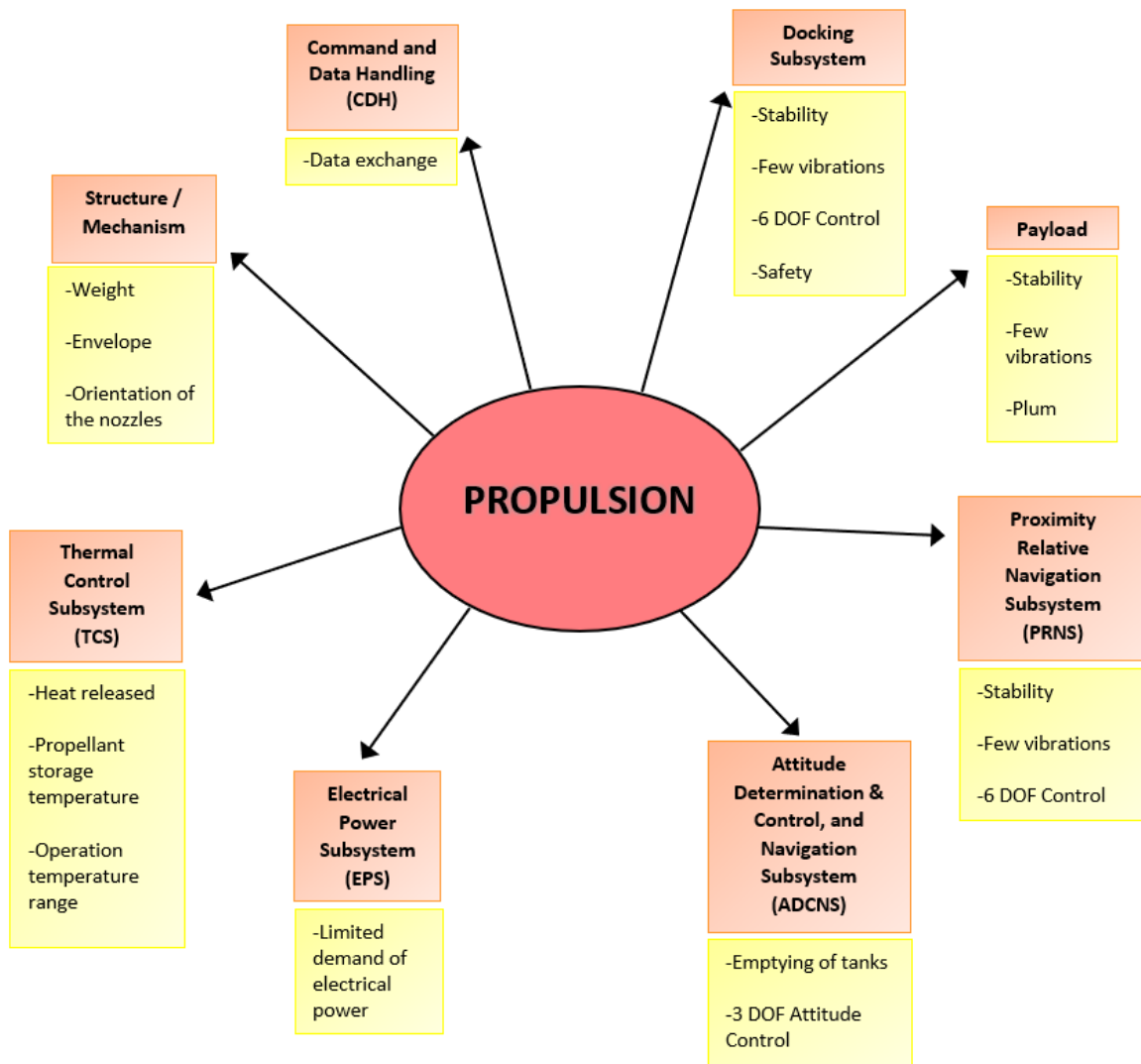


Figure 10: Interactions between the propulsion system and all the other on-board subsystems

3.1.1 Interaction between the propulsion system and ADCNS

The interaction between the propulsion system and the ADCNS consists in the way in which the tanks are emptied, as this can lead to an imbalance of the spacecraft which requires an intervention by the ADCNS to restore the desired attitude. Therefore it would be preferable to have an emptying of the tanks as symmetrical as possible so as not to create too many problems of loss of right attitude and therefore not to overload the ADCNS. Obviously, for the type of manoeuvre that we have to carry out during this mission we must have an engine that allows the control of the attitude and the thrust vector on all three axes (6 DOF).

3.1.2 Interaction between the propulsion system and PRNS

The interaction between the propulsion system and the PRNS consists in guaranteeing stability, few vibrations and a 6 DOF control in terms of thrust and attitude in order to correctly perform all the required operations.

3.1.3 Interaction between the propulsion system and the payload

The interaction between the propulsion system and the payload consists first of all in guaranteeing stability and few vibrations so as not to have photos moved by the hyperspectral camera. In addition to this there is the discourse related to the plums and therefore it is necessary to ensure that the exhaust material of the engine does not dirty the lens of the hyperspectral chamber.

3.1.4 Interactions between the propulsion system and docking subsystem

The interactions between the propulsion system and the docking subsystem are practically the same as those between the propulsion system and PRNS and that is to guarantee stability, few vibrations and 6 DOF control. In addition to what has already been said above, given that thanks to this subsystem one makes contact with another spacecraft, Space Rider, the safety aspect becomes fundamental and the propulsion system must guarantee high levels of safety and reliability.

3.1.5 Interactions between the propulsion system and CDH

The interactions between the propulsion system and the CDH that occur are solely linked to the exchange of data. These are mainly housekeeping data and data containing information on the state of health and correct functioning of the propulsion system.

3.1.6 Interactions between propulsion system and structure / mechanism

The interactions between propulsion system and structure / mechanism are fundamentally based on the weight and envelope of the propulsion system and on the orientation of the nozzles.

3.1.7 Interactions between the propulsion system and TCS

The interactions between the propulsion system and TCS are based on the amount of heat released by the engine during its operation that must be disposed of by the TCS, on the storage temperature of the propellant (in the case of monopropellant or hybrid engines) and on the operation temperature range within the propulsion system must be maintained to function properly. An important thing to

note is that if the engine releases less heat or the propellant storage temperature is included in a wider range or the operation temperature range is wider, less power is required from the EPS with consequent advantages.

3.1.8 Interaction between the propulsion system and the EPS

The only interaction between the propulsion system and the EPS is the limited demand for electrical power which must be less than a certain value.

3.2 Drivers

Once all the interactions between the propulsion system and all the other subsystems have been established, we can define all the drivers on the basis of which we choose the most suitable and most performing propulsion technology for the SROC mission.

The drivers we have identified are:

1. **Powertrain performance:**
 - 1.1. Max Thrust
 - 1.2. Minimum Impulse Bit (necessarily <5 mNs)
 - 1.3. Specific Impulse
 - 1.4. Total Impulse
 - 1.5. Delta-V (necessarily ≥ 40 m/s)
 - 1.6. Performance Density
2. **Environmental impact**
3. **Thrust Vectoring/Degrees of freedom** (necessarily 6 DOF)
4. **Safety**
5. **Envelope** (necessarily < 4 o 5 U)
6. **Mass** (necessarily <10 kg)
7. **TRL** (necessarily ≥ 5)
8. **System Complexity**
9. **Design changes**
10. **Interactions with other subsystems**
 - 10.1. Power consumption limitations (<2 W nominal, <15 W peak)
 - 10.2. Propellant storage temperature

10.3. Operation temperature range

10.4. Few Vibration

10.5. Stability

10.6. Homogeneous emptying of the tanks

Obviously these drivers do not all have the same importance in choosing the best technology for the propulsion system of the mission in question, in fact some of which have stringent conditions that must necessarily be respected (as indicated in the brackets next to each of them) and others have an importance that is not fundamental for the success of the mission but still serve to evaluate the best solution to choose. Among those that have a very significant importance there are certainly the Delta-V which must be able to guarantee the propulsion system and which must be higher than 40 m/s as calculated in the mission analysis phase; the MIB that is a measure of the smallest control torque that can be commanded to the satellite using the thruster and that for the type of manoeuvres that the spacecraft will have to perform must be limited below a certain value (<5 mNs); thrust vectoring / degrees of freedom gives the information relating to the control authority that you can have of the spacecraft and given the type of proximity relative navigation and rendezvous and docking operations, the propulsion system must guarantee a 6 DOF control to carry out the mission; safety is fundamental in this mission as the spacecraft makes contact and re-enters Space Rider; envelope and mass which must be limited as it is a 12 U spacecraft; the TRL must be greater than or equal to 5 as the launch and therefore the start of the missions are expected within a very short period and therefore ready-made technology must be adopted; the consumption of electrical power must be limited because for CubeSat we cannot have oversized EPS. The drivers we have just talked about are those that impose very specific conditions on the choice of the propulsion system and to respect these conditions you can choose a technology that offers better characteristics relative to other drivers. For example, by choosing a propellant that has a wider storage temperature range, it is possible to reduce the consumption of electrical power and therefore perhaps have a motor that consumes a higher electrical power to re-ignite because it guarantees better performance but this aspect is compensated for with a lower request for electrical power from the TCS which has to work less to keep the propulsion system in the operation temperature range. The same can be said about the emptying of the tanks which must be done in such a way as not to cause imbalances not manageable by the ADCNS and therefore an oversizing of this subsystem with the relative disadvantages. Basically, some of the drivers identified help us to evaluate the effects that the choice of a certain technology brings on the other subsystems and choosing a propulsion system that has excellent characteristics in this field brings great advantages in the design of the other subsystems, so it is very important to have this phase is a system vision of design. Other drivers of great importance are the system complexity which strongly influences the cost of the propulsion system and the difficulties in managing and assembling it and above all the design changes which give information on the level of intervention that must be done on the original design of the propulsion system. from the manufacturer to better adapt it to our needs.

3.3 Technologies^[19]

There is currently a wide range of technologies for propulsion systems, however the miniaturization of these systems for small spacecraft has been particularly challenging. Excluding some types of technologies that do not allow us to carry out our mission as demonstrated in a previous analysis made (electric thrusters and warm gas thrusters), specifically in this phase we have concentrated on the study of three types of technologies in particular: liquid monopropellant, hybrid engine and cold gas. We took these technologies into analysis despite the fact that after an initial analysis it was concluded that the best technology for the propulsion system of the SROC mission was a cold gas because in recent years there has been a lot of concentration on adapting this type of technology to CubeSat and nanosat with great results. So we thought of doing a study of the current state of the art and analysing the propulsion systems that have already flown or are ready to do so and that could also be used for our mission by making a comparison with cold gas technology.

3.3.1 Cold Gas

Cold gas systems are relatively simple systems that provide limited spacecraft propulsion and are one of the most mature technologies for small spacecraft. Thrust is produced by the expulsion of an inert, non-toxic propellant which can be stored in high pressure gas or saturated liquid forms. Cold gases are suitable for small buses due to their very low grade of complexity and are inexpensive and robust. They can be used when a small total impulse is required. Primary advantages include a small impulse bit for attitude control applications and the association of small volume and low weight. Recently, new designs have improved the capability of these systems for nanosatellite buses such as 3U CubeSats. Despite this, a completely adequate cold gas engine on the market was not found for our mission.

Figure 11 shows the current state-of-the-art for cold propulsion systems for small spacecraft.

Product	Manufacturer	Thrust	Specific Impulse (s)	Propellant	TRL Status
MicroThruster	Marotta	0.05 – 2.36 N	65	Nitrogen	9
Butane Propulsion System	SSTL	0.5 N	80	Butane	9
Nanoprop 3U	GomSpace/NanoSpace	0.01 – 1 mN	*60 – 110	Butane	9
Nanoprop 6U	GomSpace/NanoSpace	4 – 40 mN	*60 – 110	Butane	9
MiPS Cold Gas	VACCO	53 mN	40	Butane	7
MarCO-A and -B MiPS	VACCO	25 mN	40	R236FA	9
CPOD	VACCO	10 mN	40	R236FA	7
POPSAT-HIP1	Micro Space	0.083 – 1.1 mN	32 – 43	Argon	8
CNAPS	UTIAS/SFL	12.5 – 40 mN	40	Sulfur Hexafluoride	9
CPOD	VACCO	25 mN	40	R134A/R236FA	6

Figure 11: Cold Gas state of the art

A cold gas thruster developed by Marotta flew on the NASA ST5 mission (launch mass 55 kg) for fine attitude adjustment manoeuvres. It incorporates electronic drivers that can operate the thruster at a power of less than 1 W. It has less than 5 ms of response time and it uses gaseous nitrogen as propellant. Surrey Satellite Technology Ltd. (SSTL) has included a butane propulsion system in several small spacecraft missions for a wide range of applications in Low Earth Orbit (LEO) and Medium Earth Orbit (MEO). In this system, propellant tanks are combined with a resistojet thruster and operation is controlled by a series of solenoid valves. It uses electrical power to heat the thruster and improve the specific impulse performance with respect to the cold gas mode. It has been in design for more than five years and uses a RS-422 electrical interface. In June 2014, Space Flight Laboratory at University of Toronto Institute for Aerospace Research (UTIAS) launched two 15 kg small spacecraft to demonstrate formation flying. The Canadian Nanosatellite Advanced Propulsion System (CNAPS) consisted of four thrusters fuelled with liquid sulphur hexafluoride. This non-toxic propellant was selected since it has high vapor pressure and density which is important for making a self-pressurizing system. This propulsion module is a novel version of the previous NanoPS that flew in the CanX2 mission in 2008. Another flight-demonstrated propulsion system was flown in the POPSAT-HIP1 CubeSat mission (launched June 2014), which was developed by Microspace Rapid Pte Ltd in Singapore. It consisted of a total of eight micro-nozzles that provided control for three rotation axes with a single-axis thrust for

translational applications. The total Delta-V has been estimated from laboratory data to be between 2.25 and 3.05 ms^{-1} . Each thruster has 1 mN of nominal thrust by using argon propellant. An electromagnetic microvalve with a very short opening time of 1 m-s operates each thruster.

A complete cold gas propulsion system has been developed for CubeSats with a Microelectromechanical system (MEMS) that provides accurate thrust control with four butane propellant thrusters. While thrust is controlled in a closed loop system with magnitude readings, each thruster can provide a thrust magnitude from zero to full capacity (1 mN) with 5 μN resolution. The dry mass of the system is 0.220 kg and average power consumption is 2 W during operation. This system is based on flight-proven technology flown on larger spacecraft (PRISMA mission, launched in 2010). The MEMS cold gas system was included on the bus of the TW-1 CubeSat, launched in September 2015.

The CubeSat Proximity Operations Demonstration (CPOD) is a mission led by Tyvak Nano-Satellite Systems. It incorporates a cold gas propulsion system built by VACCO Industries that provides up to 186 N-s of total impulse. This module operates at a steady state power of 5 W and delivers 40 s of specific impulse while the nominal thrust is 10 mN (VACCO Industries 2015). It uses self-pressurizing refrigerant R236fa propellant to fire a total of eight thrusters distributed in pairs at the four corners of the module. It has gone through extensive testing at the US Air Force Research Lab. Endurance tests consisted of more than 70,000 firings.

Cold gas thrusters benefit from their simplicity; however, they do fall short in other respects. The following list summarizes the advantages and disadvantages of a cold gas system.

Advantages:

- A lack of combustion in the nozzle of a cold gas thruster allows its usage in situations where regular liquid rocket engines would be too hot. This eliminates the need to engineer heat management systems.
- The simple design allows the thrusters to be smaller than regular rocket engines, which makes them a suitable choice for missions with limited volume and weight requirements.
- The cold gas system and its fuel are inexpensive compared to regular rocket engines.
- The simple design is less prone to failures than a traditional rocket engine.
- The fuels used in a cold gas system are safe to handle both before and after firing the engine. If inert fuel is used the cold gas system is one of the safest possible rocket engines.
- Cold gas thrusters do not build up a net charge on the spacecraft during operation.
- Cold gas thrusters require very little electrical energy to operate, which is useful, for example, when a spacecraft is in the shadow of the planet it is orbiting.

Disadvantages:

- A cold gas system cannot produce the high thrust that combustive rocket engines can achieve.
- Cold gas thrusters are less mass efficient than traditional rocket engines.
- The maximum thrust of a cold gas thruster is dependent upon the pressure in the storage tank. As fuel is used up, the pressure decreases and maximum thrust decreases^[5].

3.3.2 Liquid monopropellant propulsion systems

Chemical propulsion systems are designed to satisfy high thrust impulsive manoeuvres. They are associated with lower specific impulse compared to their electric counterparts, but have significantly higher thrust to power ratios^[5].

3.3.2.1 Hydrazine Propellant

There are a significant number of mature hydrazine propulsion systems used in large spacecraft that present a generally reliable option as mass and volume of these compact systems allow them to be a suitable fit for some small spacecraft buses. Thrusters that perform small corrective manoeuvres and attitude control in large spacecraft may be large enough to perform high thrust manoeuvres for small spacecraft and can act as the main propulsion system. Hydrazine propulsion systems typically incorporate a double stage flow control valve that regulates the propellant supply and a catalyst bed heater with thermal insulation. Typically, they have the advantage of being qualified for multiple cold starts which may be beneficial for power-limited buses if the lifespan of the mission is short. Hydrazine specific impulses are achievable in the 150-250 s range. Because hydrazine systems are so widely used for large satellites, a robust ecosystem of components exist, and hydrazine propulsion systems are custom-designed for specific applications using available components.

Airbus Defense and Space has developed a 1-N class hydrazine thruster that has extensive flight heritage, including use on the small spacecraft, ALSAT-2. Aerojet Rocketdyne has leveraged existing designs with flight heritage from large spacecraft that may be applicable to small buses, such as the MR-103 thruster used on New Horizons for attitude control application. Other Aerojet Rocketdyne thrusters potentially applicable to small spacecraft include the MR-111 and the MR-106.

The CubeSat High-Impulse Adaptable Modular Propulsion System (CHAMPS) project leverages the miniaturization effort performed for previous small hydrazine thrusters to develop CubeSat monopropellant propulsion systems. These modules satisfy a wide range of manoeuvres from station-keeping and orbit transfers to momentum management. There are various configurations, such as the MPS-120, that support up to four 1-N hydrazine thrusters configured to provide pitch, yaw, and roll control as well as single-axis thrusting vectors. The MPS-120 was selected and funded by NASA to go through extensive testing. The 3D printed titanium isolation and tank systems were demonstrated in mid-2014 and one engine performed a hot fire test in late 2014. Currently, this system has some final development tasks remaining and depending on the level of qualification required, a first system could be delivered in the next year. The TRL is assessed at 5.

Additional versions of the MPS series are under development that use various thruster technologies such as cold gas (MPS-110), non-toxic AF-M315E propellant (MPS-130) or electric propulsion devices (MPS-160). Aerojet Rocketdyne is also developing integrated modular propulsion systems for larger small spacecraft. The MPS-220 consists of two 22-N primary engines and eight 1-N auxiliary hydrazine thrusters.

Moog ISP has extensive experience in the design and testing of propulsion systems and components for large spacecraft. These may also apply for smaller platforms as some of their flight-proven thrusters are light-weight and have moderate power requirements. The MONARC-5 thrusters flew on NASA JPL's Soil Moisture Active Passive (SMAP) spacecraft in 2015 and provided 4.5 N of steady state thrust. Other

thrusters potentially applicable to small spacecraft buses include the MONARC-1 and the MONARC-22 series. While all of these MONARC thrusters have extensive flight heritage on larger spacecraft, there is no evidence they have flown on a small spacecraft, making the TRL for small spacecraft application^[5].

3.3.2.2 Alternative green Propellants

The first analysis we did was that focused on liquid monopropellant propulsion systems by studying various products of various companies analysing their characteristics to understand if they could be possible candidates for our mission. The first thing that emerged from this first analysis was the convenience in many aspects of green propellants compared to classic propellants such as hydrazine. Alternative, 'green fuel' propellants have a reduced toxicity due to the lower danger of component chemicals and significantly reduced vapor pressure as compared to hydrazine. The 'green' affiliation results in the propellant being less flammable which in turn requires fewer safety requirements for handling, and potentially removes Self-Contained Atmospheric Protective Ensemble (SCAPE) suit requirements. This reduces operational oversight by safety and emergency personnel.

Range Safety AFSPCMAN91-710 requirements state that if a propellant is less prone to external leakage, which is seen with the alternative "green" systems due to higher viscosity of the propellant, the hazardous classification is reduced. External hydrazine leakage is considered "catastrophic," whereas using alternative "green" propellants reduces the hazard severity classification to "critical" and possibly "marginal" per MIL-STD-882E (Standard Practice for System Safety) . A classification of "critical" or less only requires two-seals to inhibit external leakage, meaning no additional latch valves other isolation devices are required in the feed system. While these propellants are not safe for consumption, they have been shown to be less toxic compared to hydrazine. This is primarily due to alternative propellants being less flammable; nontoxic gasses (such as water vapor, hydrogen and carbon dioxide) are released when combusted.

Fuelling spacecraft with green fuels, a parallel operation, may require a smaller exclusionary zone, allowing for accelerated launch readiness operations. These alternative propellants are generally less likely to exothermically decompose at room temperature due to higher ignition thresholds. Therefore they require fewer inhibit requirements, fewer valve seats for power, less stringent temperature requirements, and lower power requirements for system heaters.

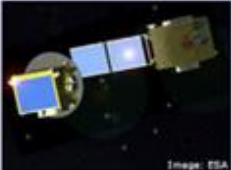
Alternative propellants also provide higher performance than the current state-of-the-art fuel and have higher density-specific impulse achieving improved mass fractions. As a majority of these non-toxic propellants are in development, systems using these propellants present technical challenges including increased power consumption and a smaller selection of materials due to higher combustion temperatures. The primary ionic liquid propellants with flight heritage or upcoming spaceflight plans are Ammonium DiNitramide (ADN)-based LMP-103S and AF-M215E, and AF-M315E, a Hydroxyl Ammonium Nitrate (HAN)-based monopropellant. Everything is summarized in the following figures^[5].

Product	AND or HAN based Propellant	Manufacturer	Thrust (N)	Specific Impulse (s)	TRL Status
GR-1	HAN	Aerojet Rocketdyne	0.26 – 1.42	231	6
GR-22	HAN	Aerojet Rocketdyne	5.7 – 26.9	248	5
1 N HPGP	ADN	Bradford Engineering	0.25 – 1.00	204 – 235	9
HYDROS-C	Other	Tethers Unlimited, Inc.	1.2	310	6
AMAC	Other	Busek	0.425	225	5
Lunar Flashlight MiPS	ADN	VACCO	0.4	190	6
Integrated Propulsion System	ADN	VACCO	4.0	220	6
ArgoMoon Hybrid MiPS	ADN	VACCO	0.1	190	6
BGT-X5	HAN	Busek	0.5	220	5
EPSS C1K	ADN	NanoAvionics	0.3	252	7
Green Hybrid	Other	Utah State	8	215	6

Figure 12: Green Propulsion Systems

As is well illustrated in the next figures, green propellants have numerous advantages and among the main ones, in addition to having a much lower environmental impact, are that of improving the performance of the propulsion system having a longer mission life with smaller tanks or a simplification in the field of handling and transport, we also have a reduction in mission costs, a reduction in physical risks to other satellites, therefore an improvement in relation to safety.

Why Green Propulsion?



Higher performance than monopropellant Hydrazine
↓
Extended mission or reduced tank volume



Much less toxic than Hydrazine
↓
Reduced fueling cost

- **IMPROVED PERFORMANCE**
 - Storable liquid monopropellant
 - Higher Specific Impulse and Density Impulse

+

- **INCREASED SAFETY**
 - Low Sensitivity
 - Low Toxicity
 - Non-Carcinogenic
 - Environmentally Benign

=

- **LOWER MISSION COSTS**
 - Simplified handling and transportation
 - Reduced cost for fueling operations
 - Compatible with available COTS hardware



Comparison Parameter	Hydrazine	HPGP (LMP-103S)
Specific Impulse	Reference	≥ 6% higher than hydrazine
Density	Reference	24% higher than hydrazine
Stability	Unstable (reactivity)	Stable > 20 yrs (STANAG 4582)
Toxicity	Highly Toxic	Low Toxicity (due to methanol)
Carcinogenic	Yes	No
Corrosive	Yes	No
Flammable Vapors	Yes	No
Environmental Hazard	Yes	No
Sensitive to Air & Humidity	Yes	No
SCAPE Required for Handling	Yes	No
Storable	Yes	Yes (> 6.5 yrs, end-to-end test is ongoing)
Freezing Point	1°C	-90°C (-7°C saturation)
Boiling Point	114°C	120°C
Qualified Operating Temp Range	10°C to 50°C	10°C to 50°C (allows use of COTS hydrazine components)
Operating Temp Range Capability	10°C to 50°C	-5°C to 60°C
Typical Blow-Down Ratio	4:1	4:1
Exhaust Gases	Ammonia, nitrogen, hydrogen	H ₂ O (50%), N ₂ (23%), H ₂ (16%), CO (6%), CO ₂ (5%)
Radiation Tolerance	Reference	Insensitive up to 100 kRad (Cobalt 60)
Shipping	Class 8 / UN2029 (Forbidden on commercial aircraft)	UN / DOT 1.4S (Permitted on commercial passenger aircraft)

Benefits to Satellite Missions:

1) Increased Performance

≥ 30% higher performance allows:

- **Longer mission lifetime** (with same tank), or
- **Smaller tank** (for same ΔV)
 - Waterfall mass reductions
 - Better utilization of limited volume & mass
- **Efficient orbit raising and/or de-orbit**

2) Simplified Handling & Transportation

Reduced propellant toxicity allows:

- **Handling in facilities not rated for hydrazine**
 - Launch sites
 - Universities and SMEs
- **Air transport** (*commercial/passenger aircraft*)
 - Shipment to launch site with s/c & GSE
- **Fueling without SCAPE suits**
- **Increased responsiveness**
 - Shorter launch campaigns
 - Shipment of pre-fueled satellites

3) Reduced Mission Costs

Significant life-cycle cost reductions, due to:

- **All of the blue highlighted items on this slide**

4) Fewer Co-Manifest Challenges

Non-Hazardous fueling operations allow:

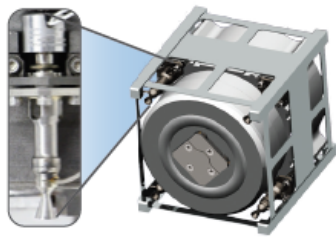
- **Reduced physical risk to other satellites**
- **Parallel processing at launch site**
 - Reduced launch schedule risk
- **More launch opportunities**

Figures 13: Advantages of Green propulsion^[6]

As part of this technology we have studied various propulsion systems. The first were the **MPS-120** and **MPS-130** both produced by the Aerojet Rocketdyne. MPS-120 uses hydrazine as a propellant and the only one studied that uses this propellant for the reasons seen above and which have also been confirmed in the comparison made between this and the other propulsion systems, while the MPS-130 uses as propellant the 'AF-M315E. Both offer performances in line with those required by the mission (obviously those of the MPS-130 are better), have a TRL of 6, are produced in an innovative way through the 3D printing of some fundamental components such as the main piston and both are proposed in two versions, a 1U and a 2U with related variations in terms of characteristics, but the main problem is that they mount only 4 thrusters configured to provide pitch, yaw, and roll control as well as single-axis thrusting vectors and therefore do not guarantee a 6 DOF control of the spacecraft and we have to see how much it would cost in terms of system complexity and changes to apply adding a sufficient number of thrusters to obtain a 6 DOF control authority.

1U Configuration Pictured

Thruster Specifications (1U and 2U)



Throughput Capability (each):	>3.0 kg
Pulses:	10,000
Total Impulse Capability (each):	>6000 N-s
MIB:	0.0004 N-s
Thrust:	.25 - 1.25 N
Isp:	206 - 217 sec

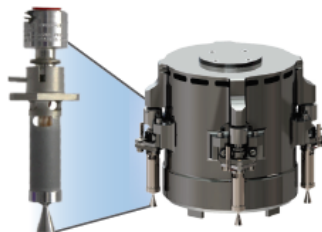
System Specifications

Parameter	Value (1U)	Value (2U)
Propellant	Hydrazine	
Operation Pressure	150-85 psi	
Dry Mass	1.06 kg	1.36 kg
Wet Mass	1.48 kg	2.38 kg
Usable Propellant	0.38 kg	0.98 kg
Total System Impulse	775 N-s	2,000 N-s
Dimensions	10x10x10 cm	10x10x10 cm
Operation Temp Range	5-60 C	
Valve Power Per Valve	0.25 W	
Valve Voltage	6-8 Vdc	
Number of Thrusters	4	
System (tank) Heater Power (avg) **	10 W	
MRL/TRL	6/8	

Figure 14: MPS-120^[7]

1U Configuration Pictured

Thruster Specifications (1U and 2U)



Throughput Capability (each):	3.0 kg
Pulses:	10,000
Total Impulse Capability (each):	6,000 N-s
MIB:	0.0004 N-s
Thrust:	.25 - 1.25 N
Isp:	206 - 235 sec

System Specifications

Parameter	Value (1U)	Value (2U)
Propellant	AF-M315E	
Operation Pressure	150-85 psi	
Dry Mass	1.06 kg	1.36 kg
Wet Mass	1.66 kg	2.76 kg
Usable Propellant	0.50 kg	1.40 kg
Total System Impulse	1,200 N-s	3,360 N-s
Dimensions	10x10x10 cm	10x10x20 cm
Operation Temp Range	5-60 C	
Valve Power Per Valve	0.25 W	
Valve Voltage	6-8 Vdc	
Cat Bed Heater Power Per Thruster	7 W	
Cat Bed Heater Voltage	12 Vdc	
Number of Thrusters	4	
System (tank) Heater Power (avg) **	10 W	
MRL/TRL	6/6	

Figure 15: MSP-130^[8]

Two other propulsion systems studied are the **BGT-X5** and the **BGT-1X** both produced by Busek. The former has better performance than the latter and both are green monopropellant thruster. Among those studied are those that have the least adaptable characteristics to our mission, above all due to the excessive power consumption and the fact that they have a single thruster mounted in a configuration that is difficult to modify.

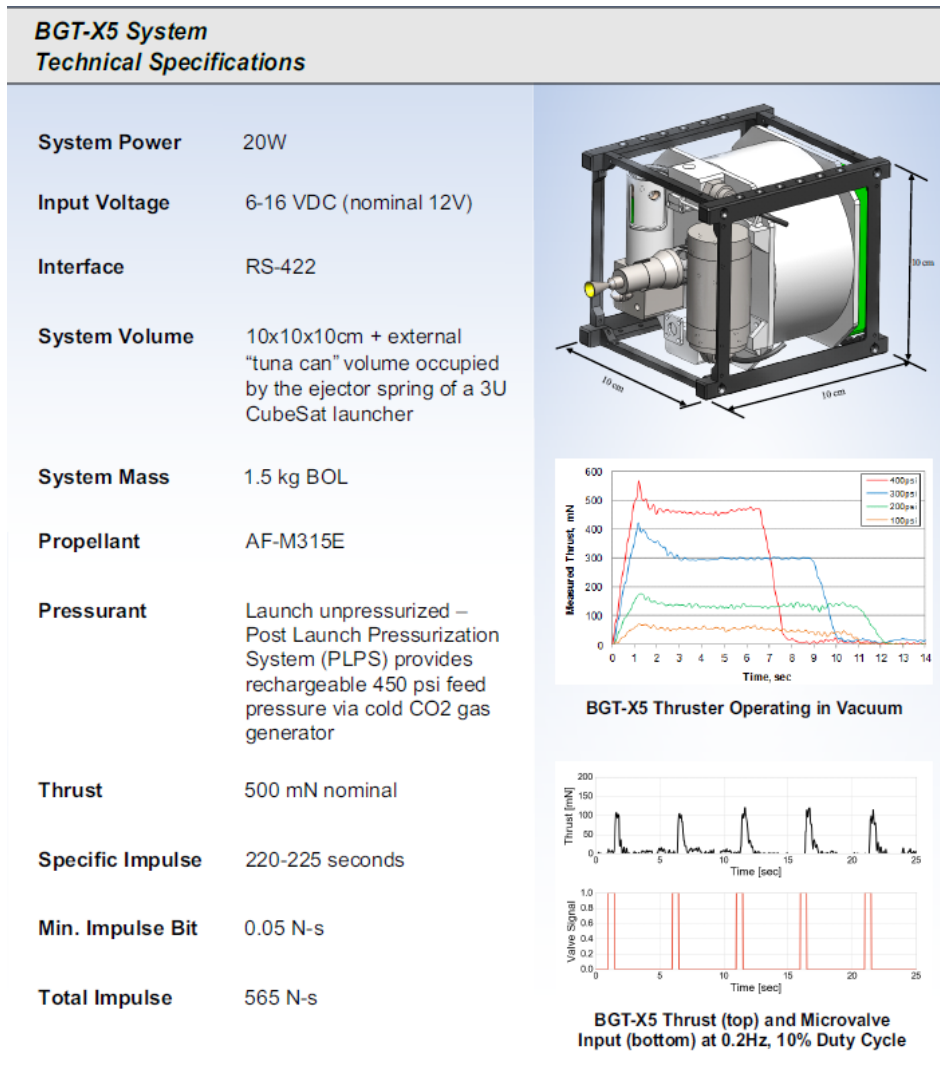


Figure 16: BGT-X5^[9]

A propulsion system that instead has interesting features is the **ADN Micro Propulsion System**. The VACCO / ECAPS CubeSat ADN Delta-V propulsion system is a high performance micro propulsion system (MiPS) specifically designed for CubeSats. The ADN Delta-V MiPS is a self-contained subsystem that can be scaled from 0.5U to >1U. Four high-thrust, high specific impulse (Isp) and thrusters deliver 1,828 N-Sec of total impulse using only integral propellant. The smart feed system can independently throttle each thruster to provide thrust vector control during Delta-V burns. Reliability is ensured through simplicity of design, welded titanium construction and frictionless valve technology. The performance of the propulsion system and the most important characteristics are all adequate for the

purposes of the mission, but thrusters canted for thrust vector control and not for attitude control so also in this case we cannot have a 6 DOF control authority and consequently they are necessary design changes with the addition of thrusters and it is necessary to understand from the manufacturer if it is possible to introduce these changes and at what cost in terms of system complexity.



Max Operating Pressure	244 psia	Vibration	23 Grms
Proof Pressure	366 psia	Cycle Life	900,000 firings
Burst Pressure	610 psia	Total Impulse	1,808 N-Sec
Total Thrust.....	400 mN	Minimum Impulse Bit.....	2 mN-Sec
Internal Leakage	3.0 scc/hr	Operating Voltage	9 to 12.6 vdc
External Leakage	1.0 x 10 ⁻⁶ scch	Dry Mass	909 grams
Operating Temperature.....	0°C to +50°C	Propellant Mass	720 grams
Non-Operating Temperature.....	-10°C to +60°C	Total Mass	1,800 grams

Figure 17: ADN Micro Propulsion System^[10]

Another propulsion system analysed with particular interest as used for a mission similar to SROC, the PRISMA mission, is **High Performance Green Propulsion (HPGP)**. This engine uses a green propellant the LMP-103S and offers very important performances especially in terms of low weight. In the basic version it has only two thrusters, but already in the PRISMA mission to these two thrusters are added another six hydrazine-powered, so this thing demonstrates a great versatility that allows you to reach a 6 DOF spacecraft control through a few configuration changes. This propulsion system represents a truly suitable candidate for our mission that combines all the advantages of a green propellant we have already discussed with great performances and full compliance with basic requirements that can be achieved through simple changes of design or configuration.

1 N HPGP Rocket Engine Characteristics	
Propellant	LMP-103S
Inlet Pressure Range	5.5 - 22 bar
Thrust Range	0.27 - 1 N
Isp <i>vacuum</i>	2010 – 2300 Ns/kg (205 - 235 sec)
Density Impulse	2850 Ns/L
Minimum Impulse Bit	0.01 – 0.05 Ns
Overall Length	176 mm
Mass	0.34 kg
Demonstrated Life	
Total Impulse	50 kNs
Pulses	60 000
Propellant Throughput	25 kg
Accumulated Firing Time	24 hours
Longest Continuous Firing	1.5 hours
Status	
Ready for flight on PRISMA 2009 TRL 7	



1 N HPGP Thruster (FM)

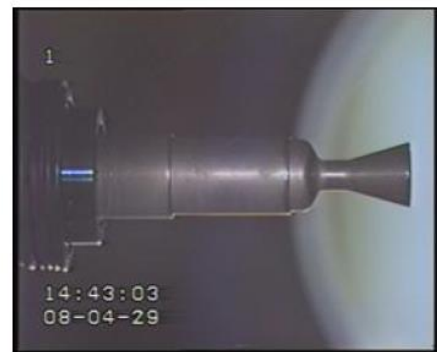


Figure 18: ECAPS HPGP thruster^[11]

Another system that introduces a truly innovative technology being considered is HYDROS. The **HYDROS** thruster is a modular and scalable system. HYDROS-C is sized for CubeSat spacecraft and it is a water electrolysis propulsion system which fits into a 1U volume and uses water as propellant. On-orbit, water is electrolyzed into oxygen and hydrogen and these propellants are combusted as in a traditional bi-propellant thruster. This thruster provides an average thrust of 1.2-N with 310 s Isp. The current TRL for this unit is 6 as it has not yet flown. This propulsion system, in addition to offering a truly innovative technology, also has very interesting performances and general characteristics suitable for our mission, the only thing is that in the first version it was produced with a single thruster and therefore with only the control of uniaxial thrust and being the very compact configuration we consider difficult a modification that allows an increase in thrusters for a 6 DOF control.



SPECIFIC IMPULSE ->310s	SIZE Ø 381 x 191 mm	TOTAL IMPULSE DELIVERED ->18,000
ORBIT-AVERAGED THRUST 6.8 mN	POWER 7.40 W	WATER CAPACITY 6.0 kg
THRUST EFFECIENCY 0.16 mN/W	COMMAND INTERFACE RS-422, Ethernet	DRY MASS 7.7 kg
IMPULSE PER THRUST EVENT ->1.75 Ns	QUALIFICATION LEVEL TRL 6+	WET MASS 13.7 kg
TOTAL # THRUST EVENTS 10,300	THRUST ->1.2 N	TIME TO REFILL GAS PLENUMS 269s
	LIFETIME 3 years LEO	MOUNTING Deck or Rail Mount Options

Figure 19: HYDROS-M^[12]



SPECIFIC IMPULSE ->310s	SIZE 190x130x92 mm	TOTAL IMPULSE DELIVERED ->2,151
ORBIT-AVERAGED THRUST 2.2 mN	POWER 5.25W	WATER CAPACITY 0.5 kg
THRUST EFFECIENCY 0.13 MN/W	COMMAND INTERFACE RS-422, Ethernet	DRY MASS 2.2 kg
IMPULSE PER THRUST EVENT ->1.75 Ns	QUALIFICATION LEVEL TRL 6+	WET MASS 2.7 kg
TOTAL # THRUST EVENTS 761 Msps	THRUST ->1.2 N	TIME TO REFILL GAS PLENUMS 825 s
	LIFETIME 3 years LEO	MOUNTING Deck or Rail Mount Options

Figure 20: HYDROS-C^[13]

The last studied green monopropellant propulsion system is the **Vacco's Green Propulsion System**. VACCO's Green mono-propellant Micro Propulsion System (MiPS) provides a highly reliable solution for a fully self-contained CubeSat attitude control and main propulsion system. The VACCO Green MiPS is approximately 3U in volume and uses four 100 mN thrusters to develop 3,320 N-sec of total impulse that provides 237 m/s of Delta-V for a 14 kg CubeSat. Each thruster independently operates to perform both Delta-V and ACS manoeuvres controlled by an integrated microprocessor controller^[14]. Easily configured for different mono-propellants: ADN green (LMP-103S/LT) and Air Force green (AF-M315E). This system offers really excellent performances and introduces a technology that seems to be very suitable for our mission and that is through the use of an integrated microprocessor controller it is possible to have both the thrust vector control and the attitude with the use of only 4 thrusters. We need to investigate this aspect and if a 6 DOF control is effectively guaranteed this could be a propulsion system ready to be used for the SROC mission.



Operating Parameters

Propellant MDP.....	5.17 Bar (75 psia)	Total Impulse @10°C.....	3,320 N-s
Propellant Proof Pressure.....	7.76 Bar (150 psia)	Dry Mass.....	3.0 kg Max
Propellant Burst Pressure.....	2.18 Bar (300 psia)	Wet Mass 95% Fill @ 10°C.....	5.0 kg Max
GHe MDP.....	29.1 Bar (422 psia)	Operating Voltage For Telemetry.....	5±0.25 V _{DC}
GHe Proof Pressure.....	43.66 Bar (633 psia)	Operating Voltage For Heaters & Valves.....	9.5-12.6 V _{DC}
GHe Burst Pressure.....	58.21 Bar (844 psia)	Standby Power.....	10 W Max
Internal Leakage.....	1.0 x 10 ⁻⁴ sccs GHe	Warmup Power.....	1W
External Leakage.....	1.0 x10 ⁻⁶ sccs GHe	Thruster Operating Power (4 thrusters).....	15 W Max
Operating Temp.....	10°C to 40°C	Data Interface.....	RS-422
Non-Operating Temp.....	-34°C to 60°C		

Figure 21: Green Propulsion System

Another propulsion system that deserves attention is the **Palomar Micro Propulsion System** which uses liquid isobutane as propellant but other propellants available. The Palomar Propulsion System is a fully integrated CubeSat micro propulsion system that includes a propellant tank, plenum and eight thrusters. The Palomar MiPS is designed to occupy the centre of a 3U CubeSat. This smart system is designed to interface with the spacecraft through an I²C data bus for command and control. The Palomar MiPS is primarily a reaction control system with thrusters arranged so that use of all six degrees of freedom (DoF) in rotation and translation are possible. Additional propellant is available by stretching the tank lobes, allowing for a custom propulsion system mass and volume based on specific

mission needs^[15]. Upgrades to other propellants available. This propulsion system offers 6 DOF control as required by the mission under consideration, but unfortunately it was designed for smaller spacecraft than SROC so it offers too low thrust and Delta-V values. We believe the system could be adapted to a 12 U CubeSat without too much effort and changes from the initial design.



Operating Parameters

Max Operating Pressure	150 psia	Cycle Life	120,000 firings
Proof Pressure	225 psia	Total Impulse	85 N/sec
Burst Pressure	375 psia	Minimum Impulse Bit.....	0.75 mN/sec
Thrust.....	35 mN	Operating Voltage	4.75 to 5.25 vdc
Internal Leakage	3.0 scc/hr	Peak Power.....	<5 watts (two thrusters)
External Leakage	1.0×10^{-6} scc/hr	Dry Mass	890 grams
Operating Temperature.....	0°C to +50°C	Propellant Mass	173 grams
Non-Operating Temperature	-10°C to +60°C	Total Mass	1,063 grams
Vibration.....	23 Grms		

Figure 22: Palomar Micro Propulsion System

3.3.2.3 Hybrid

" **Hybrid** " technology deserves a separate discussion. The hybrid rocket is an alternative to conventional bipropellant engines. The term hybrid refers to the difference in phase between the fuel and the oxidizer, they typically use a solid fuel grain and a liquid or gaseous oxidizer. Hybrid rocket motors embody certain advantages such as improved safety, reduced cost, throttleability over a wide range, and flexible packaging. Hybrid propulsion is well suited to achieve the required large ΔV for interplanetary missions because of its high performance (Isp around 300 s) and dense fuel. In addition,

hybrid rocket motors are restartable, allowing them to complete all orbit insertion and trajectory correction manoeuvres. This is of particular importance for science missions that typically require multiple orbit corrections, particularly during fly-bys of moons. Propellant selection is a key factor that defines a propulsion systems criticality to hazards such as leakage, explosive yield, fire, and pressure. Propellant options are also available for hybrid rocket motors that are relatively insensitive to the space environment and comparatively safe. Most hybrid fuels are inert and the separation in phase between the fuel and oxidizer makes hybrid rocket motors safer than alternative chemical propulsion systems. Hybrid motors also have propellant options well-suited to extended storage at a range of temperatures. This reduces the need for propellant temperature control systems, and can have dramatic implications for the overall power budget of the spacecraft. As part of this technology we have deepened the study of a JPL project of a propulsion system for a 12 U CubeSat for an interplanetary mission. The potential benefits of a hybrid motor as a propulsion system on a secondary spacecraft are explored by examining the design for a 12 U spacecraft with a total wet mass of 25 kg. The 12 U envelope is defined by the CubeSat community as 36,6 X 23,9 X 22,9 cm , which is slightly larger than 12 nominal units but fits within the notional deployment mechanism. The propulsion system was designed to deliver a total Delta-V of around 800 m/s across eight to twelve burns, representative of orbit insertion and trajectory corrections. The hybrid motor propulsion system consists of a single hybrid motor that utilizes Poly[MethylMethAcrylate] (PMMA) as the fuel and gaseous oxygen as the oxidizer. The hybrid motor is located in the centre of the spacecraft for thrust alignment. The oxidizer tanks are located symmetrically around the motor, see Figure 23. Four oxidizer tanks are required in order to accommodate the full volume of oxygen within the 12U form factor. The oxygen gas acts as a dual use propellant, working both as the main motor oxidizer, and as the propellant for cold gas thrust vector control and attitude control thrusters. The hybrid motor uses an augmented spark igniter fed with a small amount of the oxygen gas and methane gas. Such augmented spark igniters have been used extensively on liquid systems but have seen only limited use on hybrid rocket motors in the past. The system uses four TVC thrusters and eight ACS thrusters. The main motor is designed for a mean nominal in space thrust of 44 N, an ideal specific impulse of 334,5 s, and a total impulse of 17,6 X 103 Ns. The current design has 11.5 kg available for total non-propulsion mass^{[16][17]}.

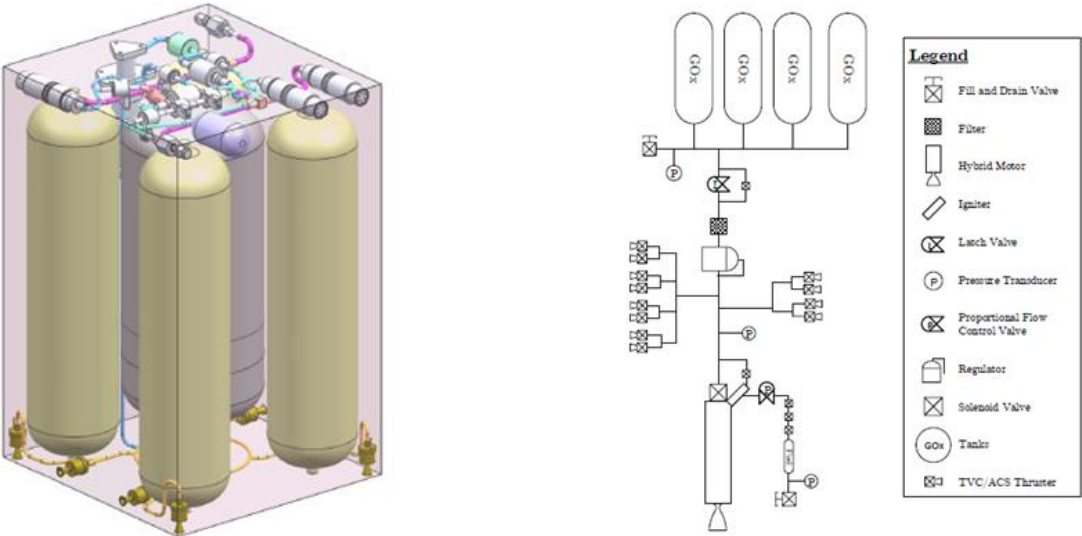
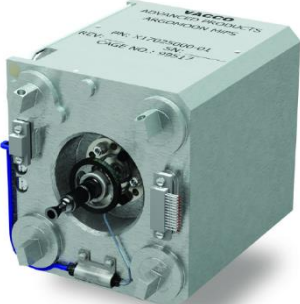


Figure 23: JPL project of a hybrid propulsion system

This propulsion system is certainly the one with the best performance and features. It also offers the best characteristics in the context of the interaction with the other subsystems that thus can be put in conditions to operate in better conditions and not be oversized. The only problem is that this propulsion system is designed for a mission other than SROC with a large Delta-V and large thrust values so consequently the mass and envelope of the system exceed the maximum limits imposed, but obviously a downsizing of the tanks made based on the thrust values we need and the Delta-V estimated for the SROC mission would lead to a drastic reduction in mass and envelope. So only a sizing suitable for our mission needs to be made without substantial design changes and this, given the performance and 6 DOF control, makes this propulsion system the potentially ideal candidate for our mission.

Even Vacco produced a hybrid system for CubeSat called **Argomoon Propulsion System**. VACCO's hybrid Micro Propulsion System (MiPS) combines green mono-propellant and cold gas propulsion in a single system to provide attitude control and orbital manoeuvring. Argotec's ArgoMoon program utilizes VACCO's hybrid propulsion system to achieve high levels of total impulse in a limited volume to accomplish the mission requirements. The VACCO ArgoMoon MiPS is approximately 1.3U plus the tuna can volume and uses one 100 mN green thruster to develop 783 N-sec of total impulse that provides 56 m/s of Delta-V for a 14 kg CubeSat. The four 25 mN cold gas thrusters develop 72 N-sec of total impulse. Each thruster independently operates to perform both Delta-V and ACS manoeuvres through an integrated microprocessor controller^[18]. Easily configured for different mono-propellants: ADN green (LMP-103S) and Air Force green (AF-M315E). Also in this case, as in the case of the other two propulsion systems discussed above, which use the technology with the integrated microprocessor controller to control the thrust vector and attitude with only 5 thrusters, it is necessary to deepen to understand if it guarantees control 6 DOF of the spacecraft. For the rest, the characteristics are adequate for our mission even if they are not excellent (especially as regards the Delta-V) and therefore it would be necessary in case you thought you wanted to use this propulsion system if they can be improved by combining other types of propellants or non-substantial changes to the design.



Operating Parameters

Propellant.....LMP-103S & R134a	Total Impulse @10°C.....72 & 783 N-s
MDP.....16.8 Bar (244 psia)	Dry Mass.....1.430 kg Max
Proof Pressure.....25.2 Bar (366 psia)	Wet Mass 95% Fill @ 10°C.....2.065 kg Max
Burst Pressure.....42.1 Bar (610 psia)	Operating Voltage For Telemetry.....9.0-12.6 V _{DC}
Internal Leakage BOL.....<1X10 ⁻⁴ sccs GHe	Operating Voltage For Heaters & Valves.....9.0-12.6 V _{DC}
Internal Leakage EOL.....<1.0 x10 ⁻³ sccs GHe	Standby Power.....1 W Max
External Leakage.....<1.0 x 10 ⁻⁶ sccs GHe	Warmup Power.....20 W Max
Operating Temp.....10°C to 40°C	Thruster Operating Power4.3 W Max
Non-Operating Temp.....-34°C to 60°C	Data Interface.....RS-422

Figure 24: ArgoMoon Propulsion System

3.4 Trade-off analysis

In this section we proceed with the trade-off of the different technologies evaluated for the propulsion system of the SROC mission. The technologies taken into consideration for this analysis are: cold gas, green monopropellants and hybrid propulsion systems (green monopropellant + cold gas). We did not take into account the classic monopropellants (for example hydrazine) for what was said in the previous section in which it was explained that this type of propulsion systems have much worse characteristics than green monopropellants.

The first thing to do is a pairwise comparison table between the different drivers identified previously in order to calculate the weight of each driver which is a fundamental parameter for the final trade-off table.

	Powertrain performance	Environmental impact	Thrust Vectoring/Degrees of freedom	Safety	Envelope	Mass	TRL	System Complexity	Design changes	Interactions with other subsystems	Sum	Weight	Final weight
Powertrain performance	1	1	0	1	0,5	0,5	1	0,5	1	1	7,5	0,136363636	0,136
Environmental impact	0	1	0	0	0	0	0	0	0	0	1	0,018181818	0,018
Thrust Vectoring/Degrees of freedom	1	1	1	1	1	1	1	1	1	1	10	0,181818182	0,182
Safety	0	1	0	1	0	0	0,5	0	0,5	0,5	3,5	0,063636364	0,064
Envelope	0,5	1	0	1	1	0,5	1	0,5	1	1	7,5	0,136363636	0,136
Mass	0,5	1	0	1	0,5	1	1	0,5	1	1	7,5	0,136363636	0,136
TRL	0	1	0	0,5	0	0	1	0	0,5	0,5	3,5	0,063636364	0,064
System Complexity	0,5	1	0	1	0,5	0,5	1	1	1	1	7,5	0,136363636	0,136
Design changes	0	1	0	0,5	0	0	0,5	0	1	0,5	3,5	0,063636364	0,064
Interactions with other subsystems	0	1	0	0,5	0	0	0,5	0	0,5	1	3,5	0,063636364	0,064
											55	1	1

Table 4: Drivers weights

Table shows the process for the definition of the drivers weights that rise analysing the relative importance comparison among the PP. When one is more important than another, "1" is put in the related cell of the matrix; instead "0" is put when the performance parameter is less important than that compared. If the parameters have the same importance, "0.5" score is assigned to both.

Following table illustrates the trade off analysis results obtained using a matrix approach. The scores assigned to the investigated configurations belong to a range between 0 (worst value) and 5 (best value). The scores assigned must be multiplied by the weight of each driver and for each of the three technologies the various products relating to each of the drivers must be added up. The technology with the highest score will turn out to be the best for our purpose.

Technology	Powertrain performance	Environmental impact	Thrust Vectoring/Degrees of freedom	Safety	Envelope	Mass	TRL	System Complexity	Design changes	Interactions with other subsystems	
Weight	0,136	0,018	0,182	0,064	0,136	0,136	0,064	0,136	0,064	0,064	1
Cold Gas	3	5	5	5	5	5	5	5	4	5	4,664
Green Monopropellant	4	4	4	4	4	4	4	4	3	3	3,872
Hybrid	5	4	5	4	4	4	3	4	3	4	4,19

Table 5: Trade-off of the different technologies for the SROC propulsion system

Cold gases are those that, in terms of performance, are able to offer less than the other technologies evaluated, while hybrid propulsion systems manage to excel in this field by offering unrivalled performance from the other two technologies. The environmental impact is good for all three technologies but obviously, speaking of inert gas, cold gases are those with the lowest environmental impact. As for the thrust vectoring / degrees of freedom we have already designed cold gas and hybrid propulsion systems that are able to guarantee the 6 DOF control of the spacecraft while for the green monopropellants we have for now 6 DOF solutions obtained through more complex combinations. As far as safety is concerned, all the technologies are absolutely excellent, even if cold gases are certainly the safest technology of all as it uses inert gas. For envelope and mass we have achieved miniaturization levels for all three technologies that are fully compatible with the requirements of the SROC mission, but with cold gas technology it is easier to have less bulky and lighter systems. As far as the TRL is concerned, the most ready technology is certainly cold gas, while the monopropellant greens are at a really good level of technological development and we have propulsion systems very similar to the one we need for our mission that have already flown; on the other hand, the technological level of hybrid propulsion systems is the lowest as we have products that have already passed the test phase but have not yet flown or in any case very few have done so. Obviously when we talk about system complexity we take into account various factors including cost, schedule, manufacturing, testing and transport logistics as well as the complexity of the system itself; by characteristics cold gases are propulsion systems that have a lower system complexity and using an inert gas bring with them the propellant that is easier to handle, while the other two technologies have an absolutely comparable system complexity. As far as design changes are concerned, none of the three technologies offers a product ready and available on the market for our mission, but certainly at the moment cold gases offer solutions that are closer to our needs. As regards the interaction with other subsystems, cold gases are those that require less effort from the TCS and a lower consumption of electrical power; from this point of view, hybrids are more optimized than monopropellant greens.

From the trade-off analysis we have not obtained a definitive result as the values attributed to the 3 technologies are very close to each other. We can certainly say that the most ready technology is that of **cold gas**, but the one with the greatest potential and that could offer superior performance and characteristics is that of hybrid propulsion systems.

4 Engine Model

From the analyses made in the previous chapter we concluded that the best technology for SROC's propulsion system is cold gas. The Tyvak company is developing a specific cold gas engine for the SROC mission called Perseus. In this chapter we will see in detail the characteristics of a cold gas engine and those specific to Perseus in order to create a model to be added to the similar environment in order to obtain increasingly validating results.

4.1 Cold gas technology

A cold gas thruster (or a cold gas propulsion system) is a type of rocket engine which uses the expansion of a (typically inert) pressurized gas to generate thrust. As opposed to traditional rocket engines, a cold gas thruster does not house any combustion and therefore has lower thrust and efficiency compared to conventional monopropellant and bipropellant rocket engines. Due to the absence of a combustion process, a Cold Gas system requires only one propellant (without an oxidizer), and hence can be designed with minimum complexity and their design consists only of a fuel tank, a regulating valve, a propelling nozzle, and the little required plumbing. They are the cheapest, simplest, and most reliable propulsion systems available for orbital maintenance, manoeuvring and attitude control.

The simpler design of a Cold gas system leads to a smaller system mass and lower power requirements for regulation purposes. However, these advantages come at the cost of a monotonically decreasing thrust profile over a period of time. The thrust produced is directly proportional to the pressure of the propellant inside the tank (propellant storage) and over the course of the mission, tank pressure decreases (due to propellant usage) resulting in a decrease of the maximum thrust that is generated by the system^[20].

The schematic of a typical Cold gas system is shown in Figure.

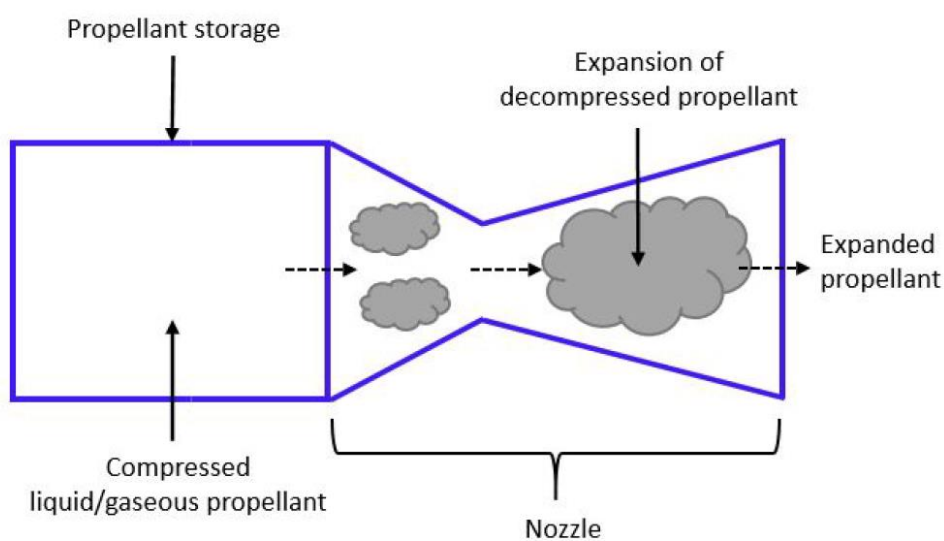


Figure 25: Schematic of a Cold Gas Propulsion System

The nozzle of a cold gas thruster is generally a convergent-divergent nozzle that provides the required thrust in flight. The nozzle is shaped such that the high-pressure, low-velocity gas that enters the nozzle is expanded as it approaches the throat (the narrowest part of the nozzle), where the gas velocity matches the speed of sound.

Specific impulse (shown in the next equation) of a Cold gas system mainly depends on the exit-to-chamber-pressure (P_e/P_c) and characteristic velocity (c^*). The exit-to-chamber-pressure is related to the expansion of the propellant, while Poisson constant (γ) is the ratio of specific heats at constant pressure and constant volume. Characteristic velocity of a Cold gas system at any instant is a function of the velocity of propellant in Mach number. Exit velocity is another important performance factor that not only depends on the exit-to-chamber-pressure, but also on the chamber temperature (T_c). The mathematical relations summarizing these relationships are described below:

$$I_{sp} = \frac{\gamma c^*}{g_0} \sqrt{\frac{2}{\gamma-1} \left(\frac{2}{\gamma+1}\right)^{\frac{\gamma+1}{\gamma-1}} \left(1 - \frac{P_e}{P_c}\right)^{\frac{\gamma-1}{\gamma}}}$$

$$c^* = \frac{a_0}{\gamma \left(\frac{2}{\gamma+1}\right)^{\frac{\gamma+1}{2(\gamma-1)}}}$$

$$v_e = \sqrt{\frac{2\gamma T_c}{\gamma-1} \left(1 - \frac{P_e}{P_c}\right)^{\frac{\gamma-1}{2}}}$$

where g_0 is standard gravity and a_0 is the sonic velocity.

Thrust is generated by momentum exchange between the exhaust and the spacecraft, which is given by Newton's second law as $F = \dot{m}v_e$ where \dot{m} is the mass flow rate, and v_e is the velocity of the exhaust. In the case of a cold gas thruster in space, where the thrusters are designed for infinite expansion (since the ambient pressure is zero), the thrust is given as:

$$F = A_t P_c \gamma \left[\left(\frac{2}{\gamma-1}\right) \left(\frac{2}{\gamma+1}\right) \left(1 - \frac{P_e}{P_c}\right) \right] + P_e A_e$$

Where A_t is the area of the throat, P_c is the chamber pressure in the nozzle, γ is the specific heat ratio, P_e is the exit pressure of the propellant, and A_e is the exit area of the nozzle.

4.2 SROC propulsion system

SROC propulsion system is the cold gas engine that the Tyvak company is building for the SROC mission. In this section we report the main characteristics on the basis of which in the following sections we will proceed with the creation of the model to be inserted in the simulation environment.

The propulsion system that Tyvak International want to develop is a monopropellant thruster for a 6U CubeSat able to deliver a thrust in the range of Millinewton in 6 degrees of freedom, torque and thrust for each of the three principal axes, using a cold gas storable at low pressure.

The general fluidic schematic of Perseus configuration is shown in the figure below.

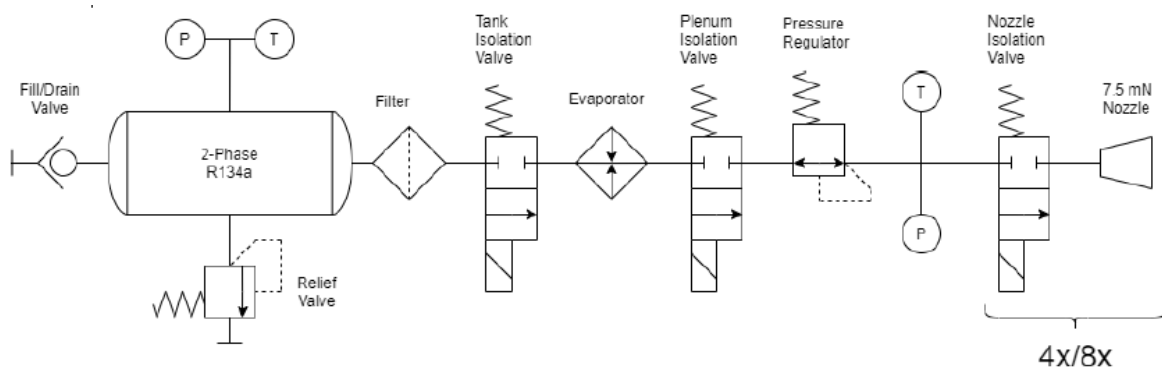


Figure 26: Perseus general configuration fluidic schematic

The fluidic part has a configuration such that the propellant can flow directly to the nozzle and then ejected outside in gaseous state.

The propellant is stored in the tank (in a bi-phasic state at ambient temperature). To keep the propellant in ideal pressure and temperature for thrusting and as a further guarantee of maintaining the propellant in a gaseous state one heater is placed on the tank and one along the line. While to avoid the passage of debris that could clog the nozzles a filter is placed on the tank outlet. Upon exit from the tank, the propellant flows in the pipes of the high-pressure stage, through a filter and then a set of 2 redundant and independent NC-valves, up to the pressure regulator, where its pressure is set to 1.5 bar. A dedicated heater/evaporator device set between the tank and plenum isolation valves ensures that only gaseous R134a reaches the regulator. The low-pressure stage follows, composed of 4 to 8 lines (depending on the configuration), each of which includes a NC-valve (independently controlled) and a nozzle^[21]. Nozzles models can be selected to provide either 8.75 mN per nozzle (only 4 thrusters can be turned on at the same time).

Along the fluidic line, before the pressure regulator, there are two normally-closed valves to prevent the propellant flowing down the line when the system is not firing. The same kind of valve is placed on each of eight branches before the nozzles.

On the tank two valves are provided: one to fill and drain the propellant into the tank, one for pressure relief. The thruster module also includes two temperature and pressure transducers: one to monitor the propellant status and one, after the pressure regulator, to measure parameters before the branching.

To generate thrust the temperature and pressure in the tank and along the pipes shall be in the range that maintain the propellant in gaseous phase, while to perform a manoeuvre, due to the nozzle configuration and orientation, at most four valves should be open at the same time in addition to the two valves along the fluidic line, used as inhibits in order to avoid unintentional propellant flow.

Nozzles are placed and angled in a configuration which allows to provide full 6 DOF control to the spacecraft (with 8 nozzles in total). Nozzles angles can be selected to maximize efficiency given the expected manoeuvres distribution among the various axes. The firing time is ideally limited only by the main tank size, since the nozzles are fed directly from the main tank and no buffer tank is inserted in the fluidic line. Moreover, the system is almost “ready to fire” since no particular pre-firing operation are needed (e.g. no buffer tank filling and heating).

While the Perseus preliminary design initially targeted a 400+ Ns total impulse module for 6U proximity operations applications (with the thruster module mounted in the central 2U), extensions are now baselined for:

- 12U applications, with double the total impulse;
- Compact 6U application, with 120 Ns max total impulse and a “twin module” configuration, with two identical 0.5U modules (with smaller tanks) placed only on the extremes of the central 2U volume – i.e. facing out the middle of the two 3U faces^[22].

The development of the full configuration is already ongoing and is expected to reach TRL 8 in mid-2021.

The preliminary specifications for this thruster module are shown in the next Figure.

	Perseus/Frostbite 6U Full config
Safety	2+ Fault Tolerance Cold Gas (R134a) No hot exhaust/plasma
Max Thrust	35 mN typical depends on nozzle config
Minimum Impulse Bit	< 5 mNs
Total Impulse	480 Ns
Delta-V	40 m/s for 12 kg 6U
Thrust Vectoring / Degrees of Freedom	6 DOF (3+3) Full 3-axis thrust vectoring Full 3-axis attitude control
Envelope	< 210 x 95 x 150 mm (3.0 L or 2.2U in a 6U)
Performance Density	160 Ns/L
Mass	< 4.0 kg wet
Power	< 2 W ready, stand-by < 22 W peak power
MEOP	≈ 17 bar (tank + high-pressure lines) 1.5 bar (low-pressure lines)
Proof Pressure	≈ 30 bar TBC
Burst Pressure	≈ 30 bar
Temperature Limits	-10°C / +50°C (operational) -20°C / +60°C (survivability)

Figure 27: Thruster module specifications

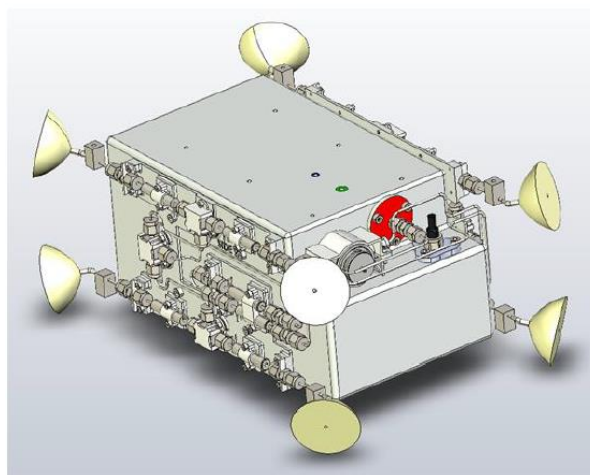


Figure 28: Perseus 6U full configuration at preliminary design

4.3 Thrusters position

The CubeSat is equipped with 8 thrusters.

Every nozzle is inclined with respect to the body reference frame of the angles:

- $\alpha = \frac{\pi}{4}$ with respect to x-axis;
- $\beta = \frac{\pi}{6}$ with respect to z-axis;

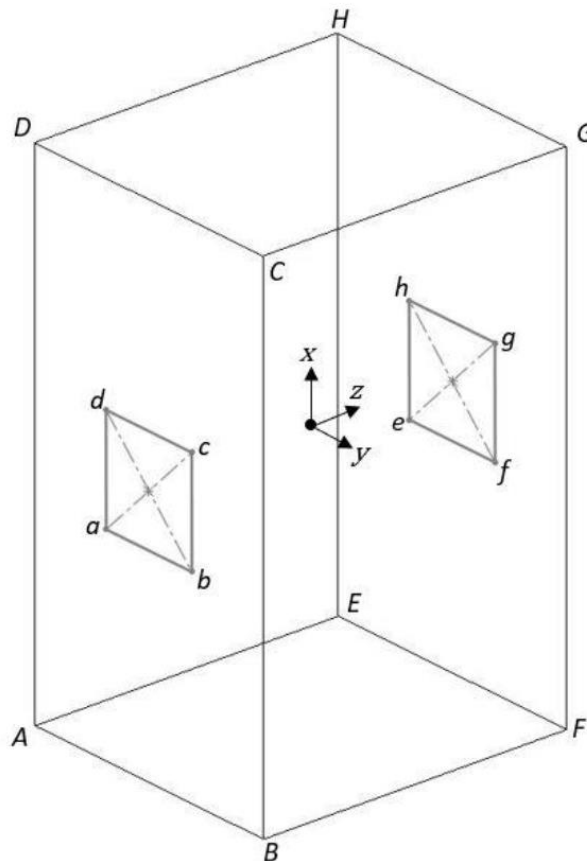


Figure 29: Thrusters position

From specifics of Perseus propulsion system listed in the previous section, it is known that the maximum thrust which the propulsion system is able to provide is equal to 35 mN, and being that a maximum of 4 thrusters can be turned on at the same time we have that maximum thrust provided by each thruster is 8.75 mN.

For each thruster the thrust components along the 3 body axes are:

$$T_x = T \cdot \sin \beta$$

$$T_y = T \cdot \sin \alpha \cdot \sin \beta$$

$$T_z = T \cdot \cos \alpha \cdot \cos \beta$$

where $T=8.75$ mN, that is T is the maximum thrust that can be delivered by each of the thrusters.

4.4 SROC propulsion system model

At this point we have all the necessary inputs to create the model of the propulsion system of our mission in order to insert it in the simulation environment previously created on STK software in order to demonstrate that it is actually possible to carry out the mission with the Perseus engine and see the effects on the ΔV they went to consider the engine that will actually be used for the mission.

4.4.1 Thrust and I_{sp} modelling

As we explained in detail in section 3.1 talking about the characteristics of a Cold Gas engine, in a system of this type the thrust and I_{sp} depend on the pressure and temperature of the tank which are two quantities that vary during a mission. For this reason, both the thrust and the I_{sp} cannot be considered constant.

From the considerations made it was estimated that the best way to model the thrust and the I_{sp} for a Cold Gas engine is through a **polynomial development**.

Below are the relations that regulate the variation of T and I_{sp} as a function of pressure and temperature of the tank.

$$Thrust(P, T) = (C_0 + C_1P + C_2P^2 + C_3P^3 + C_4P^{E_4} + C_5P^{E_5} + C_6P^{E_6} + C_7(B_7)^{E_7}) \left(\frac{T}{T_r}\right)^{(1+K_0+K_1P)}$$

$$I_{sp}(P, T) = (C_0 + C_1P + C_2P^2 + C_3P^3 + C_4P^{E_4} + C_5P^{E_5} + C_6P^{E_6} + C_7(B_7)^{E_7}) \left(\frac{T}{T_r}\right)^{(1+K_0+K_1P)}$$

The problem consists in calculating these 15 coefficients so that the model based on this polynomial development for thrust and I_{sp} reproduces the previously listed characteristics of the Perseus engine.

Tyvak International has developed a particularly high-performance regulation system for Perseus, thanks to which the thrust and the I_{sp} are very little affected by variations in pressure and temperature of tank. For this reason it was decided to calculate the 15 coefficients useful to define the model by decreasing the tank pressure starting from the nominal value of 17 bar up to 10 bar and the temperature of the tank within the operating range, i.e. between -10° and 50° . The thrust and the I_{sp} as we have seen in section 3.1 decrease as the pressure and temperature of the tank decrease but, as mentioned on Perseus, they vary within a very narrow range, that is the thrust between 30 mN and 35 mN (which is the nominal value) and the I_{sp} between 35 s and 38 s (which is the nominal value).

Since this modelling for thrust and I_{sp} within STK must be associated with each of the 8 thrusters, for the calculation of the coefficient values, a variation of the thrust for each of the thrusters between 3.75 mN and 4.375 mN (optimal value) was considered below. The hypothesis that the propulsion

system can work with all 8 thrusters running at the same time (in reality this is not the case because only 4 thrusters can work at the same time, but in this phase this approximation is tolerable and does not have a great influence on the final results).

By doing so, the coefficients can be calculated with a system of 15 non-linear equations. Since the thrust and the I_{sp} are little affected by the pressure and temperature variation in the tank, only 3 of these 15 coefficients are non-zero. The following table shows the coefficient values calculated through a Matlab program using the "fsolve" function or the "solve" function.

Coefficients	
C_0	0.004155
C_1	0
C_2	0
C_3	0
E_4	0
E_5	0
E_6	0
C_4	0
C_5	0
C_6	0
E_7	0
C_7	0
B_7	0
K_0	0.847891
K_1	$8.00498 \cdot 10^{-7}$

Table 6: Coefficients for thrust modelling

Coefficients	
C_0	36.8712
C_1	0
C_2	0
C_3	0
E_4	0
E_5	0
E_6	0
C_4	0
C_5	0
C_6	0
E_7	0
C_7	0
B_7	0
K_0	-0.740445
K_1	$1.0575 \cdot 10^{-6}$

Table 7: Coefficients for I_{sp} modelling

The obtained values of the coefficients must be inserted in the model of our engine called "Perseus model" in the Component Browser of the previously created SROC mission scenario on STK. Everything is shown in the following figures.

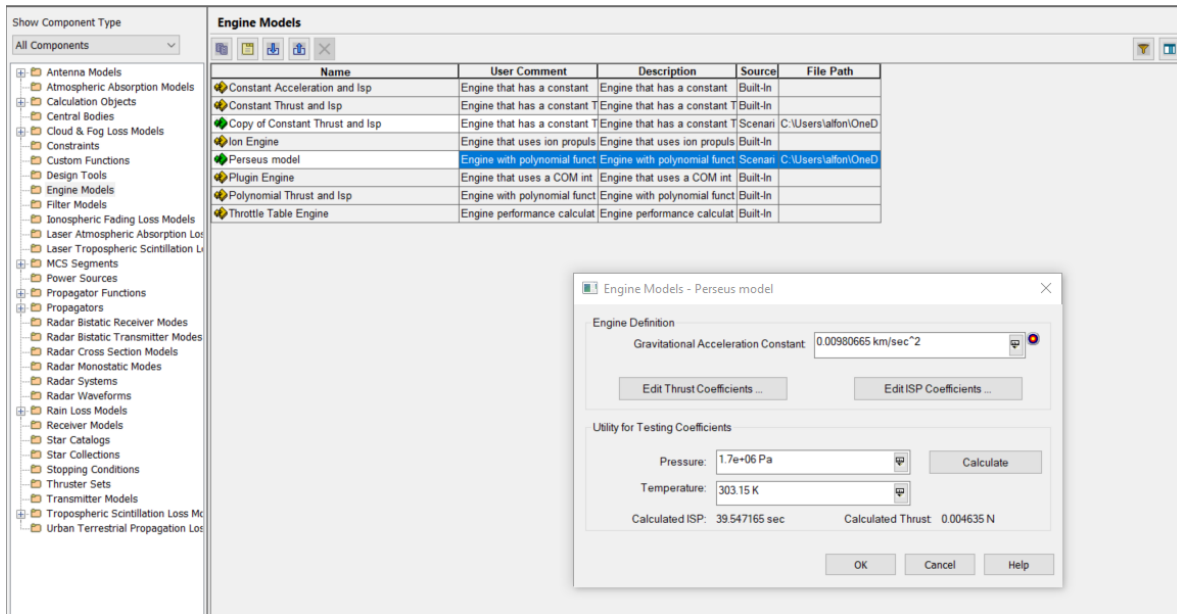


Figure 30: Perseus Model on STK

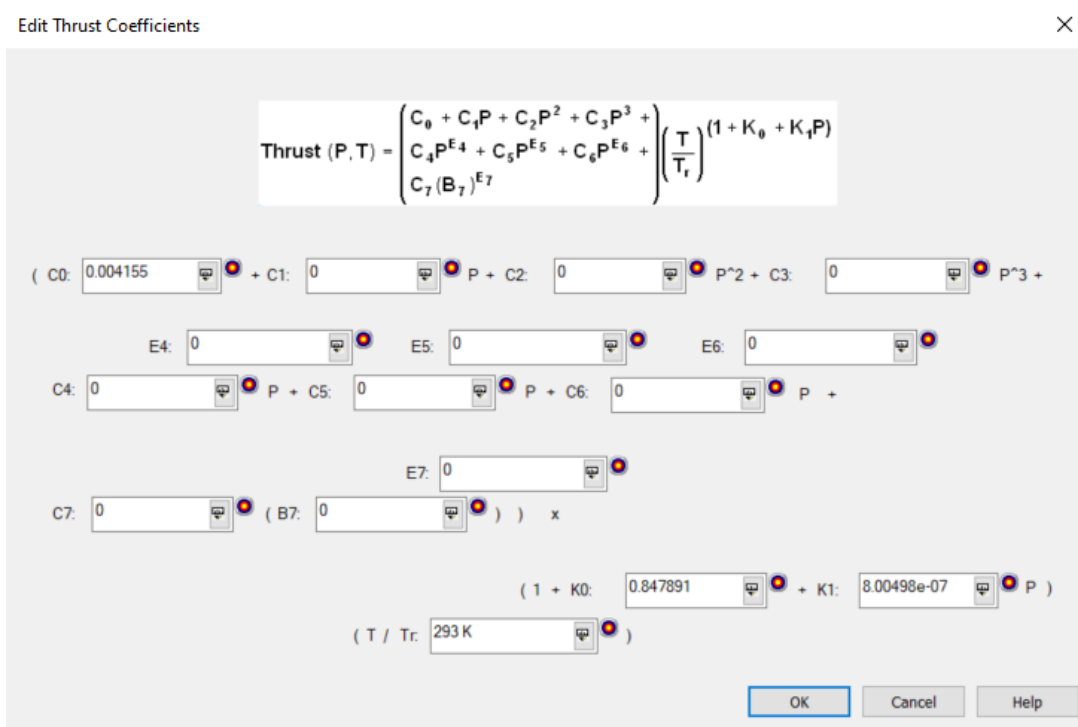


Figure 31: Edit Thrust Coefficients

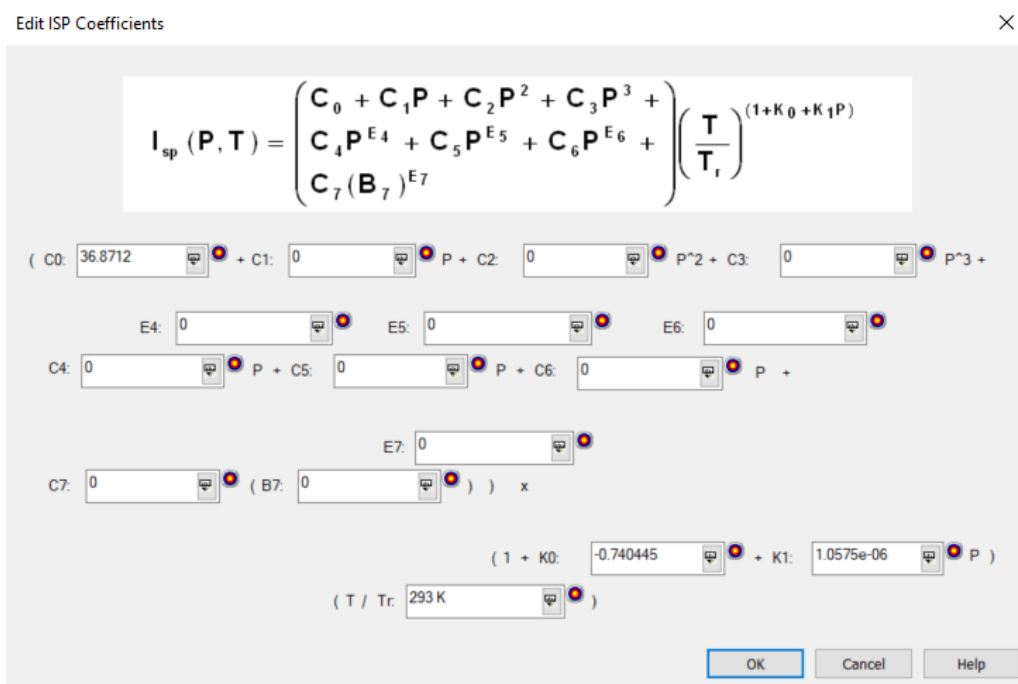


Figure 32: Edit I_{sp} Coefficients

4.4.2 Thrusters Sets

Once we have created the model that allows us to have a realistic thrust and I_{sp} trend for a Cold Gas engine to be associated with each of the 8 thrusters, we must define a Thruster Set on STK that reproduces the positioning of the thrusters characteristic of the propulsion system of the SROC mission, Perseus.

As described in section 3.3 the thrusters are positioned at an angle of $\frac{\pi}{4}$ with respect to the body x axis and at an angle of $\frac{\pi}{6}$ with respect to the body z axis. STK to define the Thrusters Sets asks us as input the **azimuth** and **elevation** angles of each thruster. Referring to the figure in section 3.3, the azimuth and elevation angles of each of the 8 thrusters are shown in the next table.

Thrusters	Azimuth	Elevation
A	135 deg	-30 deg
B	135 deg	-30 deg
C	45 deg	-30 deg
D	45 deg	-30 deg
E	45 deg	30 deg
F	45 deg	30 deg
G	135 deg	30 deg
H	135 deg	30 deg

Table 8: Thruster Sets

Once the position and orientation of each of the 8 thrusters have been defined, let's associate each of them with the model we created in the previous section and which we called " Perseus Model ". All this is done within the Component Browser of the SROC mission scenario created above on STK where a Thruster Sets called `` Thruster Sets SROC '' was created as explained in the following figure.

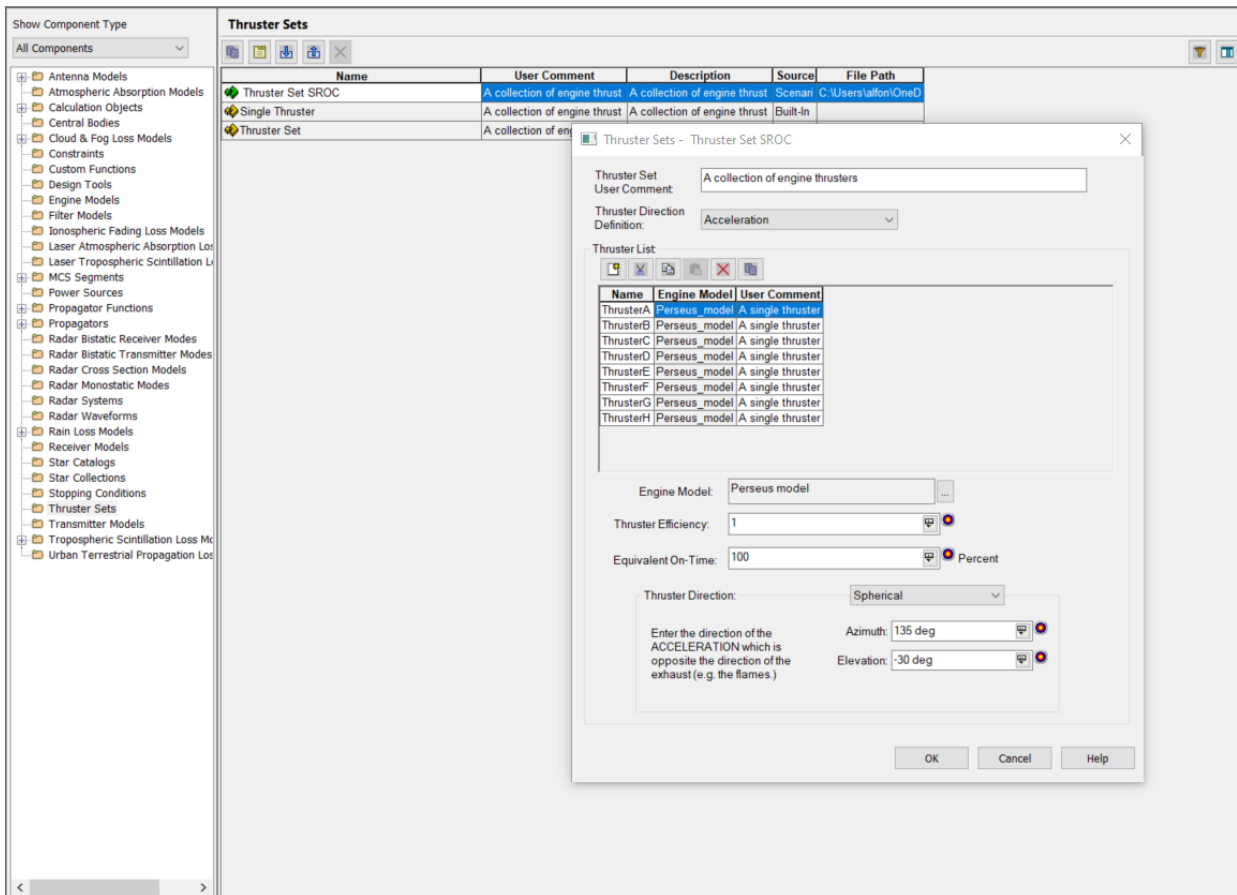


Figure 33: SROC Thruster Sets on STK

4.4.3 Finite manoeuvres and insertion of the new Thruster Sets created within each manoeuvre segment

Once we have created the Thruster Sets for the mission we have transformed all 19 manoeuvres of which the mission is formed from impulsive to finite through the command on STK `` Seed Finite From Impulsive '' which allows to generate automatically from the settings created for the manoeuvres impulsive all the useful features to transform a manoeuvre from impulsive to finite.

After transforming all the manoeuvre segments into finished manoeuvres, the previously created " Thruster Sets SROC " was selected for each of them in the appropriate " Engine " section on the Mission Control Sequence Set of STK. At this point it will be possible to simulate the mission taking into account the propulsion system that is actually developing for it. The following figure shows these two operations, for example for the Close Rendezvous of inspection 1.

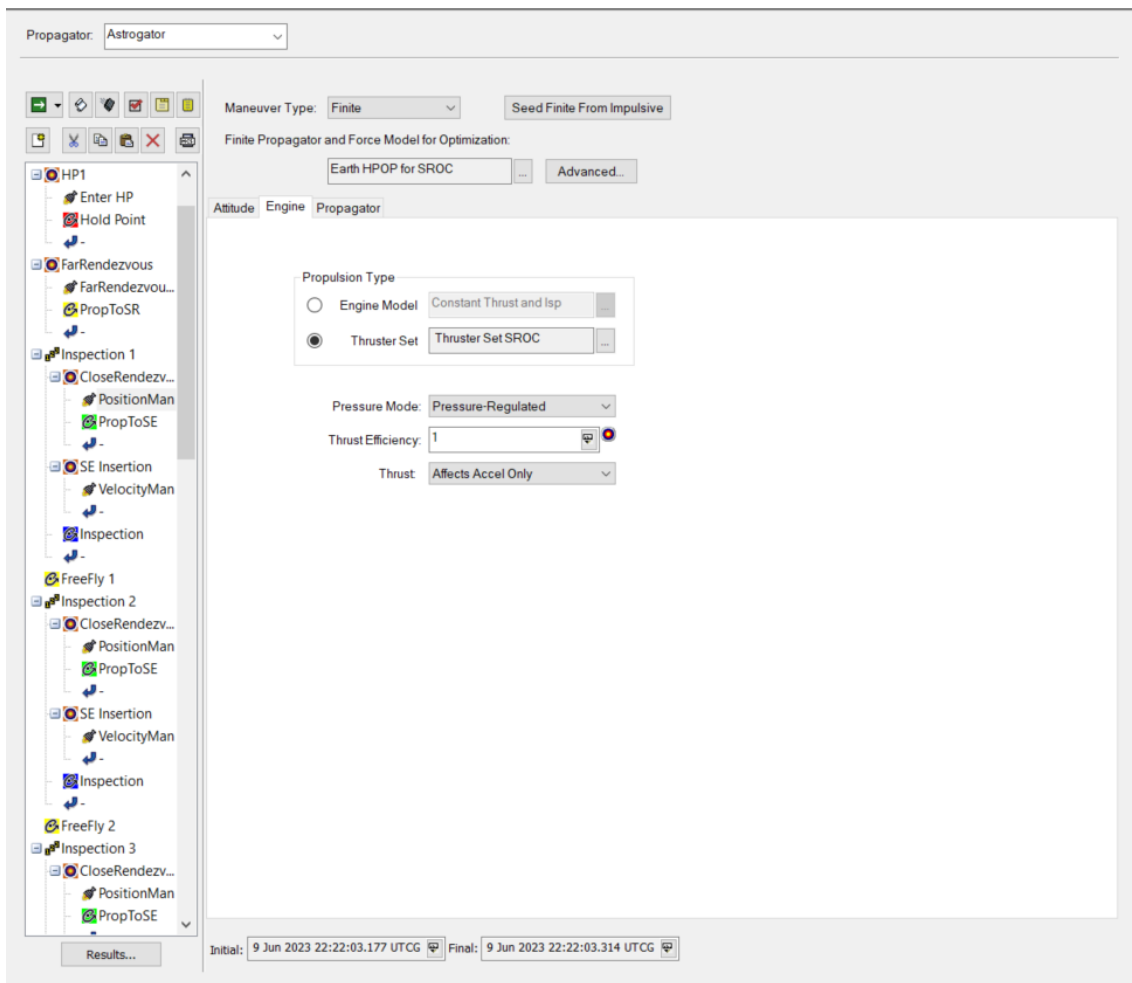


Figure 34: Finite manoeuvres and insertion of the new Thruster Sets created

4.5 Characterization of the fuel tank and estimate of the amount of propellant needed for the mission

Before launching the simulation with the new model created, all the required characteristics of the tank of our Perseus engine must be entered in the appropriate section of the STK Mission control Sequence called " Fuel Tank ".

We have set the nominal pressure and temperature which are respectively **17 bar** and **303.15 K**, the fuel density and since Perseus uses Freon R-134a as fuel it will be **4.25 kg / m³**, while the volume of the tank has been calculated by approximating the weight of the whole engine which is 8 kg with that of the tank through the equation $V = \frac{m}{\rho} = \mathbf{1.88\ m^3}$.

To estimate the mass of propellant necessary to carry out the mission, the Rocket equation or Tsiolkowski equation was used considering the worst case for ΔV , i.e. $\Delta V = 40 \text{ m/s}$, nominal I_{sp} , i.e. $I_{sp} = 38 \text{ s}$ and an initial mass of **24kg**.

$$I_{sp} = \frac{c}{g} \Rightarrow c = I_{sp} \cdot g = 38 \cdot 9.8 = 372.4 \text{ m/s}$$

$$m_f = m_0 e^{-\frac{\Delta V}{c}} = 24 e^{-\frac{40}{372.4}} = 21.556 \text{ kg}$$

$$m_p = m_0 - m_f = 2.444$$

For the calculation of the Maximum Fuel Mass we made the same steps as the previous calculation, however, considering an I_{sp} of **35 s** which is the worst case considered in the creation of the engine model (for Cold Gas the typical values of I_{sp} are those between 35 and 40 s). Obviously, considering the worst case for the I_{sp} , we would have a greater demand for fuel. Let's see the details:

$$I_{sp} = \frac{c}{g} \Rightarrow c = I_{sp} \cdot g = 35 \cdot 9.8 = 343 \text{ m/s}$$

$$m_f = m_0 e^{-\frac{\Delta V}{c}} = 24 e^{-\frac{40}{343}} = 21.358 \text{ kg}$$

$$m_p = m_0 - m_f = 2.642$$

The following figure summarizes everything said.

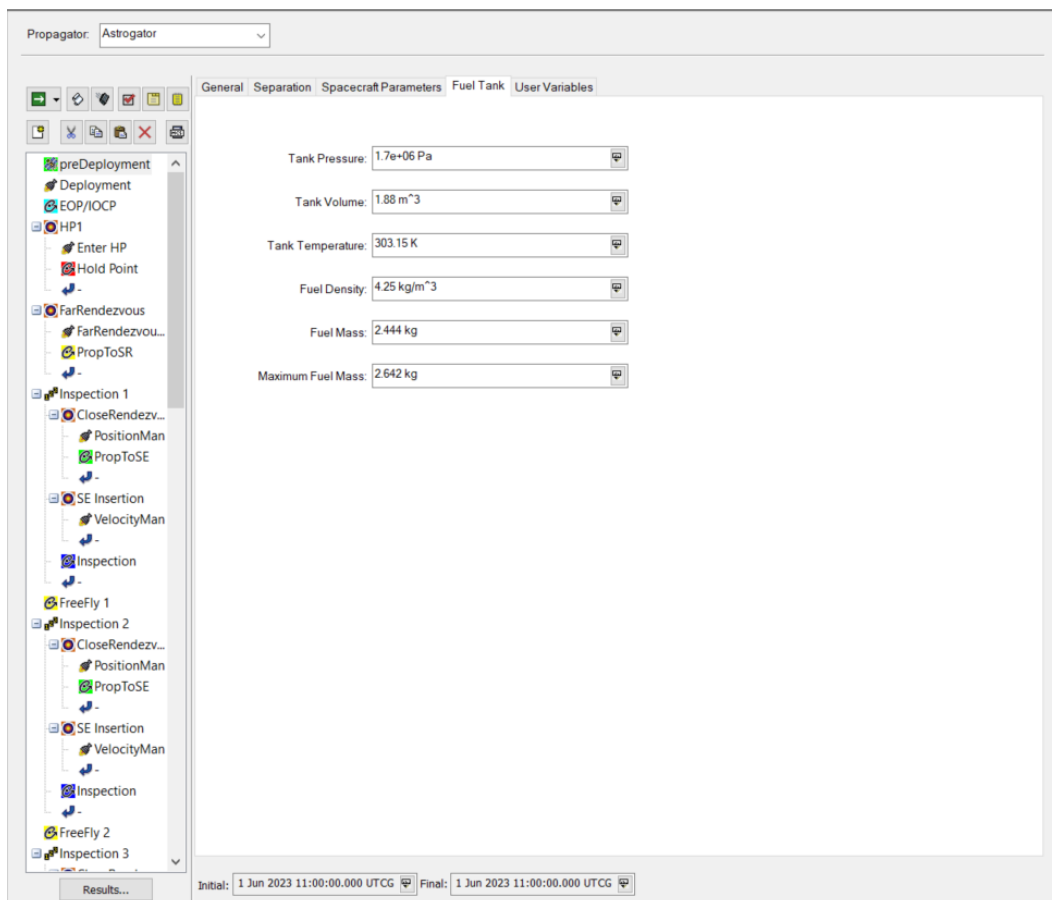


Figure 35: Characterization of the fuel tank

4.6 Simulation results

After all the steps illustrated in the previous sections we can finally launch the simulation on STK which also includes all the features of the propulsion system intended for the SROC mission.

4.6.1 ΔV

As far as ΔV is concerned, we obtained the results shown in the table.

Manoeuvre	ΔV [m/s]	Margin	ΔV with Margin
Deployment	0,008367	100%	0,016734
HP1.Enter_HP	0,003513	100%	0,007026
FarRendezvous.FarRendezvous_Man	0,003286	100%	0,006572
Inspection_1.CloseRendezvous.PositionMan	2,600655	100%	5,20131
Inspection_1.SE_Insertion.VelocityMan	0,397453	100%	0,794906
Inspection_2.CloseRendezvous.PositionMan	0,010901	100%	0,021802
Inspection_2.SE_Insertion.VelocityMan	0,059102	100%	0,118204
Inspection_3.CloseRendezvous.PositionMan	0,00147	100%	0,00294
Inspection_3.SE_Insertion.VelocityMan	0,002506	100%	0,005012
Inspection_4.CloseRendezvous.PositionMan	0,000863	100%	0,001726
Inspection_4.SE_Insertion.VelocityMan	0,003297	100%	0,006594
Inspection_5.CloseRendezvous.PositionMan	0,001503	100%	0,003006
Inspection_5.SE_Insertion.VelocityMan	0,002529	100%	0,005058
Inspection_6.CloseRendezvous.PositionMan	1,975204	100%	3,950408
Inspection_6.SE_Insertion.VelocityMan	0,003147	100%	0,006294
HP2.Enter_HP	0,000629	100%	0,001258
Docking.FlyAround.Approach	0,002219	100%	0,004438
Docking.Close_Approach.Close_Approach_Man	0,002297	100%	0,004594
Docking.Mating.Mating	0,001091	100%	0,002182
ΔV tot [m/s]	5,080030	ΔV tot with Margin	10,160064

Table 9: ΔV of the simulation with Perseus model

As can be clearly seen from the table, the ΔV obtained is **5.08 m / s** lower than the ΔV obtained in the previous simulations (the value was 7.89 m / s) which did not take into account the specific characteristics of the Perseus propulsion system. Although we have taken into account for all maneuvers a margin of 100% which is an absolutely conservative consideration that is necessary only for the last mission phases (rendezvous and docking), the full ΔV with margins is in any case lower than the total ΔV with margins calculated previously considering margins of 5% for all manoeuvres and 100% only for the final manoeuvres (the value was 11.36 m / s).

4.6.2 Duration and fuel used

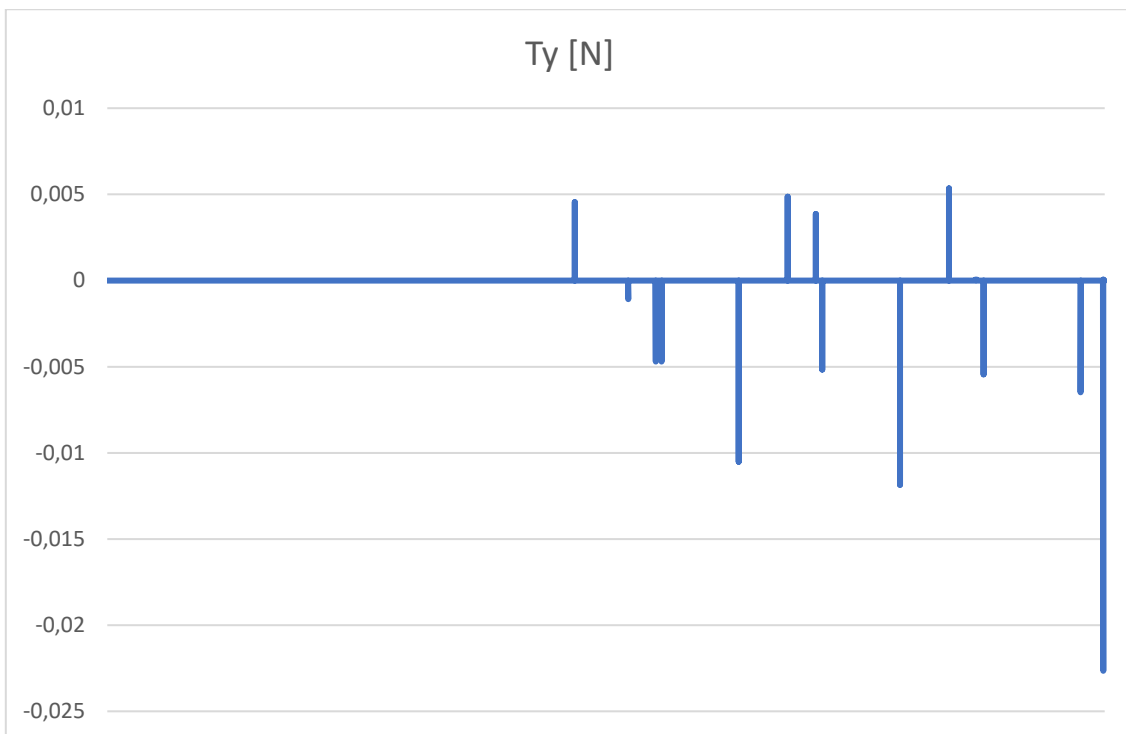
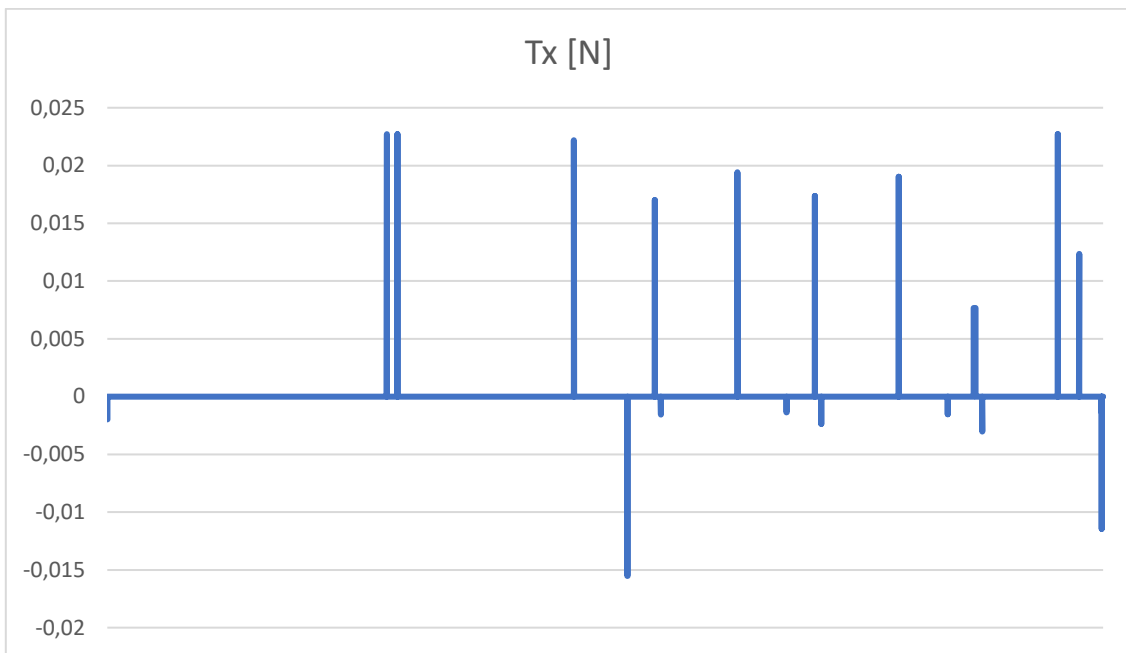
From the simulation performed, we also obtain the durations of the individual manoeuvres and the fuel consumed during the mission as outputs. We see the results obtained summarized in the following table.

Manoeuvre	Duration (s)	Finite Burn Duration	Fuel Used (kg)
Deployment	9,744	9,744	0,001
HP1.Enter_HP	4,091	4,091	0,000
FarRendezvous.FarRendezvous_Man	3,826	3,826	0,000
Inspection_1.CloseRendezvous.PositionMan	0,137	0,137	0,023
Inspection_1.SE_Insertion.VelocityMan	462,066	462,066	0,044
Inspection_2.CloseRendezvous.PositionMan	12,662	12,662	0,001
Inspection_2.SE_Insertion.VelocityMan	68,641	68,641	0,007
Inspection_3.CloseRendezvous.PositionMan	1,706	1,706	0,000
Inspection_3.SE_Insertion.VelocityMan	2,910	2,910	0,000
Inspection_4.CloseRendezvous.PositionMan	1,002	1,002	0,000
Inspection_4.SE_Insertion.VelocityMan	3,828	3,828	0,000
Inspection_5.CloseRendezvous.PositionMan	1,745	1,745	0,000
Inspection_5.SE_Insertion.VelocityMan	2,937	2,937	0,000
Inspection_6.CloseRendezvous.PositionMan	2284,083	2284,083	0,218
Inspection_6.SE_Insertion.VelocityMan	3,624	3,624	0,000
HP2.Enter_HP	0,724	0,724	0,000
Docking.FlyAround.Approach	2,555	2,555	0,000
Docking.Close_Approach.Close_Approach_Man	2,645	2,645	0,000
Docking.Mating.Mating	1,256	1,256	0,000
Tot	2870,182	2870,182	0,294

Table 10: Duration of manoeuvres and fuel consumed during the mission

It is important to note that the fuel actually used is significantly lower than that estimated in one of the previous sections (2,642 kg). Everything can be easily explained taking into consideration the fact that a ΔV of 40 m / s was used for the calculation of that value, which is a much higher value than what we actually found in the simulation.

4.7 Thrust profile



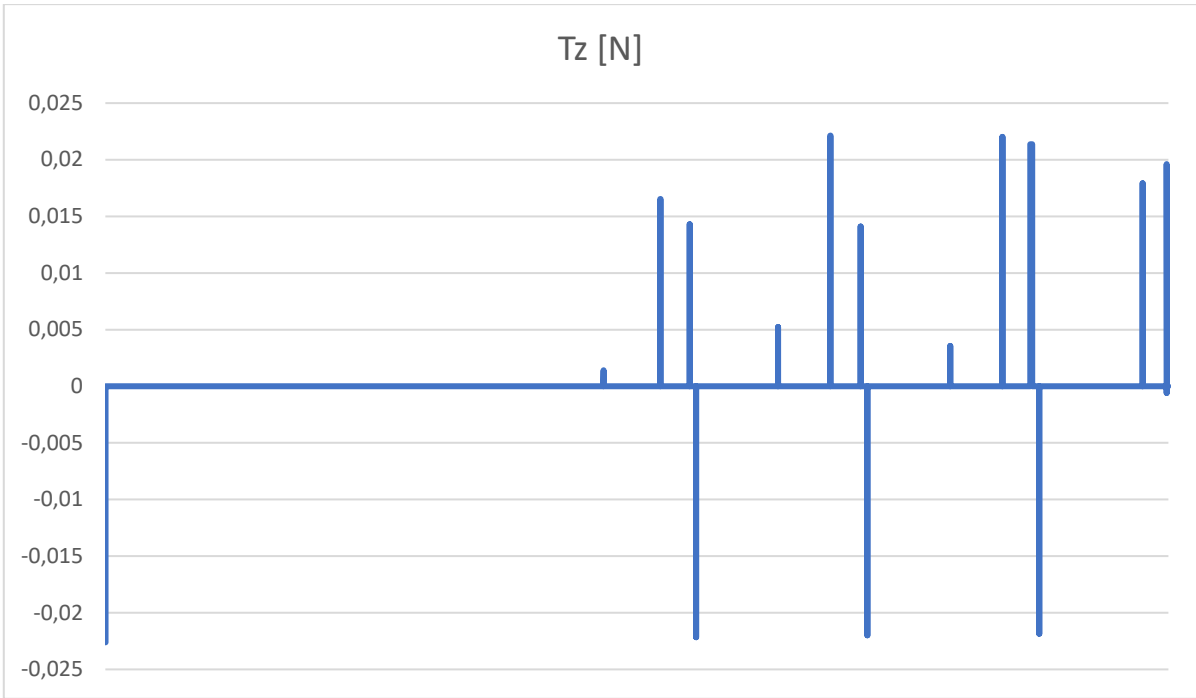


Figure 36: Thrust profile along the 3 body axes in the nominal case

These graphs show the trend of the thrust along the 3 body axes as a function of time. On the axis of the ordinate we have precisely the time while on the axis of the abscissa we have the value of the thrust in Newton. It is interesting to observe that the use of the propulsion system during the entire mission is a pulsed use, in fact the various manoeuvres can be considered practically impulsive and the time in which the thrusters remain on to perform each of them is really very short. We can get an idea of the duration of each manoeuvre from the thickness of the columns of the three figures above. Another thing we can notice is that not all manoeuvres require a push in all 3 directions. Negative thrust values mean that the direction of the thrust required is opposite to that of the body reference system taken into consideration and shown in figure 29.

Maneuver Number	Start Time (UTCG)	Tx [N]	Ty [N]	Tz [N]	Duration (sec)
1	1 Jun 2023 11:00:00	-0,00198	0	-0,022619	9,744
2	6 Jun 2023 11:40:47	0,022706	0	0	4,091
3	6 Jun 2023 16:19:47	0,022706	0	0	3,826
4	9 Jun 2023 22:22:03	0,022202	0,004541	0,001418	0,137
5	10 Jun 2023 21:22:03	-0,01551	-0,001086	0,016547	462,066
6	11 Jun 2023 08:59:55	0,017009	-0,004699	0,014289	12,662
7	11 Jun 2023 11:37:38	-0,001546	-0,00471	-0,022158	68,641
8	12 Jun 2023 20:20:07	0,019429	-0,010519	0,005235	1,706
9	13 Jun 2023 16:50:08	-0,001365	0,004859	0,022138	2,91
10	14 Jun 2023 04:34:09	0,017363	0,003857	0,014113	1,002
11	14 Jun 2023 07:11:40	-0,002351	-0,005175	-0,021983	3,828
12	15 Jun 2023 15:57:12	0,01904	-0,011848	0,003559	1,745
13	16 Jun 2023 12:27:14	-0,001526	0,005352	0,022013	2,937
14	16 Jun 2023 23:31:20	0,007679	0,000062	0,021368	2284,083
15	17 Jun 2023 02:46:54	-0,003025	-0,005447	-0,021834	3,624
16	18 Jun 2023 10:57:44	0,022706	0	0	0,724
17	18 Jun 2023 19:57:45	0,012349	-0,006492	0,017914	2,555
18	19 Jun 2023 04:57:47	-0,001409	-0,022654	-0,0006	2,645
19	19 Jun 2023 04:59:50	-0,011437	0,000049	0,019614	1,256

Table 11: Duration and thrust values along the 3 body axes for all manoeuvres

The table above shows for each of the manoeuvres the starting date and time, the duration and the value of the thrust required along each of the 3 body axes to carry it out. This summary table confirms all the considerations made previously commenting on figure 36. It is evident from this table that for each manoeuvre the sum of the thrust values along the 3 axes never exceeds 35 mN, demonstrating that with the chosen engine the mission can be completed successfully.

5 Causes of deviation from the planned trajectory^[23]

In this chapter we will deal with all those disturbances that can affect the SROC spacecraft during its operational life. After the analysis of all these possible disturbances we will insert offsets within the simulation environment created on STK (which now also includes the model of the Perseus engine) in order to better simulate the effects of these disturbances in order to validate the choice of the Perseus engine for our mission also in relation to the presence of a non-ideal environment. We will see how ΔV and fuel consumption vary as the value of these offsets varies.

Potential causes of deviations of the real trajectory from the planned one are the following:

1. **Thrust vector errors** : are deviations in magnitude and direction from the assumed applied
 - 1.1. Thrust force and duration errors
 - 1.2. Thrust direction errors
 - 1.3. Duty cycle of thrusters
2. **Thruster failures**: could, strictly speaking, also be covered by the term 'thrust vector errors'.
 - 2.1. Thrusters-closed failures
 - 2.2. Thrusters-open failure
3. **Orbital disturbances** : are forces acting on the spacecraft that change its trajectory.
 - 3.1. Drag due to residual atmosphere
 - 3.2. Disturbances due to geopotential anomaly
 - 3.3. Solar pressure
 - 3.4. Dynamic interaction of thruster plumes between chaser and target
4. **Navigation errors** : are the differences between the state as perceived by the on-board system and the real state (position, velocities, attitude, angular rates) of the vehicle. Initial navigation errors can be amplified over time by effects of orbital dynamics and by thrust manoeuvres
 - 4.1. Position measurement errors
 - 4.2. Velocity measurement errors
 - 4.3. Attitude and angular rate measurement errors
5. **Control errors** : are the differences between the proper corrections of the values to be controlled and the ones actually produced by the controller. The effects of control errors are due in equal part to navigation errors and to thrust vector errors.

5.1 Trajectory deviations due to thrust errors

Thrust errors can be caused by errors in the magnitude of the thrust force , in the actual mass of the spacecraft , in the thrust duration and in the thrust direction. These errors can be due to mounting errors, to misalignments of the exhaust flow velocity vector, to impingement of the thrust plumes on the structure of the own spacecraft, to deviation of the actual specific impulse from the nominal one, to non-linearities of the delivered ΔV w.r.t the valve opening time, etc.

Thrust direction errors can be caused by the attitude error of the vehicle, by geometric misalignment of the thruster hardware, or by a misalignment of the thrust vector w.r.t. the centre line of the thruster nozzle. This latter may be caused by flow-dynamic asymmetries. As in the case of attitude measurement errors, thrust direction errors lead to a component of thrust in a perpendicular direction.

5.2 Trajectory deviations due to thruster failures

Under the term ‘thruster failure’ two failure conditions are understood; these correspond to the inability to close the thruster valves at the end of operation (thruster-open failure) and to the inability to open the valves for operation (thruster-closed failure). Other failure conditions, where a thruster permanently produces a partial thrust level, are qualitatively equivalent to a thruster-open failure.

Depending on the direction of the failed thruster, thruster-open failures, if not counteracted in time, can lead to any type of trajectory. The magnitude of the eventual trajectory and velocity errors depends on the duration of the failure condition. As a result, there is no other protection against thruster-open failures but to detect this failure condition as early as possible and to stop the thrust force. The residual maximum possible trajectory and velocity errors can then be calculated from the worst case time difference between failure occurrence and closure of the faulty thruster.

Thruster-closed failures, if no more redundancy is available and if not resolved in time, lead to loss of attitude control around one axis and loss of trajectory control in one direction. A resulting uncontrolled angular motion about this axis may, after time, cause a coupling of trajectory control forces from one axis in the others, resulting in trajectory deviations. The effects of an unresolved thruster-closed failure are, in the short term, the inability to perform a planned trajectory manoeuvre and, in the longer term, the loss of attitude and the build-up of trajectory deviations. If the failed thruster can be identified, and as long as redundancy is available, the obvious solution is to inhibit the failed thruster and to switch over to a redundant one.

5.3 Orbital disturbances

The effect that each of the disturbances that we will discuss in this section generates depends a lot on the type of orbit of the mission and the manoeuvres that are carried out. We will make a general overview.

5.3.1 Drag due to residual atmosphere

The drag force by the residual atmosphere acting on a spacecraft is:

$$F_D = -\frac{\rho}{2} V_x^2 C_D A$$

where V_x is the orbital velocity; C_D is the drag coefficient; A is the cross section of the body.

As is evident from the equation, the resistance depends on the altitude and the more we are at low altitudes, the stronger this effect is and causes a gradually greater decay of the orbit. For instance, on the side illuminated by the Sun, the atmosphere will expand and denser parts of the atmosphere will rise to higher altitudes. The density at a certain orbital height will, therefore, not be constant but will increase (solar bulge) on the illuminated side of the orbit, and vice versa on the opposite side. A large influence on the density of the atmosphere at a certain orbital height is the solar flux, which heats up the outer atmosphere.

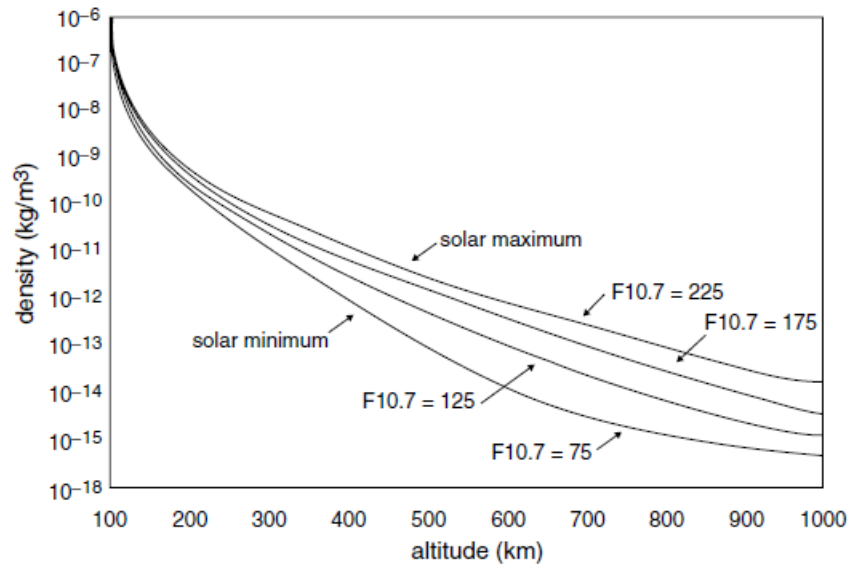


Figure 37: Density vs Altitude at various levels of solar flux

5.3.2 Disturbances due to geopotential anomaly

Due to the fact that the shape of the Earth deviates from an ideal sphere, and that its mass is not distributed homogeneously inside its body, the gravitational forces are not entirely directed toward the orbit centre, but can have components in other directions in and out of the orbit plane. These forces will vary over one orbital revolution and can cause changes in the orbital parameters.

The effect of the oblateness of the Earth on the orbits results in the following motions:

- a motion of the line of nodes called the 'drift of nodes' or 'regression of nodes'
- a rotation of the line of apsides for an elliptical orbit.

5.3.3 Disturbances due to solar pressure

Solar radiation produces a force on a spacecraft in the Sun–satellite direction:

$$F_{SP} = -p \cdot A \cdot \vec{u}_s$$

where p is the radiation momentum flux, A is the cross section of the satellite, m is the mass of the satellite and \vec{u}_s is the Sun–satellite direction unity vector. The radiation momentum flux varies periodically with the orbit of the Earth around the Sun

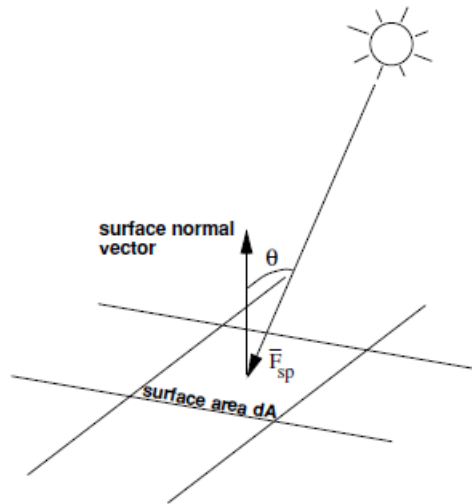


Figure 38: Solar pressure force on surface area

As the forces due to solar pressure have in- and out-of-plane components, depending on the Sun direction w.r.t the orbital plane, the solar pressure will have some effect on all orbital parameters, with the most important ones being on eccentricity and on inclination. Depending on orbital height and Sun direction, the force will be intermittent, i.e. the force will be zero when the satellite is in the shadow of the Earth.

5.3.4 Dynamic interaction of thruster plumes between chaser and target

In the case of the SROC mission where a rendezvous and docking manoeuvre is carried out, this type of disturbance is also of great importance.

Plume interaction becomes an important disturbance when spacecraft are operating in close proximity. Depending on the size of the thrusters and the geometric extension of the opposite spacecraft's surfaces, the effects are significant in a range below a few tens of metres through a few hundred metres. As thruster plumes are limited in their extension, and since the various spacecraft surfaces are at those distances equal to or larger than the plume diameter, there is no possibility of treating the disturbance more globally. Rather, the forces must be integrated over the various surfaces, taking into account the thrust direction w.r.t. the particular surface and the pressure distribution of the plume as a function of range and angle from the centre line.

The force exerted by a thruster plume on a surface element dS can be described by the plume pressure $P(r, \theta)$ and the direction γ of the gas flux with respect to the surface:

$$dF = -P(r, \theta) \cos(\gamma) dS$$

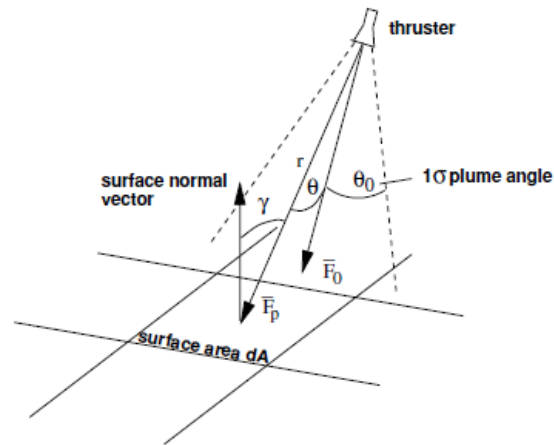


Figure 39: Thruster plume force on surface area

Accelerations due to plume interaction from one spacecraft on another one can (at short distance) be one to two orders of magnitude higher than that of air drag. Braking boosts close to the spacecraft, where the plume is directed toward the target vehicle, must therefore be avoided. Attitude control thrust could be in all directions, but the single thrusts are relatively short in time.

5.3.5 Trajectory deviations generated by the spacecraft system (navigation errors)

Navigation errors are the deviations of the measured or predicted state vector of the vehicle from the real one. Such deviations can result from alignment errors between the sensor and the spacecraft axes, from measurement performance limitations of the sensors used, from aberrations caused by the measurement environment, and from performance limitations of the information processing in the navigation filter.

The parameters that are measured are: the position, the speed and attitude and angular rates and what must be evaluated for each of these measurements is the effect that the error that is committed in carrying out these has on the trajectory measurements.

5.4 Simulations

Now we have to make sure that all these disturbances that we have analysed are taken into account within the simulation environment on STK. As for the "Orbital disturbances", the STK software already takes them into account through specific models in order to provide results, considering the type of orbit and the time period during which the mission is operational, which take these into account disturbances. While with regard to all those disturbances related to thrusters that we have extensively analysed in the previous sections, we take them into consideration by adding offsets within the scenario created on STK in the attitude panel of each manoeuvre segment where the thrust vector is specified. The figure shows the procedure.

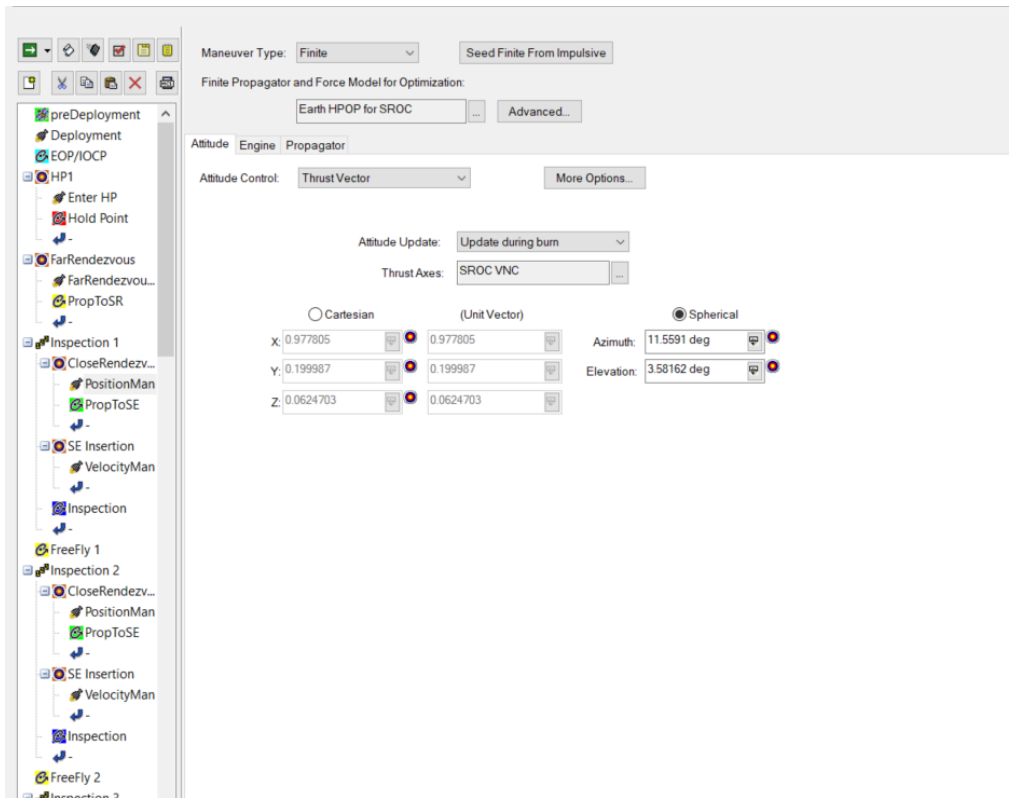


Figure 40: Nominal values

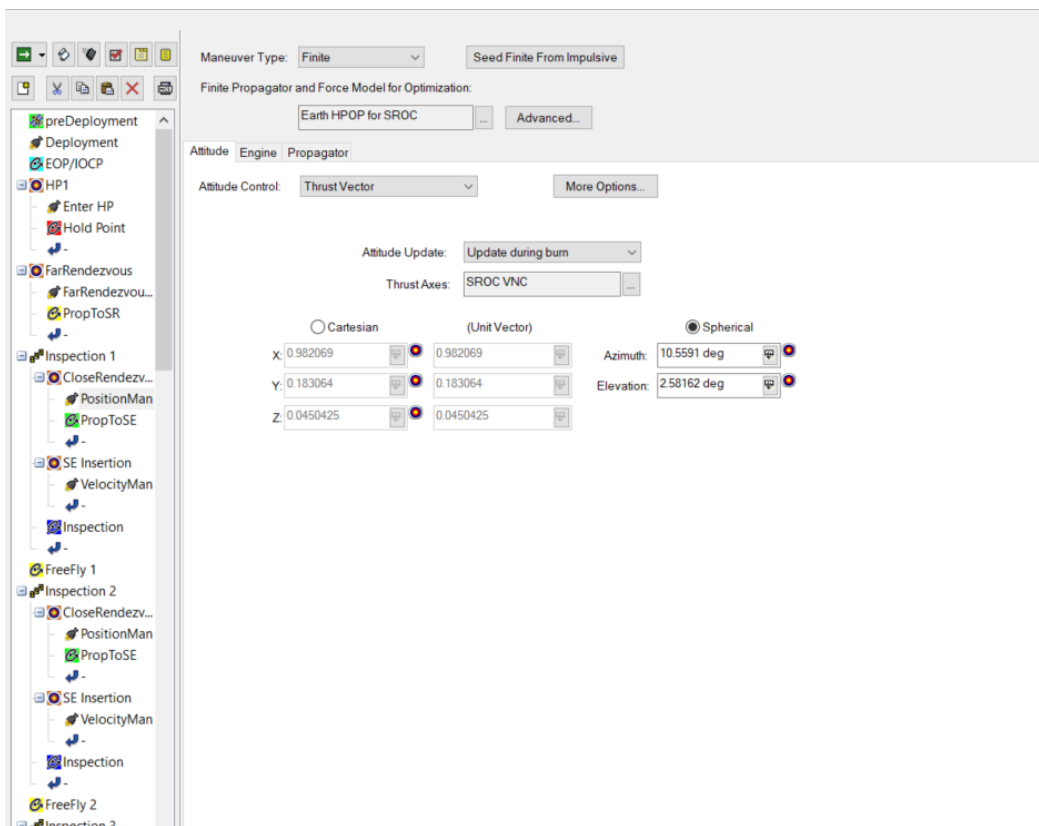


Figure 41: Added 1 degree offset on both azimuth and elevation angle

As shown in the figure we are going to vary the azimuth and elevation angles with respect to their nominal values by a maximum of 5 degrees (more and less) in 1 degree steps and let's see how the ΔV and fuel consumption vary following the introduction of these offsets.

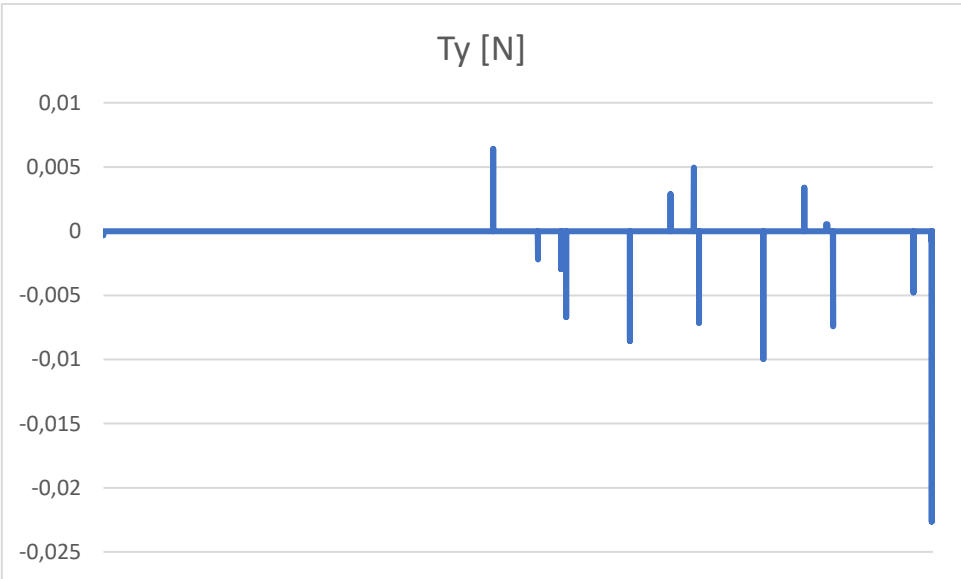
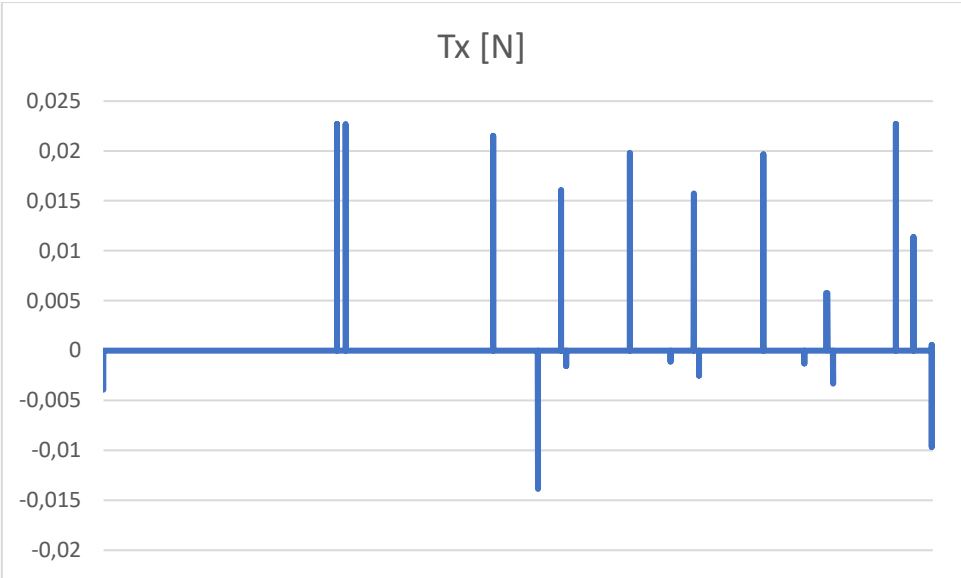
We went to do some simulations by inserting an offset only on one of the two between azimuth and elevation up to a maximum of 5 degrees and then we went to evaluate the worst cases, i.e. variations for both of +/- 5 degrees. The results of all simulations are shown in the following table.

	Azimuth	Elevation	ΔV	Fuel Used
Offset [°C]	1	0	5,08	0,294
Offset [°C]	2	0	5,08	0,294
Offset [°C]	3	0	5,08	0,294
Offset [°C]	4	0	5,08	0,294
Offset [°C]	5	0	5,08	0,294
Offset [°C]	0	1	5,08	0,294
Offset [°C]	0	2	5,08	0,294
Offset [°C]	0	3	5,08	0,294
Offset [°C]	0	4	5,08	0,294
Offset [°C]	0	5	5,08	0,294
Offset [°C]	1	1	5,08	0,294
Offset [°C]	2	2	5,08	0,294
Offset [°C]	3	3	5,08	0,294
Offset [°C]	4	4	5,08	0,294
Offset [°C]	5	5	5,08	0,294
Offset [°C]	-1	0	5,08	0,294
Offset [°C]	-2	0	5,08	0,294
Offset [°C]	-3	0	5,08	0,294
Offset [°C]	-4	0	5,08	0,294
Offset [°C]	-5	0	5,08	0,294
Offset [°C]	0	-1	5,08	0,294
Offset [°C]	0	-2	5,08	0,294
Offset [°C]	0	-3	5,08	0,294
Offset [°C]	0	-4	5,08	0,294
Offset [°C]	0	-5	5,08	0,294
Offset [°C]	-1	-1	5,08	0,294
Offset [°C]	-2	-2	5,08	0,294
Offset [°C]	-3	-3	5,08	0,294
Offset [°C]	-4	-4	5,08	0,294
Offset [°C]	-5	-5	5,08	0,294
Offset [°C]	5	-5	5,08	0,294
Offset [°C]	-5	5	5,08	0,294

Table 12: Results of simulations with offsets

As can be seen from the summary table, there are practically no variations due to the ΔV and fuel consumed offsets taken into consideration compared to the nominal case, the values of which are summarized in table 6 and table 7.

Among the outputs that we can obtain from the STK software there is also the variation of the thrust vector in its components along the body axes as a function of time and we note that the insertion of these offsets generates a variation of the thrust profile. The thrust profiles for two of the worst cases are shown in the figure, i.e. 5 degrees offset for both azimuth and elevation and 5 degrees offset for azimuth and -5 degrees for elevation.



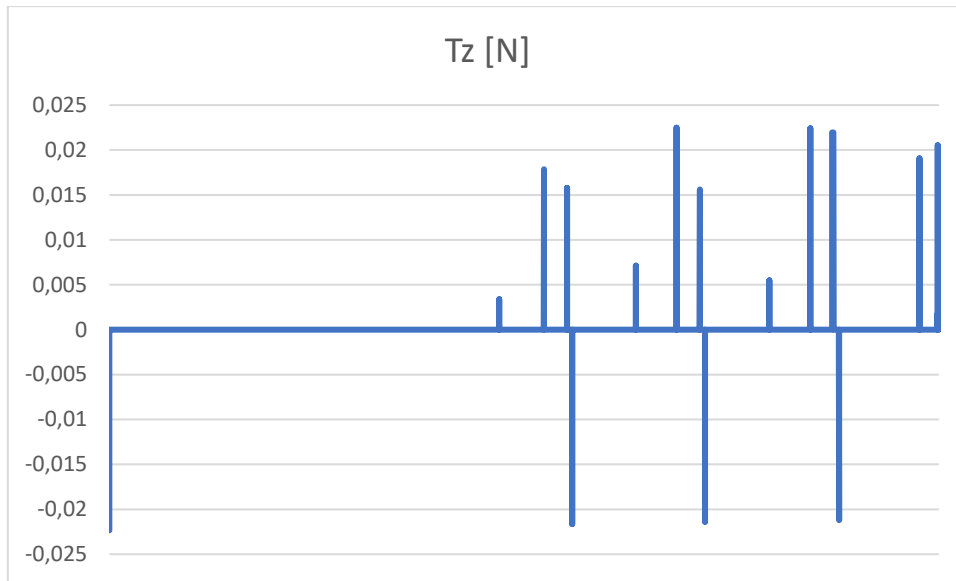
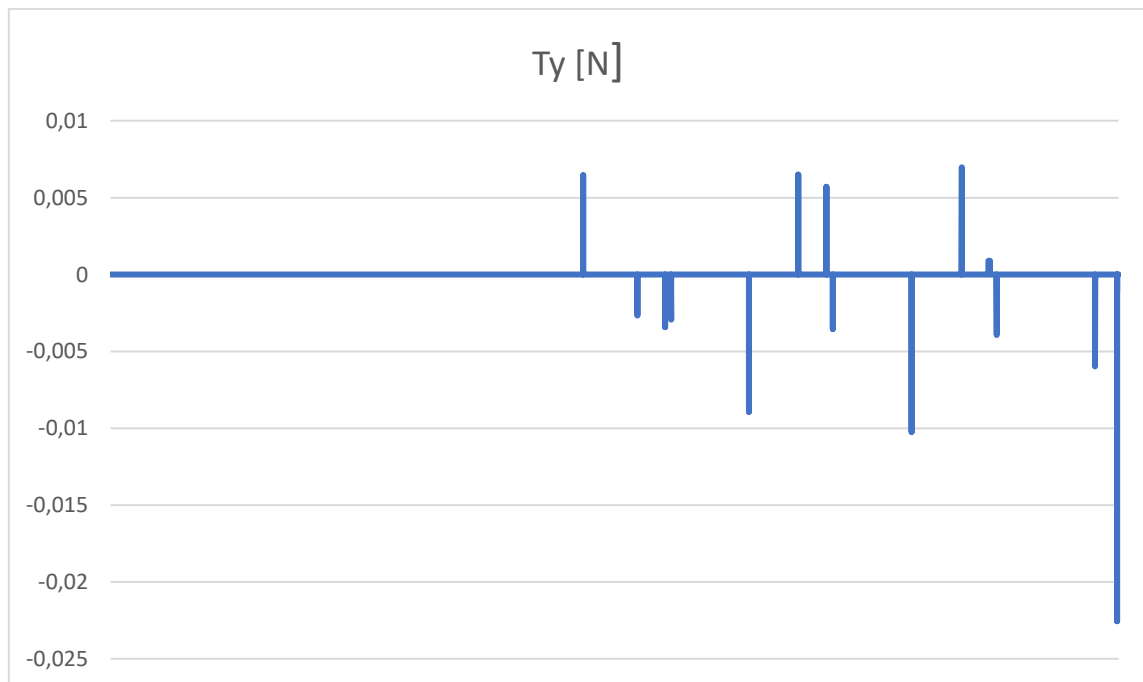
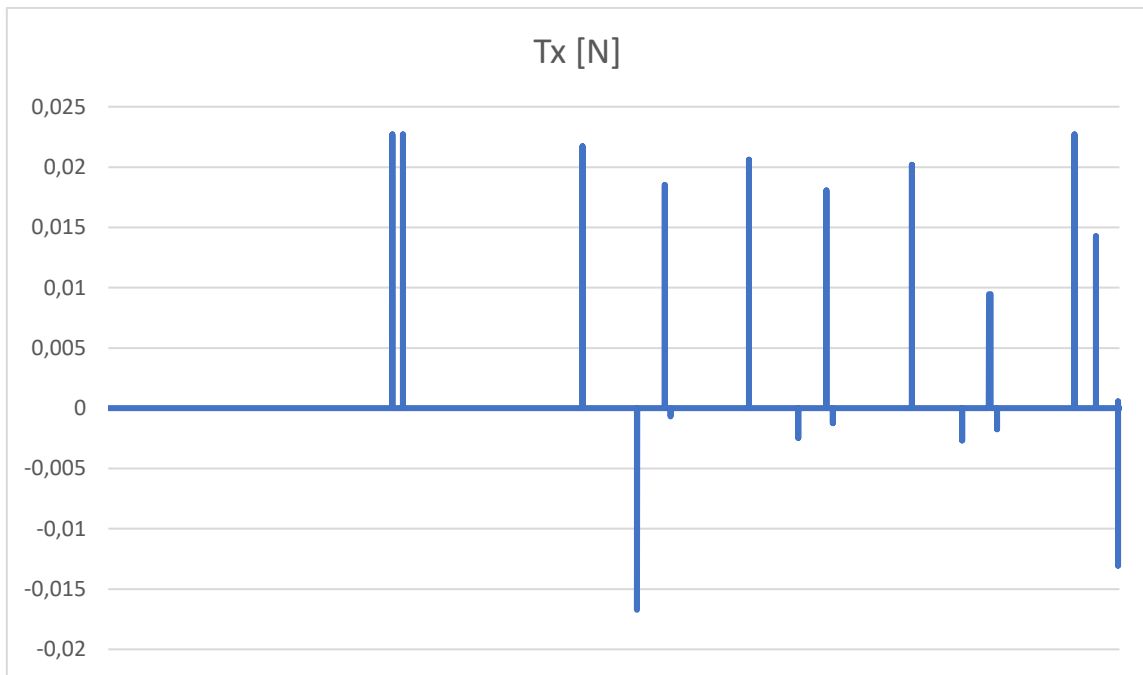


Figure 42: Thrust profile for the case with 5 degree / 5 degree offsets

Maneuver Number	Start Time (UTCG)	Tx [N]	Ty [N]	Tz [N]	Duration (sec)
1	1 Jun 2023 11:00:00,000	-0,003929	-0,00034	-0,02236	9,744
2	6 Jun 2023 11:40:48,057	0,022706	0	0	4,091
3	6 Jun 2023 16:19:48,106	0,022706	0	0	3,826
4	9 Jun 2023 22:22:01,516	0,02152	0,006399	0,003388	0,137
5	10 Jun 2023 21:22:01,653	-0,013874	-0,0022	0,017839	462,066
6	11 Jun 2023 08:59:59,550	0,016063	-0,00296	0,015772	12,662
7	11 Jun 2023 11:37:42,212	-0,001566	-0,00669	-0,02164	68,641
8	12 Jun 2023 20:21:33,771	0,019776	-0,00857	0,00714	1,706
9	13 Jun 2023 16:51:35,477	-0,001095	0,002898	0,022493	2,910
10	14 Jun 2023 04:35:36,073	0,015724	0,004965	0,01561	1,002
11	14 Jun 2023 07:13:07,075	-0,002522	-0,00715	-0,0214	3,828
12	15 Jun 2023 15:58:11,885	0,019647	-0,00997	0,0055	1,745
13	16 Jun 2023 12:28:13,630	-0,001294	0,003387	0,022414	2,937
14	16 Jun 2023 23:32:03,877	0,005762	0,000551	0,021956	2284,083
15	17 Jun 2023 02:47:37,961	-0,003304	-0,00741	-0,02121	3,624
16	18 Jun 2023 10:57:20,719	0,022706	0	0	0,724
17	18 Jun 2023 19:57:21,443	0,011379	-0,00477	0,019062	2,555
18	19 Jun 2023 04:57:23,998	0,000569	-0,02263	0,001787	2,645
19	19 Jun 2023 04:59:26,643	-0,009651	-0,0008	0,020537	1,256

Table 13: Duration and thrust values along the 3 body axes for the case with 5 degrees / 5 degrees offsets



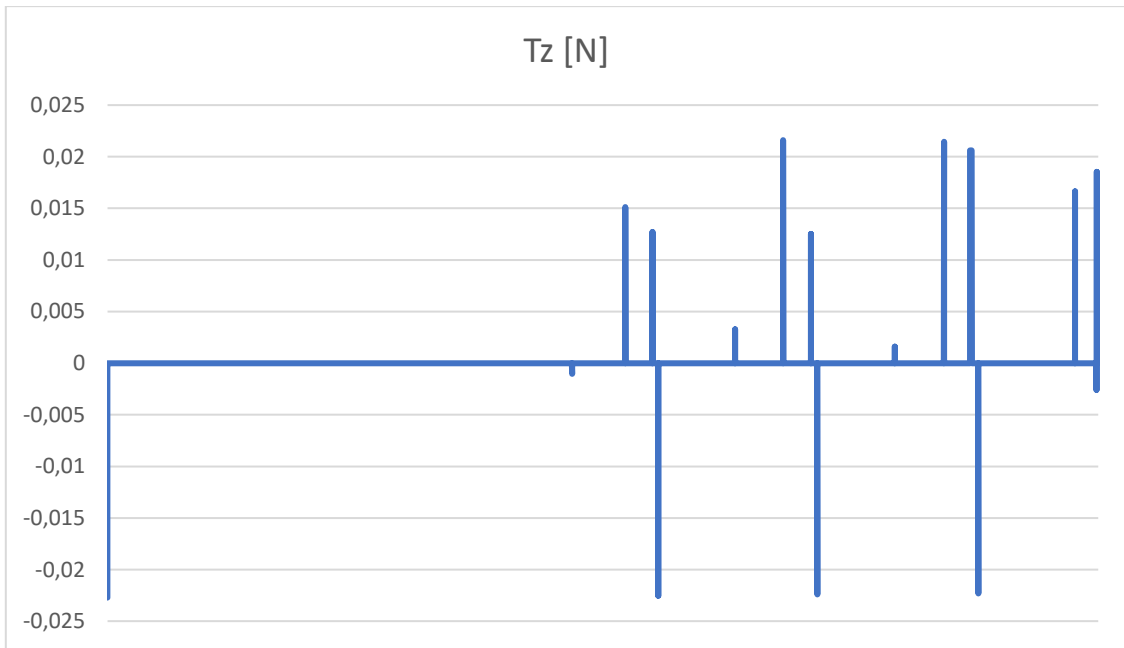


Figure 43: Thrust profile for the case with 5 degree / -5 degree offsets

Maneuver Number	Start Time (UTCG)	Tx [N]	Ty [N]	Tz [N]	Duration (sec)
1	1 Jun 2023 11:00:00	-0,000001	0	-0,022706	9,744
2	6 Jun 2023 11:40:48	0,022706	0	0	4,091
3	6 Jun 2023 16:19:49	0,022706	0	0	3,826
4	9 Jun 2023 22:22:06	0,021742	0,006465	-0,001023	0,137
5	10 Jun 2023 21:22:06	-0,016722	-0,002651	0,015129	462,066
6	11 Jun 2023 08:59:56	0,018512	-0,003412	0,012696	12,662
7	11 Jun 2023 11:37:39	-0,000685	-0,002928	-0,022506	68,641
8	12 Jun 2023 20:20:40	0,020613	-0,008934	0,003289	1,706
9	13 Jun 2023 16:50:42	-0,002458	0,006508	0,021614	2,91
10	14 Jun 2023 04:35:07	0,018069	0,005705	0,01251	1,002
11	14 Jun 2023 07:12:38	-0,001247	-0,003533	-0,022394	3,828
12	15 Jun 2023 15:57:55	0,0202	-0,010245	0,001591	1,745
13	16 Jun 2023 12:27:56	-0,002663	0,006971	0,021444	2,937
14	16 Jun 2023 23:31:49	0,009469	0,000906	0,020617	2284,83
15	17 Jun 2023 02:47:23	-0,001753	-0,00393	-0,022294	3,624
16	18 Jun 2023 10:56:55	0,022706	0	0	0,724
17	18 Jun 2023 19:56:56	0,014259	-0,005974	0,01663	2,555
18	19 Jun 2023 04:56:58	0,000567	-0,022552	-0,002576	2,645
19	19 Jun 2023 04:59:01	-0,013059	-0,001086	0,018543	1,256

Table 14: Duration and thrust values along the 3 body axes for the case with 5 degrees / -5 degrees offsets

Here are represented the thrust profiles with the relative values reported in the tables for two of the worst cases. Differences from the nominal case discussed in section 3.7 can be noted. In fact, with the addition of the offsets, the thrust values along the 3 body directions necessary to perform each manoeuvre vary according to the degree of offsets considered. This means that the thrust profile, i.e. the trend of thrust as a function of time, varies with respect to the nominal case and is also different between the two worst cases taken into consideration. It is interesting to underline that the duration of each manoeuvre does not vary in the presence of offsets as can be seen from the tables above compared with that of the nominal case. As for the nominal case, even for the two worst cases the sum of the thrust values necessary along the 3 directions for each manoeuvre does not exceed 35 mN and this shows that even in the presence of offsets that could be present in reality during the carrying out the mission, the selected engine is adequate to successfully carry out the mission.

6 Conclusions

The study done in this thesis, in a first phase, has shown that the best technology for the propulsion system of a mission like SROC is cold gas as this type of thrusters are simple, not bulky and light, inexpensive and very effective for the purposes of the mission in question, in addition to the fact that at the moment they are the most used for missions with CubeSat and consequently it is a technology already validated in several missions and which has an average TRL higher than the others taken into consideration. During the analysis for the choice of the best technology for the mission propulsion system, very innovative technologies and solutions were also taken into consideration, which guaranteed truly excellent characteristics and performance but unfortunately have not yet been validated in orbit or the current configurations of the engine had even excessive capacity for a mission like SROC and therefore in the end, as we have seen from the results of the trade-off, the choice fell rightly on a cold gas engine.

After demonstrating that the best choice for SROC's propulsion system was a cold gas propulsion system, it was decided to use the Perseus propulsion system developed specifically by Tyvak International for this type of mission, given that there are no propulsion systems on the market ready-made completely suitable for a mission like SROC. Starting from the data provided by the manufacturer Tyvak on the main characteristics and performance of Perseus, a model was built in order to model the engine chosen for the mission. Once this model was created, it was inserted into the simulation environment previously created through the STK software in which all the maneuvers from which the SROC mission is composed were reproduced. In addition to the creation of the Perseus model, all the characteristics of the " fuel tank " had to be calculated and inserted in the simulation environment in order to make the simulations more and more realistic. Once this was done, simulations could be carried out which showed that with the chosen propulsion system the mission could actually be carried out and that the ΔV values obtained taking into account 100% margins have even decreased compared to the previous simulations that took into account a standard propulsion system included in the software and even the ΔV required to perform the entire mission was found to be lower. The fuel consumption values were also found to be compliant with those predicted and previously calculated through the analyzes reported in this thesis.

Once the model was created and the characteristics of the fuel tank calculated in order to refine the simulation environment, we did all the analyzes of the nominal case, but we wanted to validate the propulsion system and analyze the results even in non-nominal cases. So it was decided to take into consideration a whole series of possible disturbances and situations that could cause a deviation from the nominal case and to simulate them by inserting a whole series of offsets within the simulation environment in order to analyze the results. It has been seen from the results of the simulations that the propulsion system chosen is valid even in the worst cases taken into consideration and that the ΔV and fuel consumption values do not change compared to the nominal case but the thrust profile changes, i.e. the thrust value required over time. of mission along the 3 body direction changes in the presence of offsets with respect to the nominal case. Although the thrust profiles change with respect to the nominal case, the maximum values are in any case lower than the total 35 mN for each maneuver segment, therefore the chosen engine is also valid for managing the off-nominal conditions analysed.

7 References

- [1] <https://www.focus.it/scienza/spazio/che-cosa-sono-i-cubesat>
- [2] Sabrina Corpino, Loris Franchi, Daniele Calvi, Luca Guerra, Serena Sette, Fabrizio Stesina, Small satellite mission design supported by tradespace exploration with concurrent engineering: Space Rider Observer Cube case study, IAF Space Systems Symposium (D1) Innovative and Visionary Space Systems(1), 70th International Astronautical Congress (IAC), Washington D.C., United States, 21-25 October 2019.
- [3] Sabrina Corpino, Daniele Calvi, D1.1-Assessment of the SROC mission and preliminary functional specification.
- [4] Sabrina Corpino, Fabrizio Stesina, Daniele Calvi, Filippo Corradino, D4.2-SROC: Technology Assessment Dossier.
- [5] NASA/TP-2018-220027, State of the Art Small Spacecraft Technology, Small Spacecraft Systems Virtual Institute, Ames Research Center, Moffett Field, California, https://www.nasa.gov/sites/default/files/atoms/files/soa2018_final_doc.pdf
- [6] Aaron Dinardi, ECAPS, High Performance Green Propulsion (HPGP), On-Orbit Validation & Ongoing Development, <https://forum.nasaspaceflight.com/index.php?action=dlattach;topic=32444.0;attach=546154>
- [7] Aerojet Rocketdyne, MPS-120 Innovative Propulsion Solutions for SmallSats, https://www.rocket.com/files/aerojet/documents/CubeSat/MPS-120_data_sheet-single_sheet.pdf
- [8] Aerojet Rocketdyne, MPS-130 Innovative Propulsion Solutions for SmallSats, https://www.rocket.com/files/aerojet/documents/CubeSat/MPS-130_data_sheet-single_sheet.pdf
- [9] Busek Space Propulsion and Systems, BGT-X5 Green Monopropellant Thruster, https://static1.squarespace.com/static/60df2bfb6db9752ed1d79d44/t/61292af2a097083a87c4cbc0/1630087925107/BGT_X5_v1.0.pdf
- [10] Vacco, ADN Micro Propulsion System, <https://www.cubesat-propulsion.com/wp-content/uploads/2015/10/adn-micropropulsion-system.pdf>
- [11] ECAPS, A Stable Liquid Mono-Propellant based on ADN, <https://ndiastorage.blob.core.usgovcloudapi.net/ndia/2009/insensitive/8Asjoberg.pdf>
- [12] Tethers Unlimited, Hydros-M, Water Propulsion System, <https://www.tethers.com/wp-content/uploads/2020/07/TUI-DATA-SHEETS-2-compressed.pdf>
- [13] Tethers Unlimited, Hydros-C, Water Propulsion System, <https://www.tethers.com/wp-content/uploads/2021/01/HYDROS-C-1.pdf>
- [14] Vacco, Green Propulsion System, <https://cubesat-propulsion.com/wp-content/uploads/2019/08/X19041000-Green-Propulsion-System-data-sheet-073019.pdf>
- [15] Vacco, Palomar Micro Propulsion System, https://cubesat-propulsion.com/wp-content/uploads/2015/10/Palomar_Micro-propulsion-system.pdf
- [16] Elizabeth T. Jens, Ashley C. Karp, Barry Nakazono, Jason Rabinovitch, Hybrid Propulsion System Enabling Orbit Insertion

Delta-Vs within a 12 U Spacecraft.

[17] Elizabeth T. Jens, Ashley C. Karp, Jason Rabinovitch, Barry Nakazono, Antonietta Conte, David Vaughan, Design of Interplanetary Hybrid CubeSat and SmallSat Propulsion Systems, AIAA Propulsion and Energy Forum July 9-11, 2018, Cincinnati, Ohio 2018 Joint Propulsion Conference.

[18] Vacco, ArgoMoon Propulsion System, <https://cubesat-propulsion.com/wp-content/uploads/2017/08/X17025000-data-sheet-080217.pdf>

[19] David Krejci, Paulo Lozano, Space Propulsion Technology for Small Spacecraft, PROCC. OF THE IEEE, VOL. 106, NO. 3, MARCH 2018.

[20] Akshay Reddy Tummala, Atri Dutta, An Overview of Cube-Satellite Propulsion Technologies and Trends, <https://www.mdpi.com/2226-4310/4/4/58/html>

[21] Martina Sacco. Design, development and test of the control unit for a small cold-gas propulsion system, Rel. Sabrina Corpino, Fabrizio Stesina, Filippo Corradino. Politecnico di Torino, corso di laurea magistrale in Mechatronic Engineering, 2020.

[22] Tyvak International, Answer to ESA AO/1-10258/20/NL/GLC, HERA Mission "Second Cubesat" Phase A/B C/D & E₁, HCS2-HERA CubeSat 2.

[23] Wigbert Fehse, Automated Rendezvous and Docking of Spacecraft, Cambridge University Press, 2003.

[24] S Corpino, F Stesina, D Calvi, L Guerra, (2020), Trajectory analysis of a CubeSat mission for the inspection of an orbiting vehicle, Advances in aircraft and spacecraft science, Vol 7(3), pp 271-290, <https://doi.org/10.12989/aas.2020.7.3.271> .

[25] Corpino S., Stesina F. (2020), Inspection of the cis-lunar station using multi-purpose autonomous Cubesats, Acta Astronautica, Volume 175, 2020, Pages 591-605, <https://doi.org/10.1016/j.actaastro.2020.05.053> .

[26] Nichele, F., Villa, M. and Vanotti, M. (2018), "Proximity operations - autonomous space drones", in Proceedings of the 45 Symposium, May, Sorrento (Italy).

[27] Stesina F., Tracking model predictive control for docking maneuvers of a CubeSat with a big spacecraft, Aerospace, Volume 8, Issue 8, August 2021, Article number 197.